Cardiff University

Epigenetics and Neurodevelopmental disorders: Molecular and behavioural characterisation of an *Ehmt1/Glp* knockout mouse model

A thesis submitted for the degree of

Doctor of Philosophy (PhD)

Manal Ali Adam

2019

School of Medicine

DECLARATION

This work has not been submitted in substance for any other degree or award at this or any other university or place of learning, nor is being submitted concurrently in candidature for any degree or other award.

Signed (candidate) Date

STATEMENT 1

This thesis is being submitted in partial fulfillment of the requirements for the degree of PhD.

Signed (candidate) Date

STATEMENT 2

This thesis is the result of my own independent work/investigation, except where otherwise stated. Other sources are acknowledged by explicit references. The views expressed are my own.

Signed (candidate) Date

STATEMENT 3

I hereby give consent for my thesis, if accepted, to be available for photocopying and for inter-library loan, and for the title and summary to be made available to outside organisations.

Signed (candidate) Date

STATEMENT 4: PREVIOUSLY APPROVED BAR ON ACCESS

I hereby give consent for my thesis, if accepted, to be available for photocopying and for inter-library loans **after expiry of a bar on access previously approved by the Academic Standards & Quality Committee.**

Signed (candidate) Date

Thesis Summary

Post-translational histone modifications lead to large coordinated and dynamic changes to the chromatin in a spatial and temporally specific manner. These highly synchronised epigenetic changes control gene transcription and are critical for various cellular functions including cell cycle progression, DNA repair, and telomere maintenance. The role of epigenetics in neurodevelopment is wide-ranging therefore it is highly unsurprising that epigenetic modifiers have been implicated in neurodevelopmental disorders (NDDs). I used an *in vivo* and *in vitro* approach to understand the role of histone modifier *Ehmt1* in development and disorder.

In this thesis I describe a distinct behavioural phenotype in a forebrain specific *Ehmt1* haploinsufficient mouse model, *Ehmt1*$^{D6cre/+}$ (**Chapters 2 & 3).** These behavioural findings were then related to the role of *Ehmt1* in adult hippocampal neurogenesis, *in vivo* (**Chapter 4**) and *in vitro* (**Chapter 5**). Finally using publically available RNA-seq data, enrichment analyses were used to determine the effect of *Ehmt1* reduction on key phenotypes associated with memory and learning, as well as identifying genes associated with neurodevelopmental disorders (**Chapter 6**).

In summary, this thesis aims to draw connections between *Ehmt1's* function in the forebrain, particularly the hippocampus, and the deficits seen in cognition and executive functioning in a number of associated neurodevelopmental disorders. Using interesting results from data mining, along with findings from behavioural and cellular analyses; identification of potential downstream targets for further research of disease pathogenesis could be possible.

Acknowledgements

All work in this thesis was conducted by myself unless otherwise stated.

First and foremost, I would like to thank my supervisors, Professor Anthony Isles and Dr. Trevor Humby, for all their support and guidance throughout the length of this degree. The advice and knowledge I've gained from them, both in regards to academia and life in general, will stick with me for a lifetime.

To the Isles lab PhDs: Kira, Simona, Matt, & Sylvia, thank you for the support and friendship through the years. I will never forget the ups and downs of circumnavigating this PhD with you all. To Dr.Hugo Creeth and Dr. Grainne McNamara, I am glad I had people to look up to not so far removed to the struggles of the second year blues, and uncooperative genotyping! Your moral support, even though at times just shared misery, helped with the long days.

Thank you to Dr.Andrew Pocklington and Dr. Robert Andrews for their expertise and guidance in the steep-learning curve that is bioinformatics and statistics. A special thank you to Dr. Niels Haan for his friendship and unofficial supervisory role spending days on end in the cell culture room with me. I am grateful to having built a large network of friends during these years; thank you Rae for all of your lunch time rants, and shared pizzas on the couch; thank you Jo for your baked goods and cat gifs. To Jeff, I am so entirely grateful for you; I don't know where I would be without your almost overbearing support, thanks for all the nagging.

To everyone outside of work for their continuous, almost undeserving, diehard support; Sonia, Hannah, Hidaya, thanks for reminding me of who I am on a constant basis and providing a personal get-away from world of academia.

Lastly, I could never have achieved any success, academic or elsewise, if it were not for the most supportive family I could have asked for. Thank you to my mother for being my constant advocate, cheerleader, and pillar. To my siblings for bringing me back from the brink numerous times, and never letting me lose sight of what's important. To my uncles for their love and support through it all.

This thesis is dedicated to my father, the strongest & most caring man I have ever met. Thank you for being my biggest champion my entire life. I hope I make you proud.

Table of Contents

Index of Tables

Index of Figures

List of Abbreviations

AHN- Adult hippocampal neurogenesis

ASD- Autism spectrum disorders

ASR- Acoustic startle reaction

BDNF- Brain-derived neurotrophic factor

bHLH- Basic helix-loop-helix

BrdU- 5-bromo-2'-deoxyuridine

CNV- Copy number variants

CpG- Cystosine-phosphate-Guanine

DAPI- 4′,6-diamidino-2-phenylindole

DCX- Doublecortin

DIV- Days *in vitro*

EGF- Epidermal growth factor

EHMT1- Euchromatic histone-lysine N-methyltransferase 1

EPM- Elevated plus maze

FGF- Fibroblast growth factor

GFAP- Glial fibrillary acidic protein

ID- Intellectual disability

KS- Kleefstra Syndrome

LMA- Locomotor activity

LTP- Long term potentiation

NeuN- Neuronal Nuclei

NOL- Novel Object Location

NOR- Novel Object Recognition

PAX6- Paired box 6

PBS- Phosphate buffered saline

PPI- Prepulse inhibition

REST- RE1-Silencing Transcription factor

SOX- SRY (sex determining region Y)-box

TTX- Tetrodotoxin

WT- Wildtype

Chapter 1 General Introduction

1.1. Epigenetics

Epigenetics was originally termed by Conrad Waddington to explain how a genotype brings about a phenotype. The term has since then evolved in order to integrate the growing knowledge within the field. It now stands that epigenetics refers widely to the stable and reversible alterations in genetic expression above and beyond changes to the DNA sequence. This broad definition encompasses a range of mechanisms involved from gene to protein, in which highly sophisticated regulated processes control gene expression at almost every level. These epigenetic mechanisms include DNA methylation at cytosine-phosphate-guanine, CpG, islands and post-translational modifications of histones (Figure 1.1). The reversible nature of such mechanisms allow for incredibly dynamic expression patterns, as seen during the development of the CNS (Mehler 2008).

1.1.1. DNA Methylation

DNA methylation occurs at cytosine residues at the promoter rich CPG islands, which often span approximately 1000 base pairs of which CG density exceeds that seen elsewhere in the genome (Deaton & Bird 2011). The majority of protein coding promoters are found within CpG islands, an aspect found to be evolutionarily conserved from mouse to human, suggesting an important function to these regions. DNA methylation at these sites leads to transcriptional silencing, and dynamic processes involving *de novo* methylation as well as demethylation lead to tissue specific methylation patterns and thus tissue specific gene expression (Ghosh et al. 2010). Neurons have been found to be able to alter their methylation patterns in response to stimuli (Saunderson et al. 2016).Here it was

shown that a stressful event, in the form of a forced swim challenge, lead to CpG-specific demethylation at the gene promoter regions of *c-Fos and Egr-1.* This implicates DNA methylation patterns to normal neuronal functioning and behaviour.

1.1.2. Histone Modification

Another group of epigenetic processes are the post-translational modifications of histones. Histones in a nucleosome, along with DNA, form chromatin (Bannister & Kouzarides 2011; Rudenko & Tsai 2014; Lawrence et al. 2016). Chromatin is found in two conformations, in either euchromatic or heterochromatic forms. Euchromatin refers to an open, relaxed form in which regions of the genome are accessible for transcription; heterochromatin confers a condensed, compact structure. Histones form the core of nucleosomes. Each nucleosome is made up of two copies of each histone protein: H2A, H2B, H3, and H4. Each of these histones has protruding tails to which modifications can be added (Lawrence et al. 2016). Changes in these chemical modifications alter the 3D structure of chromatin, impacting gene expression through adjusting the accessibility to regions of the chromosome. The most extensively modified histone is the H3 protein (Bannister & Kouzarides 2011), in which specific chemical marks on specific residues on its tail can confer altered gene expression patterns. These chemical modifications including acetylation, methylation, and phosphorylation can be added to the tails using “writer” enzymes, including HMTs - histone methyltransferases, and HATs, histone acetyltransferases. These marks can be deciphered by “reader” enzymes regions such as chromodomains, and in turn removed by “eraser” enzymes, e.g. histone deacetylases, HDACs (Benevento et al. 2015).

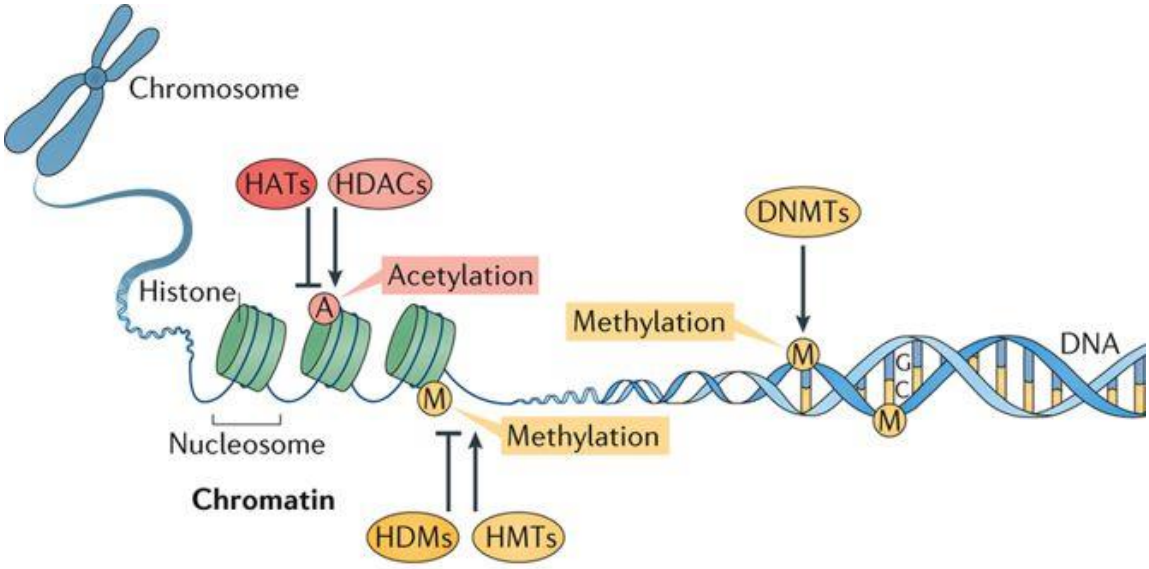

Figure 1.1 Summary of epigenetics. Chromatin is made up of DNA wrapped around repeating units of nucleosomes. These nucleosomes are composed of histones. Chemical tags can be added to histone tails to lead to either the repression or activation of nearby genes. DNA sequences can also be directly methylated at CpG sites to alter expression of genes. (Image taken from Niederberger et al. 2017)

1.1.3. Histone Modifier : EHMT1

Over the years, various enzymes involved in the writing, reading, and erasing of these biochemical tags have been associated with, and linked to, neurodevelopmental disorders (Millan 2013). This is understandable when taking into account the known significance of dynamic spatiotemporal regulation of gene expression in the precise development of the brain. Euchromatic Histone Methyltransferase-1 (EHMT1), also known as GLP (G9a-like protein), is a protein that is important for development and associated with neurodevelopmental disorders. EHMT1, along with G9a, is a member of the euchromatic lysine histone methyltransferase family (Tachibana et al. 2001; Tachibana et al. 2005; Shinkai & Tachibana 2011).

These proteins are part of a superfamily of lysine-methyltransferases characterised by the presence of a SET domain. Within this superfamily EHMT1 and G9a are a part of the Suv39h1 subfamily of lysine methyltransferases

responsible for the mono-, di-, and tri-methylation at lysine residues (Trievel et al. 2002). The SET/pre-SET domains are vital for methyltransferase activity (Herz et al. 2013). These proteins are highly conserved through evolution with a large number of orthologues having been characterised in other species, including *Ehmt* in *Drosophila melanogaster*, a single gene that appears to share functional similarities with both EHMT1 and G9a (Kramer et al. 2011). Within the Suv39h1 family of lysine methyltransferases, both EHMT1 and G9a uniquely contain ankyrin repeats in their protein structure. Although unique to EHMT1 and G9a within the methyltransferase family of proteins, ankyrin repeat domains are also found in a wide range of proteins with differing functions including synaptic functioning and cell adhesion (Li et al. 1999; Lim et al. 2001) and are important for protein-protein interactions (Mosavi et al. 2004). The Ank domains in EHMT1 and G9a preferentially bind to H3 tails at mono- and di-methylated K9 (Collins et al. 2008), providing evidence of the proteins being able to recognise the marks, and perhaps self-regulate (Adam & Isles 2017).

This non-methyltransferase dependent activity is corroborated further by evidence of the SET domain superfamily of enzymes interacting with other proteins. EHMT1 and G9a have both been shown to methylate non histone target proteins such as WIZ, (Rathert et al. 2008), P53 (Huang et al. 2010), and CDYL (Rathert et al. 2008). EHMT1 has also been found to target DNMT1 and DNMT3/3a (Chang et al. 2011), although the purpose of these interactions are not understood at present.

1.1.3.1. Methyltransferase Activity

EHMT1 mediates the addition of mono- and di- methyl groups to the H3K9 within the genome, doing so by the previously described SET/pre-SET domains (Tachibana et al. 2001; Tachibana et al. 2005). This is generally associated with repression of transcription, and is associated with classical epigenetic mechanisms of transcriptional silence such as genomic imprinting (Xin et al. 2003; Zhang et al. 2016) and globally with regions of heterochromatin (Peters et al. 2002). EHMT1 is often found within repressive complexes, including forming a stoichiometric complex with G9a that is important for *in vivo* dimethylation at H3K9 (Tachibana et al. 2005). EHMT1 is also a member of the NRSF/REST complex involved in the repression neuronal genes in progenitors (Roopra et al. 2004; Mozzetta et al. 2014). EHMT1 has been shown to also form a complex with other methyltransferases including G9a, SETDB1, and Suv39h1 to regulate G9a target genes (Fritsch et al. 2010). Despite potential redundancy in the function of EHMT1 and G9a, Tachibana et al. (2005) found reduction in either protein leads to significantly reduced H3K9 dimethylation, with no further reduction being seen in a double knockout. This is indicative of a lack of compensation of function by either EHMT1 or G9A. This is further validated by the fact homozygous deletion of EHMT1 leads to embryonic lethality in the mouse, suggesting a vital role of the protein during development that cannot be compensated for by the G9a alone (Tachibana et al. 2005).

1.1.4. DNA Methylation

There is an expanding literature on EHMT1's role in the reestablishment and maintenance of DNA methylation. Reestablishment of DNA methylation upon

the formation of the hemi-methylated daughter strands is a necessary step after DNA replication. EHMT1 has been linked to this process, and knocking it down lead to a decrease in DNA methylation (Dong et al. 2008). Its methylation mark H3K9me2 is necessary for the maintenance process (Liu et al. 2013; West et al. 2014). There is some evidence of interaction between G9a and DNMT1 in regulating H3K9 methylation in the HCT116 cancerous colon immortalised cells; here knocking out DNMT1 lead to a reduction in H3K9me2 (Estève et al. 2006).

Low DNA methylation in embryonic stem cells (ESCs) was associated with decreased DNA methylation maintenance along with associated UHRF1 as well as decreased EHMT1/G9a expressions (von Meyenn et al. 2016). However the exact mechanism by which EHMT1 mediates the maintenance of DNA methylation is not fully understood. UHRF1 is known to co-localise and directly interact with DNMT1 aiding in the maintenance of the methylation by binding to hemi-methylated DNA via its SET/RING domain. This in turn recruits DNMT1 to re-establish methylation (Qin et al. 2015; Harrison et al. 2016). UHRF1 was also shown to bind to H3K9me2/3 through its tandem Tudor domain and recruits DNMT1 to mediate DNA methylation maintenance in an H3K9me2/3 dependent manner (Harrison et al. 2016).

Recently Ferry et al. (2017) have increased the current understanding of this process; DNA ligase 1 (LIG1), a novel target of EHMT1 is methylated on its H3K9 mimic, UHRF1 then binds to the mimic, leading to the recruitment of UHRF1 to hemi-methylated sites, mediating its activity (Figure 1.2). UHRF1 was also found to more readily bind to the LIG1 mimic compared to H3K9me2/3. Current

evidence is suggestive of complimentary role of EHMT1 in histone and DNA methylation (Adam & Isles 2017).

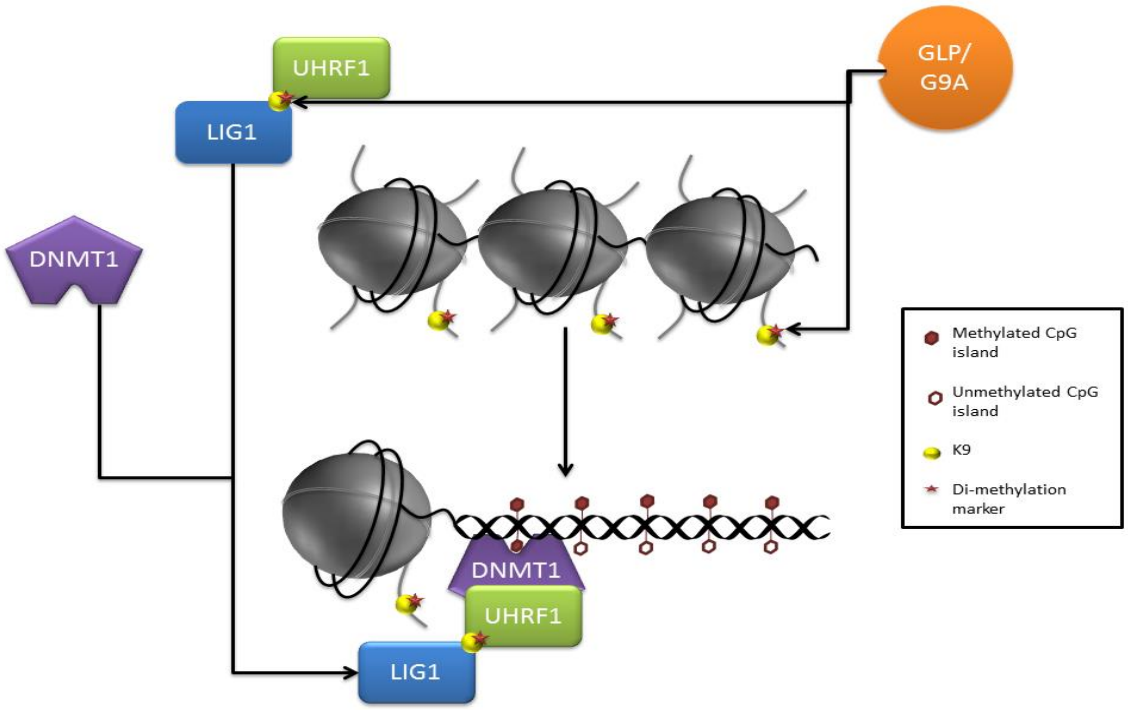

Figure 1.2 Maintenance of DNA methylation: Glp and G9a methylate the H3K9 mimic on DNA ligase 1 (LIG1). UHRF1 can recognise and bind both H3K9me2/3 marks on the methylated mimic on LIG1. UHRF1 binds to methylated LIG1 with a high affinity, mediating its activity to recognise and preferentially bind to hemi-methylated DNA strands, recruiting DNA methyltransferase 1 (DNMT1) to re-establish methylation and CpG islands.(Adam & Isles 2017)

1.2. EHMT1 in Brain Disorders

In humans, the gene encoding EHMT1, *EHMT1*, is found on the long arm of chromosome 9, specifically at q34.3. A wide range of genetic studies have linked loss of one copy (haploinsufficiency), or mutation of one copy, of *EHMT1* with a number of brain disorders, particularly neurodevelopmental disorders. These data add to the growing image of neurodevelopmental disorders being, in part, “epigeneopathies”, as *EHMT1* and various other important enzymes in histone modification have been implicated in the pathogenesis of NDDs (Millan 2013).

1.2.1. Intellectual Disability

Intellectual disability affects approximately 1-3% of the population and is characterised by reduced cognitive ability and some adaptive behaviour problems (Hamdan et al. 2014). Intellectual disability can be sporadic and isolated, or as an identifying phenotype in a complex syndrome and is a key symptom in various syndromes including Down syndrome and fragile X syndrome (Millan 2013).

EHMT1 is most notably associated with Kleefstra Syndrome, an intellectual disability multi-system syndrome associated with congenital heart defects, hypotonia, and dysmorphisms (Kleefstra et al. 2005). Kleefstra syndrome is also characterised by developmental delay, and reduced or complete lack of speech. Patients also have distinctive facial features including midface hypoplasia, synophrys, and hypertelorism (Kleefstra & de Leeuw 1993). Kleefstra syndrome is caused by the haploinsufficiency of *EHMT1*, either through single mutations, or 9q34.3 microdeletions (Kleefstra et al. 2005; Kleefstra et al. 2006). More recently patients suffering from Kleefstra syndrome that appear to not have the deletion or mutation of *EHMT1* have rather been linked to other genes found to be directly interact with *EHMT1*, such as MBD5, another epigenetic regulator (Kleefstra et al. 2012). These findings have in turn advanced the current understanding of the pathogenesis of Kleefstra syndrome, and provided further evidence of *EHMT1's* larger impact in epigenetic regulation.

Outside of Kleefstra syndrome, *de novo* deletions of *EHMT1* have been detected in severe intellectual disability copy number variant or CNV studies. (Gilissen et al. 2014; Grozeva et al. 2015; Quintela et al. 2017)EHMT1 associated chromatin regulators have also been linked to sporadic intellectual disability in

chromosomal microarray (Quintela et al. 2017) and exome studies (Hamdan et al. 2014; Han et al. 2017) of patients with intellectual disability, once again linking EHMT1 to a wider epigenetic regulatory network important to cognitive function.

Recently exome sequencing of approximately 4300 families with members suffering from developmental disorders identified *EHMT1* as a gene of interest in the pathogenesis of developmental disorders generally (McRae et al., 2017). EHMT1 was also identified as a pathogenic CNV in patients with intellectual disability and early onset epilepsy (Fry et al. 2016). Epilepsy is often associated with ID and developmental delay (Fry et al., 2016; Han et al., 2017), and some patients with Kleefstra syndrome are known to suffer from epilepsy (Hadzsiev et al. 2016).

1.2.2. Autistic Spectrum Disorders

EHMT1 has also been associated with autism spectrum disorders (ASDs). ASDs share a common base of phenotypes including dysfunctional social behaviour and restricted adaptive and repetitive behaviours (Belmonte et al. 2004). Patients diagnosed with ASD suffer from persistent social deficits, with communication being below expected levels of development. The restricted repetitive patterns of behaviour are variable but include stereotypical motoric movements or speech, ritualised patterns of thinking, as well as restricted fixated interests (American Psychiatric Association DSM-5 Task Force. 2013), While the epidemiology of autism differs between sources, incidence rate currently falls at approximately 2 cases per 1,000 people. ASD is four times more prevalent in males compared to females; however this may be due to the differences in the symptomology between sexes, with boys showing more typical behaviour found in

the diagnosable criteria compared to girls (Rynkiewicz & Łucka 2018). Interestingly, ASD is highly co-diagnosed in Kleefstra syndrome patients (Iwakoshi et al. 2004) and is known to be comorbid with a range of other developmental disorders and, significantly, with intellectual disability (La Malfa et al. 2004). CNV analysis of ASD probands identified *EHMT1* as a *de novo* mutation (O'Roak et al. 2011). This evidence is strengthened with a recent study where BCA (balanced chromosomal abnormalities) sequencing of 22 autism patients also identified *EHMT1* microdeletions as a risk gene in the development of ASD (Talkowski et al. 2012). Finally, exon sequencing of a group of Japanese autism patients also identified two novel rare missense *EHMT1* and G9a variants. G9a has been shown to be elevated in the blood of these ASD patients suggesting an increasingly restrictive chromatin in the pathogenesis of ASD (Balan et al. 2014). These studies link *EHMT1* to the overlapping phenotypes seen in intellectual disability disorders and autism.

1.2.3. Schizophrenia and Psychosis

Schizophrenia affects approximately 1% of the population. According to DSM-5, diagnosis of schizophrenia occurs after at least two symptoms from delusions, hallucinations, disorganised/catatonic behaviour, disorganised speech, and negative symptoms such as reduced emotional expression persist for a month or longer with a direct impact on normal functioning to the person's life such as work, and interpersonal relationships (American Psychiatric Association DSM-5 Task Force. 2013). This highly heterogeneous diagnosis is thought to share a molecular basis with various other developmental and psychiatric disorders, particularly autism spectrum disorders (McCarthy et al. 2014; Canitano & Pallagrosi 2017). A population based study showed an overlapping co-diagnosis of

schizophrenia and intellectual disability, with over 30% of patients diagnosed with intellectual disability being co-diagnosed with a psychiatric illness, of which schizophrenia was overrepresented (Morgan et al. 2008).

In a copy number variation analysis study Kirov et al. (2012) identified two *de novo EHMT1* CNVs as pathogenic variants in schizophrenia, linking *EHMT1* to the pathogenesis of the adult onset psychiatric disorder. Interestingly, diagnosis of schizophrenia was associated with increased *EHMT1* and H3K9me2 in post-mortem brain samples; increased *EHMT1* expression was also linked to worsening symptoms (Chase et al. 2013). Increased *EHMT1* and H3K9me2 marks, and thus a restrictive chromatin state, as seen in ASD, could therefore be considered a marker for schizophrenia, as well as a marker for potential prognosis. Another histone methyltransferase associated with schizophrenia, SETD1A (Takata et al. 2016), suggests an overarching role epigenetic regulators may play in the pathology of schizophrenia.

There is now growing evidence that Kleefstra syndrome patients have developed a regressive phenotype, leading to adult onset psychosis (Verhoeven et al. 2011; Vermeulen et al. 2017). Therefore either maintained reduction of *EHMT1*'s function, or an early developmental trigger due to *EHMT1* haploinsufficiency leads to psychosis in adulthood. Evidence presented here shows that both an increase and decrease in *EHMT1* and H3K9me2 appears to lead to similar phenotypes in psychosis, pointing towards *EHMT1*'s importance in maintaining the homeostasis of the epigenome, and changes in either direction would lead to impairment (Adam & Isles 2017). Whether these bidirectional changes of *EHMT1/H3K9me2* on developmental disorders are however a

secondary effect of a primary dysfunction is unknown; future studies assessing the causality of *EHMT1* on NDD pathology is necessary.

1.2.4. Evidence of H3K9me2 in Neurodegeneration

H3K9me2, a marker of heterochromatin, initiated by G9a and EHMT1, has been associated with neurodegeneration in human and animal models. H3K9 methylation is found to increase with age, and is linked to cognitive decline. For instance, H3K9 methylation was found to be increased in 3xTg-AD mouse model of Alzheimer's (Walker et al. 2013). Conversely in post-mortem brains of Alzheimer disease patients H3K9me2 was shown to be reduced, this was complimented by reduced H3K9me2 in Tau neurodegenerative *Drosophila* and mouse models, where there is evidence of global loss of heterochromatin (Frost et al. 2014).

α-Synuclein, a protein associated with Parkinson's disease and other neurodegenerative disorders, was found to increase the levels of H3K9me2, and overexpression of the protein would lead to an increasingly restrictive chromatin in Parkinson's disease (Sugeno et al. 2016). H3K9me2 has also been associated with Huntington's, where the marker is shown to be in the striatum of HD patients (Ryu et al. 2006). The growing evidence of H3K9me2 in the pathogenesis of neurodegenerative disorders is of notable interest due to the previously mentioned regressive phenotype in Kleefstra syndrome patients, with patients showing increased severity in behavioural and motor deficiencies, developing apathy, and also showing signs of subcortical abnormalities (Verhoeven et al. 2011) suggesting a neurodegenerative course in Kleefstra syndrome prognosis. Currently, the amount of evidence on the degenerative nature of Kleefstra

syndrome is minimal however, whether classical molecular markers of degeneration appear in ageing Kleefstra patients is yet to be determined.

1.3. *Ehmt1* in learning and memory

A notable feature shared amongst these disorders is the disruption in cognitive and executive functioning. *Ehmt1* is highly involved in the process of learning and memory. H3K9me2 post translational mark is dynamically regulated in hippocampus, entorhinal cortex, and amygdala of the rat during contextual fear learning, with differing patterns methylation when comparing different brain regions, entorhinal cortex and CA1 hippocampus, as well as temporally dynamic changes after training (Gupta et al. 2010; Gupta-Agarwal et al. 2012a; Gupta-Agarwal et al. 2014). However it is important to note that while contextual fear learning is learning task, due to it being subject to negative/aversive stimuli, whether it accurately represents other forms of learning is arguable. The mice may be sensitized differently to negative versus positive stimuli. Positive and negative memories and associated behaviour also have divergent circuitry involved (Namburi et al. 2015).

At the synapse, blocking *Ehmt1*/*G9a* function during early LTP leads to increases in BDNF expression and reinforcement of LTP. Reduction of *Ehmt1* also leads to reduced mature spine density and miniature excitatory postsynaptic currents in pyramidal cells. Evidence shows that *Ehmt1* is important for the *Grin2b*-*Grin2a* switch, required for learning and memory (Yashiro & Philpot 2008; Gupta-Agarwal et al. 2014) and is possibly involved in the repression of *Grin2b* during development (Gray et al. 2011). These convergent data point towards an

important role of *Ehmt1* both during early embryonic development and continually postnatally, for normal cognitive abilities.

1.4. Mouse models of Neurodevelopmental Disorders

In this thesis, a mouse model of *Ehmt1* haploinsufficiency is utilised. Mouse models have long been used as a tool for understanding the pathology of neurodevelopmental disorders. Some of these mouse models have identified relevant behavioural and molecular phenotypes with high translational value (Kazdoba et al. 2016). However there is growing evidence that studies classifying neurodevelopmental and psychiatric disorders in rodent models are difficult to translate to the human disorder and often overlapping across a number of other diagnoses (van der Staay et al. 2009; Jucker 2010; Silverman et al. 2010; Crawley 2012; Salgado & Sandner 2013; Kazdoba et al. 2016). For example, impairments in social behaviour, a key symptom of a number of NDDs, are presented differently in rodents compared to humans and hold different biological interpretations. Thus careful and rigorous interpretation of mouse model phenotypes is important to inform human disorder. Another important aspect is most neurodevelopmental disorders are not monogenic in their pathology, whereas most mouse models define singular gene dysfunctions. Therefore the over-interpretation of the singular candidate genes to human disorder in animal models has led to translational failure in pre-clinical and clinical studies. External validation of rodent models is an important process in evaluating their translational value; multiple rodent lines tested by multiple labs is an often used method for validation. Here, a novel *Ehmt1* haploinsufficiency model using the same floxed *Ehmt1* mice used in other labs that have generated *Ehmt1* haploinsufficient mice. Comparison of findings here to

previous literature will aid in the characterisation of the mouse model and the gene's role in neurodevelopmental disorders.

1.5. Thesis Rationale

Ehmt1 is a key regulator in neurodevelopment and thus associated widely in neurodevelopmental disorders (Kirov et al. 2012; O'Roak et al. 2012; Balan et al. 2014). These disorders are widely regarded to share a molecular pathogenesis and have high percentages of comorbidity (Matson & Shoemaker 2009; Canitano & Pallagrosi 2017). *Ehmt1's* highly dynamic and spatiotemporal function could therefore help expand current knowledge on the pathways vulnerable to dysfunction in neurodevelopmental disorders. *EHMT1* is known to have a wide pleiotropic effect on development from early autistic phenotypes to a more regressive phenotype and development of psychosis in the adult, as seen in Kleefstra patients (Kleefstra et al. 2006; Verhoeven et al. 2011). The disruption of normal *EHMT1* function from a very early embryonic time point may very likely lead to a more degenerative phenotype, with various neurodegenerative disorders showing a pathogenesis linked to continued imbalance in H3K9me2 markers (Ryu et al. 2006; Sugeno et al. 2016; Sharma et al. 2017).

Determining the role of epigenetics as a whole on the pathogenesis of neurodevelopmental disorders, with *Ehmt1* as an example, will lead to a better understanding of their pathogenesis that will likely help inform the involvement of other non-epigenetic genes to lead away from narrow pathogenic tracks such as 'synaptopathies' to a more elaborate framework of developmental genes and environment. The understanding of this interplay is of high importance for novel

and improved treatments of neurodevelopmental disorders, by either the direct targeting of epigenetic regulators or through targeting any upstream and/or downstream mechanisms identified.

In order to understand *Ehmt1* in cognition and executive functioning, a forebrain specific mouse model is utilised. In Chapter 2, the *Ehmt1* forebrain haploinsufficiency model is described and compared to other mouse models of *Ehmt1* haploinsufficiency. Basic assessment of the gross anatomical measures is described before assessing key motoric, anxiety and spontaneous behaviours.

In Chapter 3, the mouse model was assessed for cognitive impairment. Here the haploinsufficient mouse model and their WT counterparts underwent two memory tasks, an object and a location based memory task, in order to gain a better understanding of the role of *Ehmt1* in the development and maintenance of different memory types.

In Chapter 4, adult neurogenesis and its influence on behaviour and memory is described. The mouse model is assessed for both short term proliferation and long term neurogenesis *in vivo* to evaluate *Ehmt1* role in hippocampal function.

The *in vivo* findings were expanded *in vitro* in Chapter 5*;* hippocampal primary cell cultures from the *Ehmt1* forebrain haploinsufficient mice were cultured and assessed for *in vitro* proliferation rates, cell type ratios, and cell apoptosis ratios. These experiments further expand on the role of *Ehmt1* on cell survival and cell type specificity in the hippocampus, and in turn open potential areas of further research to understand their connection to the cognitive and executive functions impaired in neurodevelopmental disorders.

In Chapter 6, the large number of publically available data on *Ehmt1* reduction was mined to assess whether the knocking down of the protein lead to changes in genes specifically attributed to disorders. Here, Benevento et al. (2016) data on *Ehmt1* deficient cells both incubated with TTX, initiating synaptic upscaling, and at baseline were mined for enrichment in phenotypes and for genes associated with intellectual disability, autism, and schizophrenia. This allows for the identification of potential translational genes and pathways of interest.

1.5.1. Aims

- Assess the behavioural phenotype of the *Ehmt1*$^{D6cre/+}$ mouse model
- Evaluate *in vivo* adult neurogenesis in *Ehmt1*$^{D6cre/+}$ hippocampus
- Assess the *in vitro* phenotype of hippocampal cells from the *Ehmt1*$^{D6cre/+}$ mouse model
- Mine publically available data for functional relevant biological points of interest for future research.

Chapter 2 Basic Tissue Analysis and Characterisation of Spontaneous Behaviours in *Ehmt1*$^{D6cre/+}$

2.1. Introduction

The *Ehmt1* gene is highly conserved throughout evolution, with the mouse and human orthologs sharing 97% homology in their sequence (Shinkai & Tachibana 2011). Alongside its related protein *G9a*/*Ehmt2*, *Ehmt1* catalyses the mono- and di- methylation of lysine 9 on histone 3 of the nucleosome (H3K9me/2). H3K9me2 is a widely recognised marker for epigenetic repression, and is involved in transcriptional silencing (Tachibana et al. 2005). *Ehmt1* is expressed throughout life, with peak expression occurring during embryonic development with a decrease through early postnatal development. The human *EHMT1*, as previously mentioned, has been linked to a variety of neurodevelopmental disorders including schizophrenia and autism which have known overlapping behavioural profiles in humans (Cooper et al. 2011; Kirov et al. 2012; O'Roak et al. 2012).

Indeed, deletions or mutations in one copy of *EHMT1,* leading to haploinsufficiency of the protein, is most recognisably linked to the intellectual disability syndrome, Kleefstra syndrome (KS, Kleefstra et al. 2005) Autistic-like features are prevalent in patients with Kleefstra syndrome (Kleefstra et al. 2005). With *Ehmt1* being identified as a risk gene across these various diagnostic categories which share commonalities in adaptive behaviour and cognitive function, there is growing interest in understanding the role of *Ehmt1* in executive functions, with the use of animal models (Schaefer et al. 2009; Kramer et al. 2011;

Balemans et al. 2013). These studies have included manipulating *Ehmt1* in *Drosophila* and mice.

Haploinsufficiency of EHMT in *Drosophila* has led to changes in social behaviour in the flies, as well as changes in the locomotor behaviour as larvae (Kramer et al. 2011). Although it should be noted that *Drosophila*, which have a single orthologous EHMT gene, compared to the two seen in mice and humans, appears to have the combined function of both *Ehmt1* and *Ehmt2* (Kramer et al., 2011). Moreover this gene has a continued high expression into adulthood, unlike *Ehmt1* in rodents and humans (Balemans et al., 2012).

Various mouse models have been utilised to determine the behavioural impact of *Ehmt1* deficiency on behaviour and cognition. Mouse models have been assessed in using specialised behavioural paradigms to elucidate the roles of genes of interest on the phenotype of psychiatric disorders (Davis & Isles 2014). With the changing focus of the neuropsychiatric field away from diagnostic boundaries and towards a more holistic approach of clinically relevant symptoms, looking at common endophenotypes, quantitative and measurable biological markers correlated to disease, in the human disorders in complimentary rodent paradigms have proved to be a reliable method for deciphering components and pathways that may be altered across the different disease pathologies and diagnostic restrictions. It should be mentioned that endophenotypes, although closer to biology, are not necessary sufficient to aid the discovery of new genes in NDDs and psychiatric disorders. Endophenotype analysis using the Minnesota twin study found over 89% of genetic search strategies across 17 endophenotypes resulted in nulls results, with 8 endophenotypes analysed providing no associated

genes across all search strategies employed (Iacono et al. 2014). Endophenotypes are not specific to any one disorder due to the similarities across NDDs; a possible solution is to further breakdown disorders into more specific and unique attributes for a greater chance of gene discovery.

While homozygous depletion of *Ehmt1* is embryonically lethal in mice the *Ehmt1*$^{+/-}$ mouse model, similar to the genetic pattern seen in Kleefstra syndrome patients, has been successfully utilised in KS syndrome modelling (Balemans et al. 2010; Balemans et al. 2013). *Ehmt1* haploinsufficient mice showed changes in their locomotor activity, as well as reduction in their exploratory behaviour. This was also coupled with an increase in their anxiety in the open field and various other test paradigms, which both test the innate conflict between exploration and risk (Balemans et al. 2010). These changes, along with social behavioural changes seen in the mice (Balemans et al. 2010), point towards a link in *Ehmt1* function and the autistic-like features seen in the various neurodevelopmental disorders in which the gene has been linked. However there are limitations with this KS mouse model, where *Ehmt1* is knocked down in the entire organism with confounding factors, such as hypotonia, delayed motoric function, cranial abnormalities, and increased weight gain (Balemans et al. 2013). In order to bypass these issues, use of *CamK2a*-cre recombination led to targeted reduction of *Ehmt1* and haploinsufficiency in postnatal forebrain neurons only (Schaefer et al. 2009). Thus, there were no differences in *Ehmt1* expression prenatally. This mouse model had normal motoric function as seen on a standardised accelerating rotarod test. However in contrast to the *Ehmt1*$^{+/-}$ mouse model, *Ehmt1*$^{Camk2a\text{-}cre}$ mice had reduced anxiety compared to their wildtype littermates in the elevated plus maze task. These contradicting anxiety phenotypes in the different mouse models could

elucidate the pathway specific involvement of *Ehmt1* in the development of anxiety phenotypes.

Despite these steps taken to overcome the confounding aspects of a full heterozygous knockout, having a postnatal specific knockout does not allow for the exploration of *Ehmt1* function during development. As mentioned, *Ehmt1* is highly expressed from E12 and its expression is reduced by E18.5 and postnatally. Therefore this model may also restrict examination of its role at the point where its expression and thus function is greatly diminished. Thus the development of the *Ehmt1*$^{D6cre/+}$ mouse model, allowing for early restricted forebrain specific depletion of *Ehmt1* overcomes these barriers for behavioural analysis. In the *Ehmt1*$^{D6cre/+}$ mice, exon 23 of *Ehmt1* allele is deleted, leading to the nonsense mediated deletion of the transcript. This deletion affects SET domain of the gene. However it does not affect a number of smaller protein coding transcripts of unknown function (Figure 2.1).

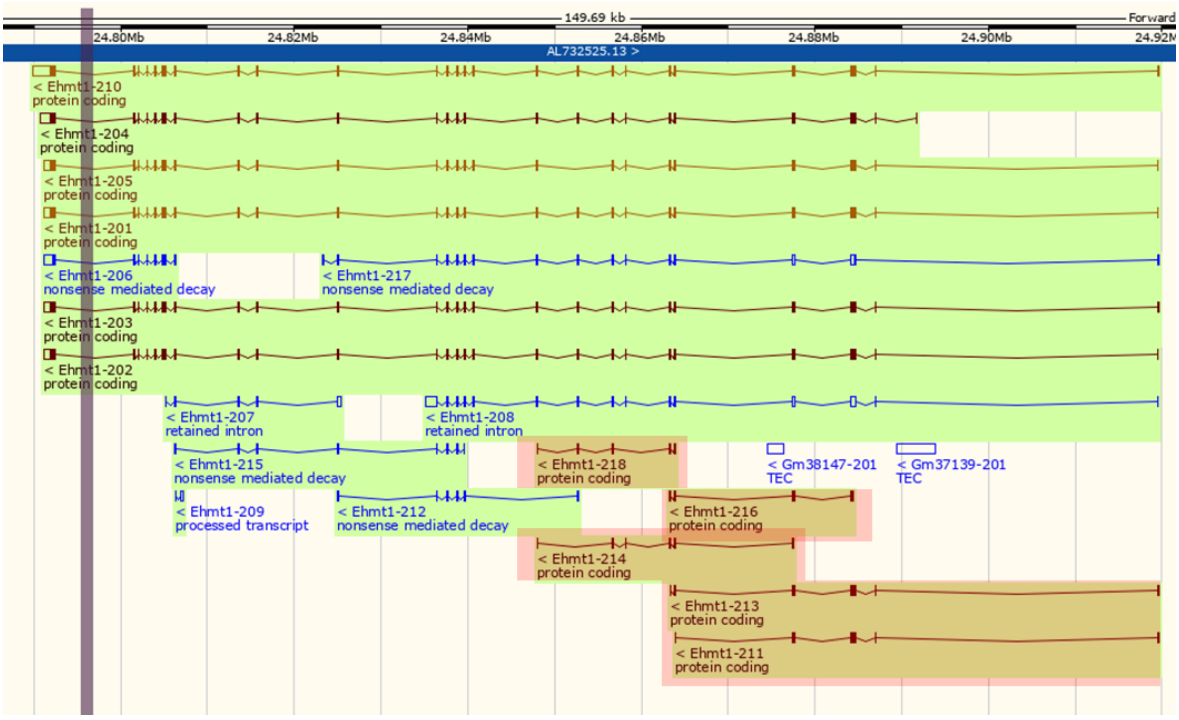

Figure 2.1 Mouse *Ehmt1* transcripts. Graph of *Ehmt1* transcripts identified. Grey line bar marks position of exon 23 where deletion occurs. Highlighted are 5 short protein coding transcripts not affected by the deletion of exon 23. Adapted from Ensembl.

In this chapter, the mouse model underwent basic characterisation. Behavioural paradigms were used to characterise spontaneous behaviours in the *Ehmt1*$^{D6cre/+}$ mouse model viewed as representative of the overarching behavioural phenotypes mutually disrupted in the developmental disorders associated with *Ehmt1* disruption. These behaviours include sensorimotor gating, and anxiety based phenotypes, as shown in previous rodent studies, are generally considered hippocampal and forebrain dependent and therefore compatible with Kleefstra syndrome phenotypes whilst being restrictive enough to aid in deciphering the biological impact of haploinsufficiency of *Ehmt1*.

2.1.1. Behavioural phenotypes of neuro-developmental disorders

There are a number of behavioural phenotypes that are considered common across neurodevelopmental and neuropsychiatric disorders. These behaviours are often analysed in animal models associated with the various disorders to

determine the different convergent genetic changes that account for commonly affected clinical areas across diagnostic categories of disorders. Here, the focus will be on a number of key basic and spontaneous behaviours that will be analysed in this chapter.

2.1.1.1. Anxiety

Anxiety is a common phenotype observed in neurodevelopmental disorders. Anxiety also plays a confounding role in assessing the behavioural phenotypes of mouse models, due to the exploratory nature of most behavioural tasks. Previous *Ehmt1* deficient mouse models showed contradicting anxiety behaviours. This is likely due to anxiety encompassing a variety of emotionality, and thus several paradigms have been designed in the past years that measure anxiety in several different forms (for review: Bućan & Abel 2002; Powell & Miyakawa 2006; Bourin et al. 2007). One such paradigm is the elevated plus maze. This paradigm allows a measure of the animal's natural tendency towards exploration against their natural aversion for open spaces and heights (Pellow et al., 1985). It has been established that "normal" behaving mice spend more time in the closed arms compared to the open arms, reflecting this conflict. If the rodents are recorded to have more entries or spend a longer duration in the open arms compared to the closed arms, it is suggestive of a reduced anxiety-like behaviour. If the rodents spend less time/ have decreased number of entries to the open arms compared to the closed arms during the test, it is suggestive of increased anxiety. This task has been validated across a number of studies, where clinically effective anxiolytics lead to significant increases in the time spent and number of entries into the open arms (Pellow et al. 1985; Anseloni et al. 1995; Walf & Frye 2007).

Hyponeophagia, or food neophobia, is generally characterised as another measure of anxiety, as well as anhedonia. Hyponeophagia refers to the restricted intake of novel foodstuff when in an unfamiliar context (Hall, 1934). This is a measure of the conflict between the animals need or choice to feed and aversion for novelty/potential poisonous consumption. Hyponeophagia paradigms have been shown as a valid measure of anxiety, where methods of manipulation in humans to either increase or decrease anxiety have been found to have similar effects with hyponeophagia in mice, including administration of anxiolytics (Bodnoff et al. 1988; Bodnoff et al. 1989), and hippocampal lesions (Aggleton et al. 1989). The mice are placed singly in empty cages, the novel environment, and are presented with access to a novel highly palatable foodstuff, such as condensed milk, as well as water. The amount consumed for both is measured and the animals are returned to their home cage. To motivate drinking, the animals are water deprived before the test. Due to their innate food neophobia, normal behaving animals consume more water than condensed milk. During successive trials, repeated sampling of the condensed milk overcomes the initial hyponeophobia and eventually leads to a preference for this more palatable foodstuff. *Ehmt1*$^{Camk2a\text{-}cre}$ mice showed a reduced preference and motivation for reward consumption when tested with sucrose water, thus suggesting *Ehmt1* plays a role in the motivation and reward circuitry. The amount consumed and the rate in which consumption increases session to session are used as indices of anxiety.

2.1.1.2. Sensorimotor gating

A relevant behavioural endophenotype for neurodevelopmental disorders is sensorimotor gating. Sensorimotor gating is the ability to filter auditory input in

order to control motor response (Powell et al. 2011). This is measurably deficient in neuropsychiatric patients, including those with schizophrenia, adults with autism, panic disorders, and Fragile X syndrome (Belmonte et al. 2004; Powell & Miyakawa 2006; Powell et al. 2011). This can be operationally measured by assessing the acoustic startle response (ASR) and prepulse inhibition of ASR (PPI). This has been proven to be a robust measure that is translational across species, and has been used in various genetic studies of schizophrenia, helping understand the impact of genes on behaviour (Powell & Miyakawa, 2006). This operational measure of abnormalities in sensorimotor gating has been shown to be a relevant measure for a fundamental component in executive processing.

ASR will be measured as the habituation to a repeated loud acoustic stimulus, and the PPI as the reactivity to a loud acoustic stimulus that is preceded immediately prior by a weaker pulse, or prepulse. This prepulse allows for the attenuation of the reactivity to the loud stimulus, and it is this measure that is determines sensorimotor gating (Powell et al., 2012). This measure is viewed as a robust measure of important drivers of executive functions, in which disorders with attention deficient phenotypes often lack. The ability to attenuate ones reactivity is viewed as regulated by multiple brain regions, including striatal, limbic and cortical regions, such as the medial prefrontal cortex and hippocampus (Swerdlow et al. 2001) where *Ehmt1* is expected to be deleted. Thus deficits in acoustic startle response and prepulse inhibition can inform the neural processes that *Ehmt1* may be involved.

2.1.1.3. Locomotor Activity

Locomotor activity, a behavioural measure of both the motoric function and spontaneous activity level in rodents has been shown to be a reliable measure, and can indicate both hyper- or hypo-activity. Hyperactivity, also known as psycho-motor agitation in clinical literature refers to the increased activity and stereotypic movements seen in schizophrenia as well as other neuropsychiatric disorders (Powell & Miyakawa 2006). This behavioural endophenotype has been recapitulated in various “schizophrenia” mouse models, including *NR1* K/O mice (Mohn et al. 1999), and dopamine transporter K/O mice (Gainetdinov et al. 1999), and thus LMA can be used to measure both baseline hyperactivity and or hyperactivity linked to novel environments and habituation to these novel environments. Psychomotor agitation can also be recapitulated in humans who use psychotomimetic drugs, such as ketamine and amphetamines (Tamminga et al. 2003), which have been shown to both mimic psychotic symptoms and cause psychosis in itself. This has led to the use of LMA as a pharmacological behavioural paradigm; this drug related hyperactivity can be attenuated with the use of antipsychotic drugs.

Previous mouse models showed reduced *Ehmt1* to subsequently lead to reduced motoric function and activity in the mice (Balemans et al. 2010), this reduced activity levels have been seen in the mice alongside various other phenotypes including hypotonia, increased weight gain, and delayed motoric development (Balemans et al. 2013). These confounding factors should not have an impact in this forebrain specific mouse model, and thus testing locomotor activity as a measure of general motoric function and activity levels of the

Ehmt1$^{D6cre/+}$ mice, as well their reactivity to a novel environment, can accurately determine if *Ehmt1* haploinsufficiency has a role in the common psychomotor agitation endophenotype found in neurodevelopmental and neuropsychiatric disorders.

2.1.2. Aims

- Confirming specificity of *Ehmt1*$^{D6cre/+}$ through region genotyping and gross brain morphology
- Characterise the basic spontaneous and anxiety behaviour of the *Ehmt1*$^{D6cre/+}$ mouse.

2.2. Methodology

2.2.1. Animals

Ehmt1$^{fl/fl}$ mice were bred from male mice on a C57BL/6 background from Dr. Alexander Tarakhovsky (Rockfeller University, NY). B6CBAF1/Tg (*Dach1-cre*) 1Krs/Kctt transgene on a (C57BL/6 x CBA)F1, *D6*-Cre, mice were transferred from Dr. Ondrej Machon (Karolinska Institute). Experimental animals were generated through breeding *Ehmt1*$^{fl/fl}$ mice with *D6-cre* heterozygous mice. Both mice were backcrossed into C57BL/6J backgrounds for over 10 generations. Breeding cohorts were intermittently rejuvenated by introduction of new C57BL/6 mice to reduce genetic drift. Behavioural cohort litters were balanced for Parent-of-Origin effects by mixing between male and female *flp* and *cre* carriers. Litters were housed together in groups of 3-5 animals per cage. Mice were not singly housed for behaviour to avoid any detrimental effects of singular housing. Male mice housed together formed natural hierarchies and thus were free to perform natural behaviour; studies have argued for the positive welfare value of group housing including reduced anxiety and the natural preference for conspecifics (Baumans & Van Loo 2013; Kappel et al. 2017). All animals were housed under standard 12hr light – dark cycles, in temperature and humidity controlled environments. All experiments were carried out in agreement with the Animals Scientific Procedures Act 1986, under license from the United Kingdom Home Office and approved by the local animal welfare and ethics review body (Cardiff University).The *Ehmt1*$^{fl/fl}$ mouse line was crossed with a *D6-cre* mouse line leading to forebrain specific deletion mouse model (***Ehmt1***$^{\mathbf{D6cre/+}}$). ***Ehmt1***$^{\mathbf{fl/+}}$ littermates were used as WT controls.

The behavioural cohort: 20 *Ehmt1*$^{flp/+}$, 17 *Ehmt1*$^{D6cre/+}$ - all male (Table 2.1). Only male mice were used during behavioural tasks due to the potential confounding effects of oestrous cycle on female behaviour. Initial behavioural tests were conducted starting at 10 weeks, as the mice were considered mature tasks that were repeated were repeated at 10 months old, coinciding with the mice entering middle age, approximately coinciding with humans 35-50 years old. Tissue cohort: 51 *Ehmt1*$^{flp/+}$, 48 *Ehmt1*$^{D6cre/+}$. Mice were culled through cervical dislocation and brains collected at 8 weeks old, coinciding with the mice reaching mature adulthood.

Table 2.1 Number of animals and age at start of experiment for each behavioural paradigm

Behavioural Paradigm	Ehmt1$^{fl/+}$	Ehmt1$^{D6cre/+}$	Behavioural paradigm
Elevated plus maze	20	17	12 weeks
Novel food preference	20	17	7 months
Acoustic startle response and Prepulse inhibition	20	17	10 weeks /10 months
Locomotor Activity	20	17	10 weeks /10 months

2.2.2. Genotyping

Mice were weaned at approximately postnatal day 24, and a 2mm diameter ear perforation was taken for identification and genotyping. For cre-specificity genotyping, mice were culled at 8 weeks old, and their brains were isolated. The brains were then dissected to isolate the cerebellum, prefrontal cortex, and hippocampus of each mouse. The tissue samples were then digested overnight in 100µl of lysis buffer (0.1 M Tris.HCl pH 8.5, 0.005 M EDTA pH8.0, 0.02% SDS, 0.2 M NaCl, 100 µg/ml Proteinase K) at 55°C. Samples were then vortexed briefly and centrifuged for 10 minutes at 13000 rpm in order to pellet cellular debris. The

supernatant was then transferred into a new Eppendorf tube and an equal volume of cold isopropanol was added to precipitate DNA. The tube was inverted to ensure thorough precipitation. The tubes were then incubated at 4°C for 20 minutes, before being vortexed briefly and centrifuged for 10 minutes at 13000 rpm to pellet DNA. The supernatant was removed and the pellet washed briefly in 1x volume of cold 70% ethanol. The tubes were vortexed and then recentifuged at 13000 rpm for 2 minutes, at which point the supernatant was removed and the pellet was left to air dry at 50°C for 20 minutes. The DNA pellet was suspended in 80µl TE buffer (10mM Tris pH8.0, 1mM EDTA pH8.0).

2.2.3. PCR Amplification

For the *Ehmt1* FLP/FLP PCR reaction 1ul of sample was used for 19ul of the PCR mix (2µl PCR buffer, 0.4µl Primer mix (Ratio of F:R1:R2 50:50:50) 0.4µl dNTPs, 0.2ul Hotstar Taq, and 16µl H_20). Floxed allele is seen at 146-bp, and the wild type allele band is visualised at 95-bp for heterozygous animals.

Amplification of target sequences was carried out the following conditions:

1. **94°C 3 minutes**
2. **94°C 20secs**
3. **60°C 20secs**
4. **72°C 30secs**
   ~ repeat steps 2-4 for 29 cycles ~
5. **72°C 10 minutes**

PCR reaction for the deleted band was optimised and ran concurrently with the previously described *Ehmt1* PCR reaction. Deleted allele band would be visible at 296-bp.

For the PCR reaction to genotype D6-Cre 1 µl of samples was used for 28ul of

PCR mix (3ul PCR buffer, 0.5 µl F primer, 0.5ul R primer, 0.5ul dNTPs, 0.2ul Hotstar Taq, 23.3µl H_20). Amplification of Cre target sequence was done under these conditions:

1. **95 ˚C 6 minutes**
2. **94 ˚C 45secs**
3. **58 ˚C 45 secs**
4. **72 ˚C 1 minute**

   ~ repeat steps 2-4 for 35 cycles ~
5. **72 ˚C 10 minutes.**

The cre band was visualised at 293 bp.

Table 2.2 PCR Primer sequences for genotyping

PCR PRIMERS	Primer sequences
5' forward primer (Glp-F)	5' – ctc agt cat tta cta aag gtg c- 3'
5' reverse primer 1 (Glp-R1)	5' – ccc gtg tat ttg cag tgc aag- 3'
5' reverse primer 2 (Glp-R2)	5' – tgc ctg gca cag aag cca tag- 3'
5' forward primer (Cre52)	5´ gtc caa ttt act gac cgt aca cc 3´
3' reverse primer (Cre32)	5´ tga agc atg ttt agc tgg cc 3´

2.2.4. Elevated Plus Maze

To examine the innate conflict between exploration and open space of the *Ehmt1*$^{D6cre/+}$ and *Ehmt1*$^{flp/+}$ mice, the mice were tested on the elevated plus maze. The apparatus includes a “plus” shaped maze on an elevated platform and made from white Perspex. Two of the four arms on the maze are “closed”, covered in all sides with 15cm high walls; two of the four arms are “open” measuring 17.5 by 7.8 cm, with no protective walls on any side. The animal is placed within the closed portion of the maze and is recorded throughout the duration of the test. Entries into

closed and open arms are recorded, as well as time spent within the arms. The maze was elevated 300mm off the ground and was evenly illuminated at 15 lux (Figure 2.2)

The mice were placed on one of the closed arms of the maze facing the centre of the maze and were allowed to explore the maze freely for 5 minutes. Optimised analysis was ran using the EthoVision Observer XT software, and the maze divided into 5 zones; 2 open arms, 2 closed arms, and the centre section of the maze. Mice were tracked with three module points by the software, front of the body, middle of the body, and end of the body. Entrances and exits were counted if the leading and middle module points entered/left any one region. Manual analysis of pilot sessions confirmed the accuracy of the tracking software, and all traces were examined for tracking-related artefacts prior to analysis.

Data from both closed arms and open arms were combined to generate total open or closed arm data to ascertain: latency to first enter, total time spent, and frequency of entries. Behavioural data including grooming, and risk assessing behaviour such as stretch-attend (the subject stretching forwards into an open arm while remaining in the closed arena) and head-dips (the subject positioning head downward over the edge of the open arm) were manually collected. These were not counted as entrances by the software as only the leading module point entered any open arm during these actions. The maze was cleaned between each subject using 2% acetic acid.

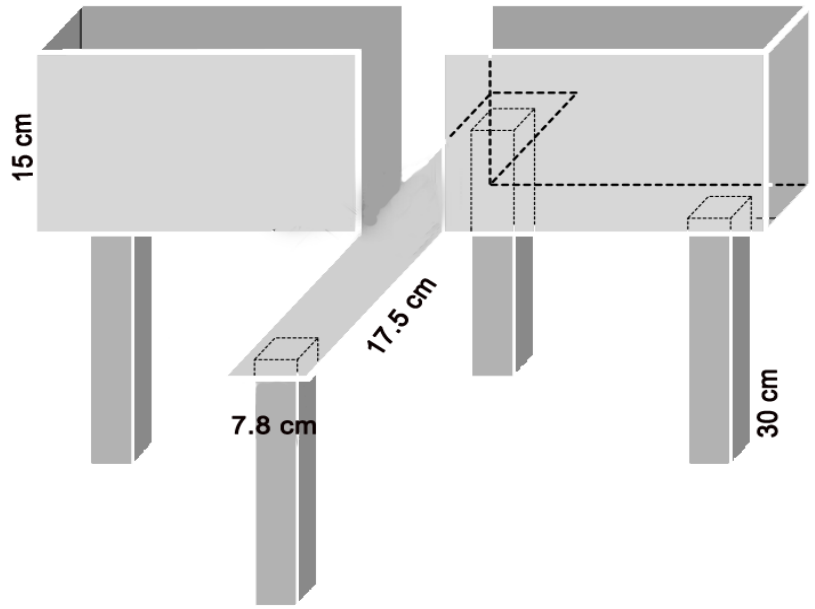

Figure 2.2 Elevated plus maze Apparatus with dimensions.

2.2.5. Food Neophobia

Reactivity to novel food was examined in mice following a period of adjustment to a water restriction schedule. The animals were assessed for a period of ten minutes for 11 consecutive days immediately before gaining two hour water access to maximise motivation to drink. The novel foodstuff presented was a 10% condensed milk solution. All testing was carried out in novel cage and the animals were presented with two containers. The containers were filled with either water or the condensed milk solution and were weighed before they are placed into the cages (Figure 2.3).

For the first two days, the mice were only presented water. Their consumption levels were measured by re-weighing the containers after the 10 minute session. Between the third and tenth day the mice were presented with an option of either water, or the condensed milk solution (novel). The position of the containers was counterbalanced at each session to avoid any spatial memory

preference. The consumption was again measured by weighing the containers before and after the session. On the final day of testing, the mice were presented only the milk solution.

Consumption data was normalised using Kleiber's 0.75 mass exponents. Percentage preference of novel foodstuff was calculated as a percentage of total consumption during the eight days where mice were presented with both liquids.

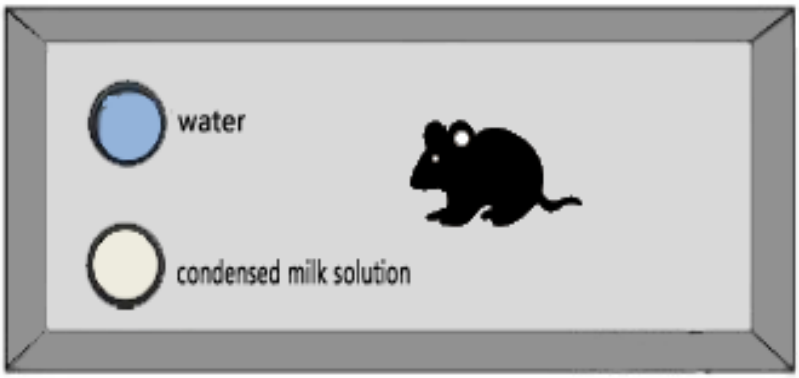

Figure 2.3 Hyponeophagia apparatus. Position of water and condensed milk was counterbalanced across genotype and sessions.

2.2.6. Acoustic startle response (ASR) and Prepulse Inhibition (PPI)

In order to measure any changes to the sensorimotor circuitry and gating, mice were tested for acoustic startle and prepulse inhibition. PPI and ASR was measured using SR Lab (San Diego Instruments, US). The mice were placed in Perspex tubes in a sound attenuated chamber that is both lluminated and ventilated by a fan (Figure 2.4).The tubes were cleaned after each animal using 2% acetic acid and aired out before the next test. ASR was measured through voltage measurement of movement by a piezoelectric sensor linked to a computer. To avoid confounding factors, all animals were tested for hearing ability from on an

80dB above background to 150dB above background, there were no genotype differences and no animals used showed hearing impairment.

Startle pulses analysed were at 120dB, with prepulse trials for both consisting of 4, 8, and 16 dB above background pulses. The thirty minute sessions recorded a series of 91 trials, starting with a 5minute habituation period of white noise (70dB), to acclimatise the mice to the chamber. The startle response is average startle amplitude, measured in mV, collected during a 65ms window from the onset of the startle.

Six pulse-alone trials were presented and this is analysed for startle habituation. This block is followed by a block of trials including two of each prepulse from which prepulse inhibition can be measured. During this session, no stimulus trials were also presented. This allowed for the data to be normalised for movement not associated with the presence of a stimulus. Pulse alone trials consisted of a 40ms stimulus, whereas prepulse stimuli lasted 20ms. Sporadic measurement of no stimulus was taken as a control for normal movement.

Percentage Prepulse Inhibition (PPI) is measured as a percentage difference in the amount of startle of the prepulse trials compared to eh pulse alone trials.

PPI score for each trial was calculated:

$$\%PPI = 100 \times \frac{(ASR_{startle\ pulse\ alone} - ASR_{prepulse + startle\ pulse})}{ASR_{startle\ pulse\ alone}}$$

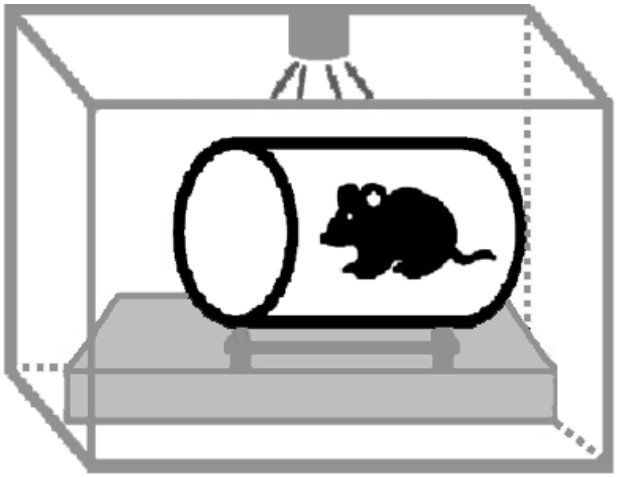

Figure 2.4 Acoustic startle response and prepulse inhibition apparatus. Mice were presented with 120dB pulses and their reactivity to the pulses was measured. Pre-pulse amplitudes of 4, 8, and 16 dB above background were pseudorandomly interjected to measure their prepulse inhibition.

Measurements were adjusted for weight using Kleiber's 0.75 mass exponents (Schmidt-Nielson, 1990).

2.2.7. Locomotor Activity

Spontaneous locomotor activity was measured in a group of 12 clear Perspex chambers. The mice we placed into chambers for 2 hours, their movement's tracked using two equipped transverse infrared beams spaced equally along the length of the chamber (Figure 2.5). Using a computer running a custom programme on ARACHNID, Each beam break, indicative of short range movement, is recorded in a series of five minute blocks across the two hour session for a total of 24 blocks. Runs were measured as both the front and rear beams being broken in succession during the time period.

Chambers were cleaned with 2% acetic acid between mice. The animals were tested in the dark for three consecutive days during their early light cycle, between 8:00-12:00, allowing for measurements in both gross locomotor characterisation and reactivity to novelty. Prior to the LMA task, all animals were

tested for their motor coordination as a potential confounding factor, with no genotype differences emerging.

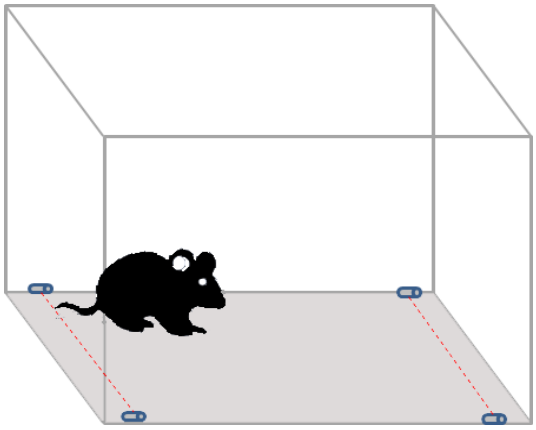

Figure 2.5 Locomotor activity apparatus. Two transverse infrared beams spaced equally along the length of the chamber record movement of the mouse in the chamber.

2.2.8. Statistics

All data were analysed using SPSS 25 (SPSS, USA). Brain and body weight differences was analysed using two-way ANOVA examining the effects of SEX and GENOTYPE. Most behavioural data were analysed using ANOVA repeated measures to examine the effect of genotype on performance, with main between subject factors being GENOTYPE (*Ehmt1*$^{D6cre/+}$ or *Ehmt1*$^{flp/+}$). ***Elevated Plus maze*** Analysis of elevated plus maze, and where appropriate, student t-test was used. The following within-subject factors were also analysed: ***Food Neophobia*** Session (day of testing). ***Locomotor activity*** Session (day of testing); AGE (10 weeks, 10 months). ***Acoustic Startle Response and PPI*** PRESENTATION (startle trial); PREPULSE INTENSITY (PPI intensity 4, 8, or 16 dB) AGE (10 weeks, 10 months) . All data was tested for normality. Mauchly's test of sphericity of the covariance matrix was applied to repeated measures ANOVAs due to their high susceptibility to violating sphericity and therefore leads to an increase in Type

I error rates. Where the sphericity was violated, Huynh–Feldt corrections to the F-ratio were applied as necessary, and adjusted degrees of freedom are provided. The behavioural data was corrected for multiple comparisons across the number of behavioural measures analysed across the tests using Benjamini-Hochberg FDR with a q-value of 0.05, and adjusted p-values are presented in text.

2.3. Results

This chapter aims to characterise the basic behavioural phenotype of *Ehmt1*$^{D6cre/+}$, an *Ehmt1* haploinsufficient mouse model. First, verification of the function and specificity of the D6 driven cre-lox recombination and deletion was completed. Brain and body weights were taken from *Ehmt1*$^{D6cre/+}$ and *Ehmt1*$^{flp/+}$ mice to assess whether *Ehmt1* D6-cre haploinsufficiency leads to possible confounding effects for exploratory driven behaviours. Finally, the basic and anxiety behavioural phenotype of *Ehmt1*$^{D6cre/+}$ was assessed.

2.3.1. *D6*-Cre recombination lead to forebrain specific deletion of *Ehmt1* allele

Conditional forebrain ablation of *Ehmt1* at E10.5 was achieved by breeding *Ehmt1*$^{flp/flp}$ mice to *D6*-Cre mice. This leads to the deletion of exon 23 in *Ehmt1* allele on E.10.5, leading to the haploinsufficiency of *Ehmt1* in the developing neocortex and hippocampus. Expression of *D6*-cre remains restricted in the adult forebrain and hippocampus (van den Bout et al. 2002). Verification of cre-specificity was assessed using isolated prefrontal cortices, hippocampi and cerebellums from *Ehmt1*$^{D6cre/+}$ and *Ehmt1*$^{flp/+}$ mice and the presence of the deleted allele was visualised using PCR and gel electrophoresis. The presence of the deleted allele was only seen in the *Ehmt1*$^{D6cre/+}$ mice with no apparent 'leakage' of cre recombination in the cerebellum (Figure 2.6).

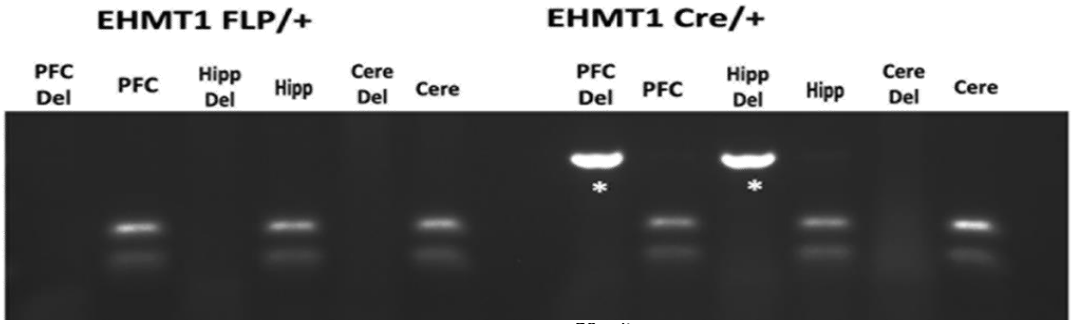

Figure 2.6 Verification of Cre Specificity in *Ehmt1*$^{D6cre/+}$ mice. Separate PCRs were run on the same samples to amplify the deleted allele, and the Flp & WT allele bands. Gel electrophoresis on PCR products visualised here show deleted alleles highly visible in PFC and Hippocampus of Ehmt1$^{D6cre/+}$ sample

2.3.2. *Ehmt1*$^{D6cre/+}$ mice have normal body and brain weight

Ehmt1$^{D6cre/+}$ and *Ehmt1*$^{flp/+}$ mice were taken for adult body and brain weight analysis at 8 weeks old. Mice were weighed prior to culling and harvesting of brain. Brain to body mass ratio was also calculated. *Ehmt1*$^{D6cre/+}$ mice displayed normal body mass, compared to their wildtype counterparts, with males weighing more than female mice [*Ehmt1*$^{flp/+}$ mean: 23.87g; *Ehmt1D6cre*$^{/+}$ mean: 24.35g] (main effect of GENOTYPE, $F_{1,95}$=0.628, p=0.430) (main effect of SEX, $F_{1,95}$=21.933, p<0.001) (Figure 2.7A). Despite there being a sex difference in body weight, there was no interaction of genotype (SEX*GENOTYPE, $F_{1, 95}$= 1.403, p=0.239). No differences were found when analysing their gross brain mass as well, with *Ehmt1*$^{D6cre/+}$ mice averaging 461mg compared to *Ehmt1*$^{flp/+}$ mice at 453.86mg (main effect of GENOTYPE, $F_{1, 95}$= 3.424, p=0.067) with no sex differences seen (main effect of SEX, $F_{1,9\ 5}$= 0.371, p=0.544) (Figure 2.7B). Both groups also displayed equivalent brain to body mass ratio (main effect of GENOTYPE, $F_{1,95}$=0.025, p=0.874). There was however sex differences, female mice had a higher brain to body mass ratio due to their smaller body mass (main effect of SEX, $F_{1, 95}$=23.163, p<0.001). This difference was not associated to the genotype of the mice (SEX*GENOTYPE $F_{1, 95}$= 0.841, p=0.361) (Figure 2.7C).

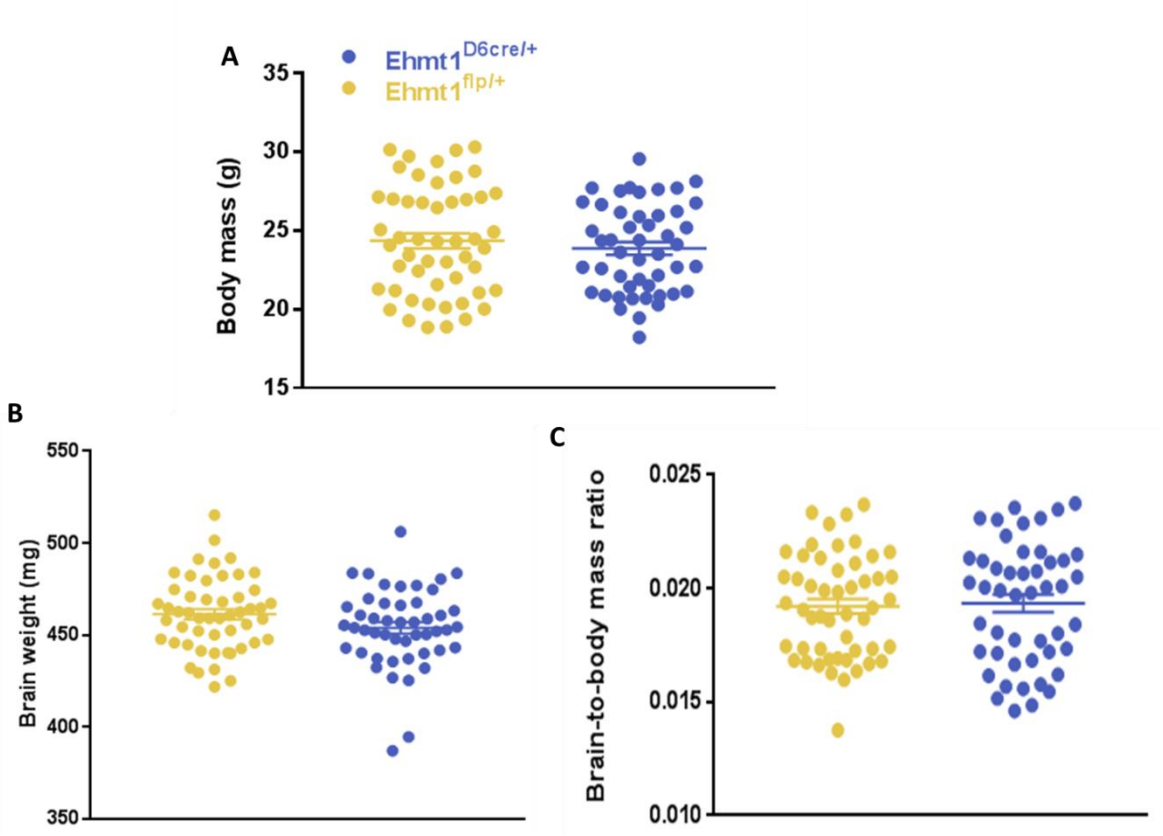

Figure 2.7 *Ehmt1*$^{D6cre/+}$ mice display normal body and brain weights compared to *Ehmt1*$^{flp/+}$ mice. A) At 8 weeks old, mice were weighed and culled for body and brain weight analysis. There was no difference between *Ehmt1*$^{D6cre/+}$ and *Ehmt1*$^{flp/+}$ mice in total body mass at 8 weeks old. **B)** *Ehmt1*$^{D6cre/+}$ mice also showed equivalent brain mass compared to their wildtype counterparts. **C)** These findings translated to normal brain-to-body mass ratio in the *Ehmt1* haploinsufficient mice.

2.3.3. *Ehmt1*$^{D6cre/+}$ mice show no differences in the elevated plus maze

Mice underwent the elevated plus maze task for 5 minutes. As expected, all the mice found the open arms of the EPM anxiogenic, thus spending the majority of their time in the closed arms (~73% of total test time). There were no differences in the time spent on the open arms of the maze between the *Ehmt1*$^{D6cre/+}$ and *Ehmt1*$^{Flp/+}$ mice Figure 2.8A, t_{35}=0.276, p=0.859). Furthermore, both groups of mice made a comparable number of entries into the open arms (Figure 2.8B, t_{35}=1.056, p=0.298), entered an open arm for the first time with a similar latency (Figure 2.8C, t_{35} = 0.563, p =0.748) and exited the starting closed arm at similar times (Figure 2.8D, t_{35} =-0.550, p = 0.748).

In addition to tracking the movement of the mice, other anxiety related behaviours during the test were also collected and analysed (Table 2.3). Consistent with the movement data, no differences were seen between *Ehmt1*$^{D6cre/+}$ and *Ehmt1*$^{flp/+}$ mice in the number of stretch attend positions into the open arms (t_{35} = -0.469, p=0.777), head dips over the open arm ledge (t_{35} = -1.758, p=0.876), and time spent grooming themselves (t_{35} = 0.98, p=0.582).

Table 2.3 Average number of behavioural markers measured in the EPM by genotype

Behaviours measured	Ehmt1$^{D6cre/+}$	Ehmt1$^{Flp/+}$
	Mean ± SE	Mean ± SE
Grooming	2.45±0.66	2.82±0.60
Head dips	30.40±2.33	36.82±3.01
Stretch attend	22.95±1.69	24.06±1.64

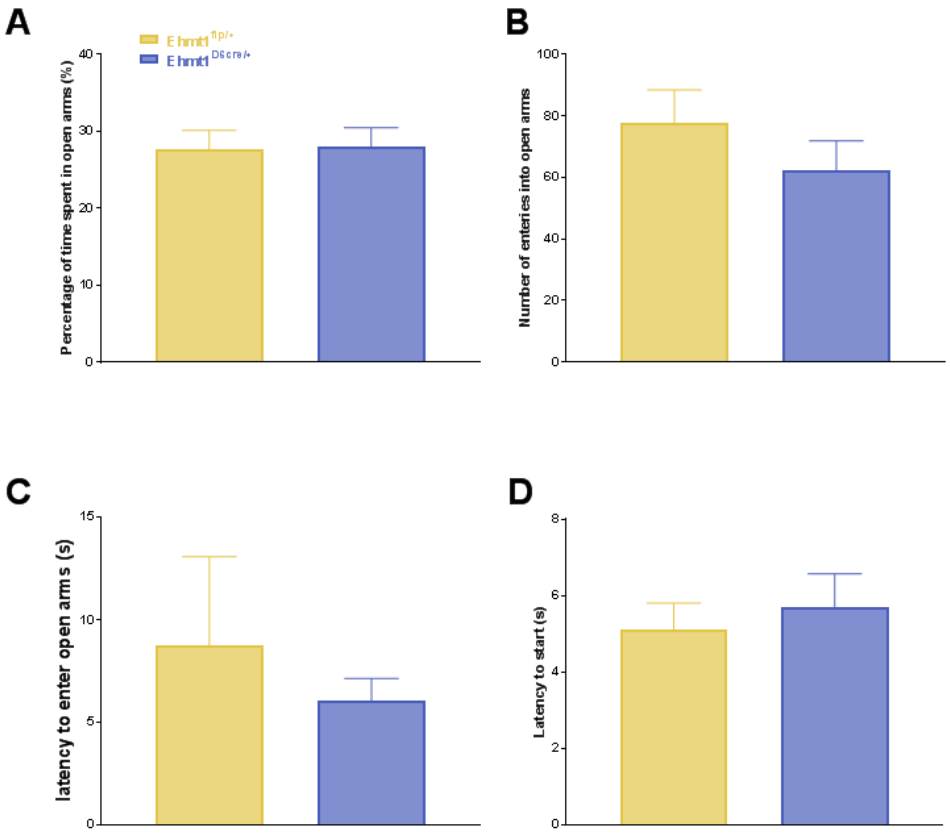

Figure 2.8 **Ehmt1D6cre/+ mice displayed no difference in the elevated plus maze task. A)** Mice underwent the EPM task for a total of 5 minutes. During this time a number of behaviours were measured. Ehmt1D6cre/+ mice spent an equivalent percentage of time in the open arms compared to the Ehmt1flp/+ mice. **B)** Both groups approached and entered the open arms at the same frequency. **C)** It took both group similar times to first enter open arm. **D)** The latency to first start by exiting the starting closed arm was equivalent between groups. Data presented as mean values with SEM. *Ehmt1*$^{flp/+}$: 20, *Ehmt1*$^{D6cre/+}$: 17.

2.3.4. *Ehmt1*$^{D6cre/+}$ mice show no differences in anxiety in a food neophobia test

Both groups of mice readily drank the solutions available during the 11 days of the test, with the volume consumed increasing daily (Figure 2.9A, main effect of SESSION, $F_{5.80,\ 202.79}$=23.10, P<0.001), and no differences between *Ehmt1*$^{D6cre/+}$ and *Ehmt1*$^{flp/+}$ mice (main effect of GENOTYPE, $F_{1,\ 35}$=0.460, p=0.799).

With the introduction of a choice between water and 10% condensed milk solution on the 3rd day of testing, overall consumption significantly increased ($F_{1,35}$=42.587, p<0.001). This was due to an increasing preference for the 10% condensed milk solution (Figure 2.9B, main effect of SESSION ($F_{5.996,\ 209.873}$ = 8.535, p<0.001). However there were no differences seen between the *Ehmt1*$^{D6cre/+}$ and *Ehmt1*$^{flp/+}$ mice groups (main effect of GENOTYPE $F_{1,\ 35}$=1.230, p= 0.571).

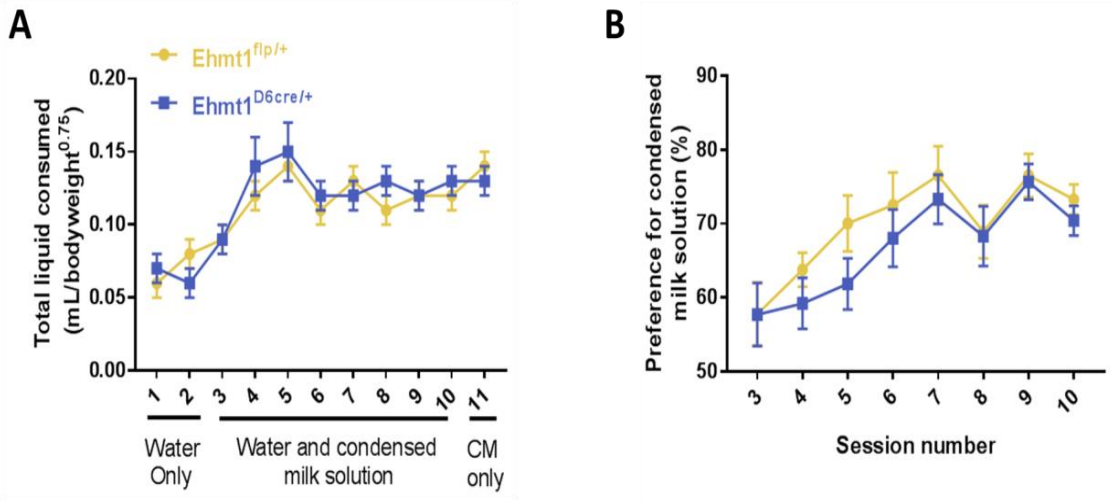

Figure 2.9 Food Neophobia and habituation. A) Total volume consumed by *Ehmt1*$^{D6cre/+}$ and *Ehmt1*$^{flp/+}$ mice across sessions (adjusted for weight) **B)** Preference for novel foodstuff, 10% condensed milk solution cross sessions. All data presented as mean values with SEM, *Ehmt1*$^{flp/+}$:20, *Ehmt1*$^{D6cre/+}$:17.

2.3.5. Locomotor activity and habituation

Locomotor activity was investigated in the mice twice in their lifetime. Initially LMA was conducted in young naive mice at 10 weeks old, across three days and the test was then repeated in the same mice at 10 months old.

Ehmt1$^{D6cre/+}$ and *Ehmt1*$^{flp/+}$ controls showed similar levels of activity across all sessions when analysing beam breaks from the mice at 10 weeks (main effect of GENOTYPE, $F_{1,35}$ =0.870, p=0.58). There was greater number of beam breaks initially, suggestive of increased locomotion during the first session and this declined subsequently, (Figure 2.10B, main effect of SESSION, $F_{2,\ 70}$ =24.626, p<0.001). Locomotor activity in both groups declined over the subsequent sessions at equal rates as the animals habituated to the novel environment (SESSION x GENOTYPE ($F_{2,\ 70}$ =0.744, p=0.688). Similar results were seen when analysing the amount of runs made, assessed as the number of consecutive breaks of both beams in the chamber, with the greatest number of runs occurring in the first session and reduces throughout the subsequent sessions, (Figure A.1, main effect of SESSION ($F_{2,70}$ =19.960, p<0.001).

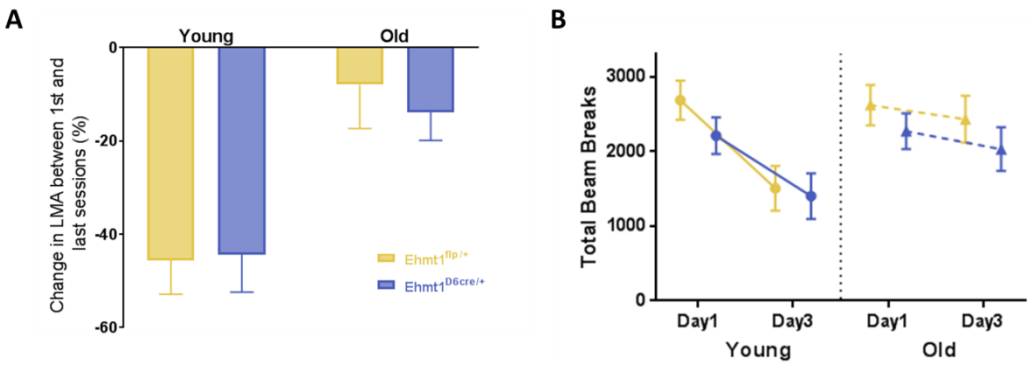

Figure 2.10 Locomotor activity and habituation at 10 weeks and 10 months old. A) Percentage change in number of beam breaks between first and last session at 10 weeks (young) and 10 months (old. **B)** Total number of beam breaks performed in the first and last session at young and old timepoints, all data presented as mean and SEM, *Ehmt1*$^{flp/+}$: 20, *Ehmt1*$^{D6cre/+}$: 17.

The analysis was repeated for locomotor activity data collected from the mice at 10 months old. This time no difference was seen between the first and last sessions in number of beam breaks, (Figure 2.10B, main effect of SESSION, $F_{2, 70}$ =2.120, p=0.29), the animals showed no habituation through the sessions, with no difference in the activity levels between the *Ehmt1*$^{D6cre/+}$ and WT controls across all sessions, (main effect of GENOTYPE, $F_{1, 35}$ = 0.790, P=0.58). Both groups showed similar locomotion in each session (SESSION x GENOTYPE, $F_{2, 70}$ = 0.133, p=0.876). When analysing runs, both groups showed comparable activity levels in the sessions, SESSION (Figure A.1, $F_{1.534, 53.678}$ = 2.879, p=0.19).

To discern whether age affected the locomotor activity of the mice, both time points were analysed together, with AGE at test as a parameter. The mice made more beam breaks in the first session compared to the last session (main effect of SESSION, $F_{2, 70}$ = 21.198, p<0.001). As the mice aged, there was an increase in beam breaks (main effect of AGE, $F_{1,35}$ = 7.724, p=0.025). There was also an interaction of age with session (SESSION x AGE, $F_{2,70}$= 13.305, P<0.001), at 10 months old the mice were no longer habituating between the sessions, and reducing their activity levels by the final session.

2.3.6. Increased startle responsivity in *Ehmt1*$^{D6cre/+}$ mice.

The reactivity of the mice to acoustic stimuli and their ability to attenuate their responses as a measure of sensorimotor gating were investigated in the same *Ehmt1*$^{D6cre/+}$ and *Ehmt1*$^{flp/+}$ mice at two ages, 10 weeks and 10 months old. At 10 weeks old, all mice showed plateaued responsivity with repeating presentation of each startle trial (Figure 2.11, main effect of PRESENTATION,$F_{4.322,151.282}$=4.355, p=0.011), with no difference between *Ehmt1*$^{D6cre/+}$ and *Ehmt1*$^{flp/+}$ (main effect of

GENOTYPE, $F_{1, 35}$ = 1.656, p= 0.268). However while *Ehmt1*$^{flp/+}$ mice appear to habituate as expected, *Ehmt1*$^{D6cre/+}$ mice did not; when group mean differences were analysed individually for each startle presentation, *Ehmt1*$^{D6cre/+}$ mice had a significantly larger startle response at the sixth presentation compared to the *Ehmt1*$^{flp/+}$ mice, (Figure 2.11, t_{35} = -2.588, p=0.03).

At 10 months old, both groups showed no habituation across the six startle presentations (Figure 2.11, main effect of PRESENTATION $F_{4.223, 147.813}$= 0.830, p= 0.513). However *Ehmt1*$^{D6cre/+}$ showed significantly higher magnitude of acoustic startle response across all startle presentations (main effect of GENOTYPE ($F_{1,35}$= 5.980, p=0.04).

To assess the impact of age on the startle responsivity of the mice to acoustic stimuli, data collected at 10 weeks and 10 months was analysed together. Robust startle responses were shown by both groups of mice at the start of each session at both ages, although the amount of startle was reduced in older animals (Figure 2.11, main effect of AGE, $F_{1,35}$=25.587, p<0.001). However, *Ehmt1*$^{D6cre/+}$ mice showed significantly greater startle response compared to the *Ehmt1*$^{flp/+}$ mice (main effect of GENOTYPE, $F_{1,35}$=5.44, p=0.047). Both groups showed differential startle response with increasing presentations (Figure 2.11, main effect of PRESENTATION, $F_{4.21, 147.22}$=3.882, p=0.015). However, the *Ehmt1*$^{D6cre/+}$ mice showed a reduced habituation to the startle presentations whereas their WT counterparts acclimatised to the repeating startle presentations, (PRESENTATION X GENOTYPE, $F_{4.206, 147.217}$ = 2.808, p=0.30). The mice's response to their startle response to repeating presentations was not affected by age (PRESENTATION X AGE (F (4.591, 160.694) = 2.374, p=0.48).

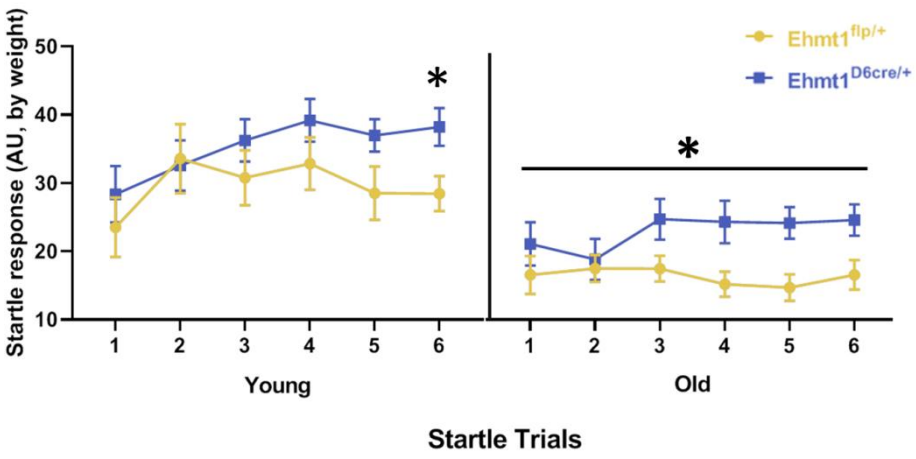

Figure 2.11 Increased startle responsivity in *Ehmt1*$^{D6cre/+}$ mice. Mice were presented with 6 120db acoustic startle trials at both 10 weeks and 10 months old. At 10 weeks old, *Ehmt1*$^{D6cre/+}$ show an increased startle to the final presentation. At 10 months old, *Ehmt1*$^{D6cre/+}$ mice startle significantly higher than *Ehmt1*lfp mice across all six presentations. Data presented as Mean and SEM, *Ehmt1*$^{flp/+}$:20, *Ehmt1*$^{D6cre/+}$: 17.

2.3.7. Impaired sensorimotor gating in *Ehmt1*$^{D6cre/+}$ mice.

Prepulse inhibition, PPI, of startle response, a measure of sensorimotor gating, was investigated by examining the startle reflex of the mice, at 10 weeks and 10 months old, to an acoustic stimulus that was preceded by a range of weaker prepulse stimuli.

At 10 weeks old, there was a tendency for *Ehmt1*$^{D6cre/+}$ to show reduced PPI compared to *Ehmt1*$^{flp/+}$ mice (Figure 2.12, main effect of GENOTYPE $F_{1,35}$=3.431, p= 0.11). A significant PREPULSE INTENSITY x GENOTYPE interaction ($F_{2,70}$=4.30, p=0.037) demonstrated that this difference was greatest with a 16db above background prepulse stimulus, confirmed by post hoc comparison ($t_{30.92}$=3.23, p=0.013). At 10 months old, the difference in PPI between *Ehmt1*$^{D6cre/+}$ and *Ehmt1*$^{Flp/+}$ mice was significantly greater (Figure 2.12, main effect of GENOTYPE, $F_{1,35}$=4.48, p=0.04), despite not surviving correction for multiple

corrections (p=0.069), suggesting impaired sensorimotor gating at all prepulse amplitudes assessed.

When analysed taking into account AGE, mice at both ages demonstrated PPI, with levels of attenuation increasing as the prepulse intensity increased (Figure 2.11), main effect of PREPULSE INTENSITY, $F_{2,70}$=80.88, p<0.001), with *Ehmt1*$^{D6cre/+}$ mice showing reductions in PPI at both ages (main effect of GENOTYPE, $F_{1,35}$=7.73, p=0.024). This difference was consistent across both ages (main effect of AGE, $F_{1,35}$= 2.72, p=0.158) although the genotype-related effect was greater in the older mice.

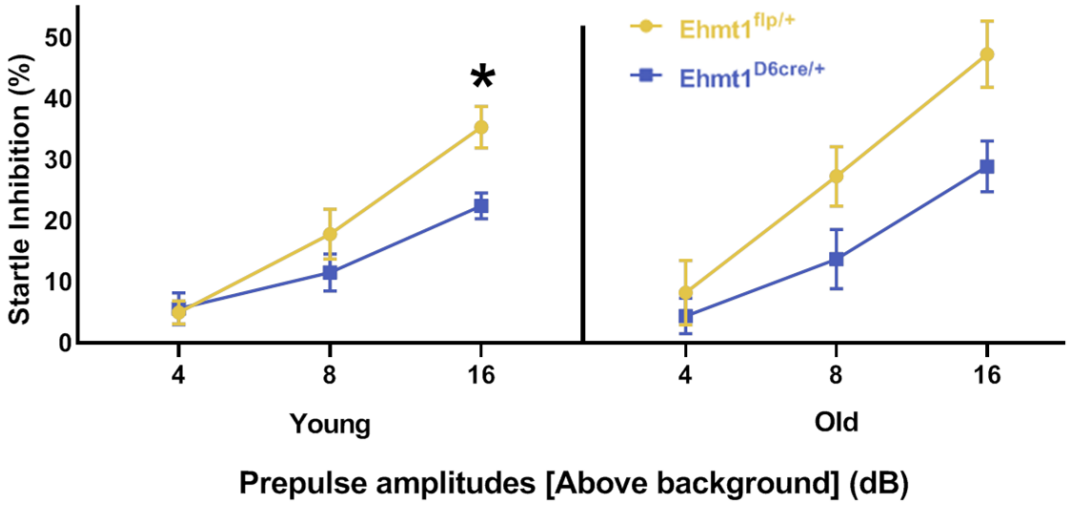

Figure 2.12 Impaired sensorimotor gating in *Ehmt1*$^{D6cre/+}$ mice. Mice were presented with 3 differing prepulse intensities; 4, 8, 16; prior to 120db acoustic startle trials at both 10 weeks and 10 months old. At 10 weeks old, *Ehmt1*$^{D6cre/+}$ show an impairment in PPI at 16db prepulse intensity. This impaired sensorimotor gating was found across all prepulse intensities at 10 months old. Data presented as Mean and SEM, *Ehmt1*$^{flp/+}$:20, *Ehmt1*$^{D6cre/+}$: 17

2.4. Discussion

This chapter investigated spontaneous behaviours, including anxiety behavioural phenotypes, sensory and motor behaviour, in the *Ehmt1*$^{D6cre/+}$ mouse model. These mice have a deletion of one copy of the *Ehmt1* gene in the frontal brain, including prefrontal cortex and hippocampal structures, with the deletion occurring from very early in development.

The deleted *Ehmt1* allele was detected in the prefrontal cortex and hippocampus of the *Ehmt1*$^{D6cre/+}$ mouse. No detection was seen in the cerebellum, acting as an internal control and in *Ehmt1*$^{flp/+}$ mouse brain regions, validating the specificity of the cre recombination. *Ehmt1*$^{D6cre/+}$ mice also had normal brain and body weights compared to *Ehmt1*$^{flp/+}$ mice.

No difference between *Ehmt1*$^{D6cre/+}$ mice and *Ehmt1*$^{flp/+}$ mice were found in a range of different anxiety measures. In the EPM task *Ehmt1*$^{D6cre/+}$ mice explored both arms equally when compared to the *Ehmt1*$^{flp/+}$ mice, and showed a normal preference for the closed arms, and avoidance of the open arms as seen in normal behaving rodents. *Ehmt1*$^{D6cre/+}$ mice also showed no difference in their consumption levels in the food neophobia/novel food preference test. *Ehmt1*$^{D6cre/+}$ mice have normal activity levels when tested in the locomotor activity chamber compared to *Ehmt1*$^{flp/+}$ mice at both 10 weeks and 10 months old.

The main finding of the chapter is *Ehmt1*$^{D6cre/+}$ mice have significantly increased response to acoustic startle compared to their *Ehmt1*$^{flp/+}$ mice. In addition to this, *Ehmt1*$^{D6cre/+}$ mice showed greatly reduced prepulse inhibition compared to *Ehmt1*$^{flp/+}$.

2.4.1. Anxiety

The elevated plus maze paradigm found no difference in “state” anxiety. In this paradigm which measures approach-avoidance conflict (Pellow et al. 1985), the *Ehmt1*$^{D6cre/+}$ mice explored both arms equally when compared to *Ehmt1*$^{flp/+}$ mice, and showed a normal preference for the closed arms, and avoidance of the open arms as seen in normal behaving rodents (Pellow et al. 1985). In the test of hyponeophagia, there were no differences between *Ehmt1*$^{D6cre/+}$ and *Ehmt1*$^{flp/+}$ mice in their overall levels of consumption or preference for a novel foodstuff.

However, these results contradict previous results found in other *Ehmt1* deficient models (Schaefer et al. 2009; Balemans et al. 2010). The *Ehmt1*$^{+/-}$ model showed a reduction in anxiety in various anxiety-related tests including open-field and light-dark box paradigms (Balemans et al. 2010) and the *Ehmt1*$^{camk2a/cre}$ model reduced anxiety in the EPM and decrease preference for a more palatable sucrose solution (Schaefer et al. 2009). However, the nature of the tests used may account for the disparity in findings between the current work and previous studies. It has been shown that anxiety tests on the same knockout rodent models lead to differing results dependent on the paradigm used (Steimer 2011; Lezak et al. 2017), and it is possible that these tests are dissociating differing neural processes of anxiety (Calhoon & Tye 2015).

In addition to this, a confounding factor of most anxiety avoidance-approach tests are exploratory in nature, and thus highly dependent on locomotor behaviour (Calhoon & Tye 2015). The constitutive *Ehmt1*$^{+/-}$ mouse model has been found to be hypoactive compared to their WT littermates (Balemans et al. 2010), and the *Ehmt1*$^{camk2a/cre}$ model made reduced arm entries in the EPM, indicative also of reduced activity (Schaefer et al. 2009). Thus, there is the possibility that in these

models reduced anxiety may be a product of hypoactivity or reduced motivation to explore rather than increased anxiety (Calhoon & Tye 2015). In our model, EPM arm entries and activity measured in a separate locomotor test (see below) did not differ between *Ehmt1*$^{D6cre/+}$ and *Ehmt1*$^{flp/+}$ mice, suggesting that activity was not a confound in terms of our measures of anxiety.

The *Ehmt1*$^{camk2a/cre}$ model has a forebrain specific promoter, leading primarily to expression in the striatum (Burgin et al. 1990), a brain region, along with other limbic structures including the hippocampus and PFC, which have long been associated with anxiety phenotypes (Lago et al. 2017), motivation and goal oriented behaviour (Mogenson et al. 1980). Motivation is linked to anxiety, and impairment in motivation can impact anxiety behaviour (Lang et al. 1998; Lago et al. 2017), and increased striatal activity can lead to increased anxiety due to enhanced motivation to avoid (Lago et al. 2017), and moreover active avoidance has been found to be striatal dependent (Darvas & Palmiter 2009). Thus it is possible that the apparent increases in anxiety and food neophobia in the *Ehmt1*$^{camk2a/cre}$ model could be due to reduced motivation. However, this hypothesis is not applicable for our model, where a forebrain specific promotor is also present, but anxiety phenotypes are absent. These, differences in performance could be accounted for by differing expression levels, regional and tissue levels or the timing of the deletion, where the *Ehmt1*$^{camk2a/cre}$ model shows homozygous depletion of *Ehmt1* in similar brain regions to the *Ehmt1*$^{D6cre/+}$ model apart from the striatum, and only postnatally. This may give rise to further ideas about the effects of *Ehmt1* on development and function which will be discussed later.

2.4.2. Locomotor exploration

As highlighted previously, on the EPM there were no fundamental differences in activity between *Ehmt1*$^{D6cre/+}$ and *Ehmt1*$^{flp/+}$ mice, which was further confirmed in a specific assessment of locomotor activity and exploration at two ages. *Ehmt1*$^{D6cre/+}$ mice have normal activity levels when tested in the locomotor activity chamber compared to *Ehmt1*$^{flp/+}$ mice at both 10 weeks and 10 months old. Again, in contrast to other *Ehmt1* mouse models, no significant differences were observed in general activity or in habituation within or between sessions, however, it should be noted that this experimental procedure is different to any used previously (Schaefer et al. 2009; Balemans et al. 2010; Balemans et al. 2013) and therefore comparisons may be difficult to determine. The absence of differences in habituation would suggest that the *Ehmt1*$^{D6cre/+}$ mice do not have any fundamental differences in habituation learning, at least with regard to environmental or contextual stimuli, suggesting that such learning may be unaffected in this model.

Interesting to note, both previous mouse models suffered from increased weight (Schaefer et al. 2009; Balemans et al. 2010). Increase in weight in adult mice would affect their exploratory behaviour and could explain the normal locomotor activity levels in this mouse model; the lack of deletion of *Ehmt1* in the cerebellum here also allows for behavioural assessments not confounded by deletion of *Ehmt1* in purkinje cells, the key cellular output of locomotor learning and behaviour (Manto et al. 2012).

2.4.3. Startle responsivity and sensorimotor gating

The acoustic startle response and PPI was measured, and showed that *Ehmt1*$^{D6cre/+}$ mice had higher levels of startle and reduced PPI compared to control

Ehmt1$^{flp/+}$ mice. These effects were present at both ages tested, although the differences were greater at 10 months, suggesting an age-related change in both responses, although overall startle was reduced at the older age in both groups of mice. Acoustic startle responding has not been previously assessed in a mouse model of *Ehmt1* deletion, so therefore these results are novel and maybe informative in determining the function of this gene. Increased startle and impaired habituation has been observed in rodent models that were administered with the psychotomimetic drugs PCP, MK-801 and D-AMP (Klamer et al. 2004), thus this may indicate that *Ehmt1* has role in the development of cognitive phenotypes in schizophrenia. Whilst acoustic startle response has been used as a measure for anxiety, the lack of other features of anxiety in this mouse model is suggestive of an impairment linked primarily to a deficit in sensorimotor gating processes.

Ehmt1$^{D6cre/+}$ mice also showed reduced prepulse inhibition compared to their *Ehmt1*$^{flp/+}$ counterparts, which was more significant when the mice were older. This is suggestive of an increasing impairment in sensorimotor gating as the animals age, although this phenomenon was present from a young age, suggesting a strong phenotype in the mice. Reduced PPI has been associated with a number of different clinical conditions, in addition to being observed in a number of rodent genetic models of schizophrenia including DISC1, Neuroligin, and BDNF (Clapcote et al. 2007; Manning & van den Buuse 2013; Chen et al. 2017).

Furthermore, although startle and PPI have not been explicitly assessed in KS, recent work shows that KS patients show increased signs of psychosis as they

age (Verhoeven et al. 2011) which could indicate that they might also show PPI deficits which may also increase with age. This suggests *Ehmt1* may play a key role in the attention regulation necessary for sensorimotor gating and deficits in *Ehmt1* can lead to growing impairment as KS patients go through adolescence and into adulthood.

2.5. Conclusion

This chapter explored the basic characterisation of the *Ehmt1*$^{D6cre/+}$ forebrain specific mouse model of *Ehmt1* haploinsufficiency. Here *Ehmt1*$^{D6cre/+}$ mice did not show anxiety-like behaviour in the anxiety-exploratory paradigms used. This was further validated with no difference seen in the exploratory locomotor behaviour.

This study provides the first evidence of compromised sensorimotor gating circuitry in *Ehmt1* haploinsufficiency, and the first to suggest an increasing impairment into adulthood. This may become noteworthy clinically when taking into consideration the increase in psychotic symptoms in the current aging KS patient cohorts.

The results laid out in this chapter suggest that although this model can be used to capture some phenotypes seen in KS, it will play a better role in understanding the function of *Ehmt1* in the development of the forebrain and within cross diagnostic endophenotypes of neurodevelopmental disorders in general. Thus, these findings provide a foundation to investigate the role of *Ehmt1* in more specific tests of learning and memory, and its effect of the development and maintenance of hippocampal and cortical structures.

Chapter 3 Dissecting the Role of *Ehmt1* in Memory

3.1. Introduction

Recently, great strides have been taken to understand the role of epigenetic regulation of learning and memory. Both DNA methylation and epigenetic post translational modifications, such as histone modifications have been attributed to the development of cognitive disorders [See review (Kleefstra et al. 2014)], with more recent work expanding their role into the development and maintenance of the biological circuitry of learning and memory. Histone acetylation, an example of a histone modification, has been long studied in memory, and was first implicated in novel taste memory (Swank & Sweatt 2001). $CBP^{-/+}$ mice, lacking a copy of a histone acetyltransferase, have impaired memory in the object recognition task (Alarcón et al. 2004; Korzus et al. 2004), contextual fear conditioning (Alarcón et al. 2004), and object location task (Korzus et al. 2004). Following the rescue of some of these impairments using a histone deacetylase inhibitor (Korzus et al. 2004), the field of research surrounding the role of these HDAC inhibitors grew, along with the communal knowledge of HDAC inhibitors in treatment of cognitive deficits (Bredy & Barad 2008; Dash et al. 2010; Peleg et al. 2010). These studies show the role of histone acetylation and histone deacetylation modulate cortical and hippocampal dependent memory.

Ehmt1 mono- and di-methylates histone 3 at the lysine 9 position. H3K9 methylation is also involved in learning and memory. H3K9me2 epigenetic mark is regulated during fear conditioning, being transiently up-regulated in the CA1 region

of the hippocampus directly after task training (S. Gupta et al. 2010; Gupta-Agarwal et al. 2012a). Inhibiting H3K9me2 in this region leads to impairment in contextual fear memory in rodents. In fact, *Ehmt1*$^{Camk2acre/+}$ knockout mice also showed impaired contextual fear memory 24 hours after training (Schaefer et al. 2009), suggestive of the role of H3K9me2, and specifically *Ehmt1*, plays in hippocampal dependent memory processes.

A role for *Ehmt1* in learning and memory is also suggested by its involvement in neurodevelopmental disorders. As previously stated, a key factor across the diagnostic lines of *Ehmt1* associated disorders is the presence of moderate to severe intellectual disability (Morgan et al. 2008; Matson & Shoemaker 2009). *Ehmt1* and other chromatin modifiers are disproportionately enriched in neurodevelopmental disorders with intellectual disability (Kleefstra et al. 2014), suggestive of a critical role at key time points during the development the highly intricate neural circuitry required for normal cognitive functioning.

This chapter will focus on characterising memory and learning phenotypes in our forebrain specific *Ehmt1* haploinsufficient mouse model.

3.1.1. Object Recognition Memory

Object recognition memory, a form of declarative memory, has long been used as a marker for memory due to the ease of testing in rodents (Ennaceur & Delacour 1988; Antunes & Biala 2012a). Declarative memory involves episodic and semantic memory, and refers to events and facts that can be remembered and consciously called upon (Riedel & Blokland 2015). Object recognition is a key

part of episodic declarative memory and refers to the recognition of previously encountered objects (Bird 2017). Hippocampal and extra-hippocampal cortical structures have been linked to the process of recognition memory (Aggleton & Brown 2005; Antunes & Biala 2012a; Vogel-Ciernia & Wood 2014; Morici et al. 2015; Bird 2017).

3.1.1.1. Novel Object Recognition Task

Object recognition memory can be investigated in rodents using a novel object recognition paradigm. This paradigm is considered to tax mechanisms analogous to human declarative memory (Rajagopal et al. 2014; Blaser & Heyser 2015). The task relies on the natural tendency of rodents to explore novel objects without the need of a reinforcer or reward (Ennaceur & Delacour 1988; Antunes & Biala 2012a; Vogel-Ciernia & Wood 2014). This preference to novelty can be elicited by allowing the rodents to freely exploration of a novel and familiar objects, the animal's preference for the novel object is thus suggestive of the maintenance of the familiar object in their memory (Antunes & Biala 2012a). This allows for large number of manipulations including number of objects and amount of time from exposure to the familiar object. The paradigm has been used to test short and long term memory as well as trying to understand the mechanisms of encoding, consolidation, and retrieval in declarative memory (Vogel-Ciernia & Wood 2014). Various studies have found novel object recognition to be impaired at different retention intervals in a number of manipulations effecting hippocampal and perirhinal cortical regions (Robert E. Clark et al. 2000; Hammond et al. 2004; Norman & Eacott 2004; Barker et al. 2007a; Broadbent et al. 2010; Gaskin et al. 2010a; Engelmann et al. 2011; Antunes & Biala 2012b).

3.1.2. Spatial Memory and Novel object Location task

Spatial memory in rodents has been used to investigate neural correlates of human cognition and memory dysfunction (Morellini 2013). There are numerous tasks that are used to assay spatial working memory, spatial reference memory and spatial learning (Morellini 2013; Vorhees & Williams 2014). Object location memory is assessed in a novel object location task to test spatial memory and discrimination in rodents (Dix & Aggleton 1999; Vogel-Ciernia & Wood 2014). This task, like novel object recognition task, relies on the preference for exploring novelty. Unlike spatial tasks such as the Morris water maze and radial arm maze, it is a relatively simple task to structure without any necessary pretraining. The core structure of this task is similar to novel object recognition (Dix & Aggleton 1999; Vogel-Ciernia & Wood 2014). However, instead of replacing an object for a novel object, one of the familiar objects is moved to a new location in the arena. The rodents are then allowed to explore both objects, one in a familiar location, and the other in a novel location, time spent exploring the objects is recorded (Dix & Aggleton 1999; Morellini 2013; Vogel-Ciernia & Wood 2014; Vorhees & Williams 2014). If the rodents spend more time exploring the object in the novel location compared to the familiar location it would be suggestive of a reference of the familiar location being maintained in their memory. This task is believed to be more hippocampal dependent compared to the novel object task (Mumby et al. 2002), with the hippocampus and hippocampal formation proving to have highly intricate neural correlates of spatial memory, including the cognitive map, including boundary, place, and grid cells (Brandon et al. 2014).

3.1.3. Aims

- To examine the effect of forebrain specific knockdown of *Ehmt1* on recognition and spatial memory in the *Ehmt1*$^{D6cre/+}$ mouse.

3.2. Methodology

3.2.1. Animals

Experimental group generated in Chapter 2 to investigate basic and spontaneous behaviours also underwent the memory tasks described here (Table 3.1).

Table 3.1 sample size and genotype and age for the behavioural cohort assayed in each memory and learning task

Behavioural Paradigm	Genotype and sample size		Age at start of Behavioural paradigm
	$Ehmt1^{fl/+}$	$Ehmt1^{D6cre/+}$	
Novel Object Recognition	20	17	4 months
Novel Object Location	20	17	4 months

3.2.2. Apparatus

Both the novel object recognition task and novel object location task took place in a 30cm x 30cm arena with 30cm high white Perspex walls. The objects and arena were cleaned after each session with 70% ethanol to remove olfactory cues. A camera, mounted directly overhead allowed the mice to be tracked using Noldus Ethovision XT software. Tracking of each subject, determined as the location of the greater body-proportion (12 frames/s), was calibrated prior to testing using mice of the same body size and fur colour as the experimental cohort. Manual analysis of pilot sessions confirmed the accuracy of the tracking software, and all traces were examined for tracking-related artefacts prior to analysis.

The arena was divided into 4 equal virtual sections, referred to as Q1, Q2, Q3, and Q4. Entries and time spent into each section were then automatically

determined by the software, in addition transitions into different halves of the arena, e.g.: movements from section 1 to section 2 (Q12 to Q34) and section 3 to section 4 (Q14 to Q23), and vice versa.

3.2.3. Objects

Mice were presented with different three- dimensional objects, which varied in colour, shape, size and texture. Any object with an obvious scent was excluded. Every object was available in triplicate and so if an object was to be presented twice in the same session a different copy could be used to avoid the possibility of odour marking. Objects for novel object recognition were: unlabelled tin can, green partially opaque glass bottle, and a black and white aerosol can. Objects used in the novel object location task were two identical wooden planks.

3.2.4. Assessment of Object/Location contact

Object exploration was defined by the mouse making contact with an object as well as facing an object within 10mm. Climbing on the object was not included within this measure, however placing the forepaws on the objects was. Each object approach was recorded by manual scoring using the video tracking system, with separate keyboard keys assigned to each familiar object/location and the novel object/location. Thus, frequency, and overall duration spent exploring objects could be determined. Objects were cleaned with 70% ethanol between trials to avoid olfactory cues. Recognition performance of the novel objects/locations was assessed using the recognition index, calculated from the formula [time exploring the novel object/location/ (time exploring the novel

object/location + time exploring the familiar object/location)], RI = $T_N/(T_N + T_F)$ (Gaskin et al. 2010b). Significantly above 0.5 is suggestive of preference towards to the novel object/location, whereas no significant difference from 0.5 is suggestive of lack of preference for the novel object, and thus a lack of recognition of novelty.

Novel Object Recognition

To investigate object recognition memory, the behavioural cohort underwent a novel object recognition task, according to the methods of Engelmann et al., 2011 (Figure 3.1). All animals were habituated to the test chambers for 5 consecutive days, with a single 10 minute session/day. Each session the subjects were placed into the empty arena and allowed to freely explore.

Immediately after the final habituation session, the subjects were returned to the arena for the acquisition phase. In this phase, two identical objects (A,A') were placed in the centre of the adjacent quadrants. During the 10 minute acquisition phase, the time spent exploring each object was measured (see above).

Object recognition was assessed after two delays: 30 minutes and 24 hours after the acquisition phase. During the test phases, one of objects was replaced with a novel object (B and C), in comparison with familiar object (A). The position of the novel/familiar objects were counterbalanced across each session, but always in the same locations used in the acquisition phase. In each retention test, the subjects could explore both objects for 5 minutes, and locomotor indices and time exploring each object was measured as previously stated.

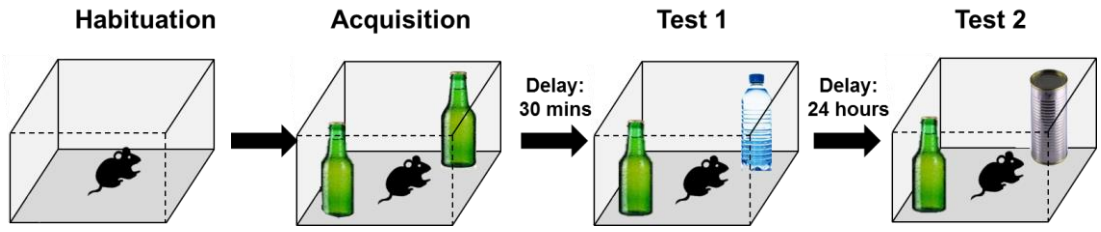

Figure 3.1 Summary of Novel Object Recognition paradigm. Schematic summarising the arena set up for novel object recognition task during the habituation, acquisition, and test phases. A 10 minute habituation phase (5 sessions) is followed by acquisition phase with two identical objects (A, A'). The first test, 30 minutes after acquisition, object A' is replaced with object B. 24 hours after initial acquisition, mice are presented with object A and C.

3.2.5. Novel Object Location

Spatial memory was investigated using a novel object location task. The task is set in the same arena as the novel object recognition task and followed a similar experimental design (Figure 3.2). In this test, all object recognition was tested following a 24 hours delay, with a novel location recognition test, and a familiar location test as control, the order of which was counter-balanced between subjects. For each test, the mice underwent 10 minute habituation and acquisition sessions and a 5 minute test session. New objects were used in these tests.

During acquisition, directly after a habituation phase, the subjects explored two identical objects placed in adjacent corners (D_{f1}, D_{f2} or E_{f1}, E_{f2}). 24 hours after acquisition the subjects were tested in either the familiar (objects in the same positions as acquisition, D_{f1}, D_{f2} or E_{f1}, E_{f2}) or novel (on object moved to a new location, D_{f1}, D_n or E_{f1}, E_n) tests. The time spent exploring these object locations were measured along with locomotor indices, and the recognition index was measured to analyse preference for novelty (see above).

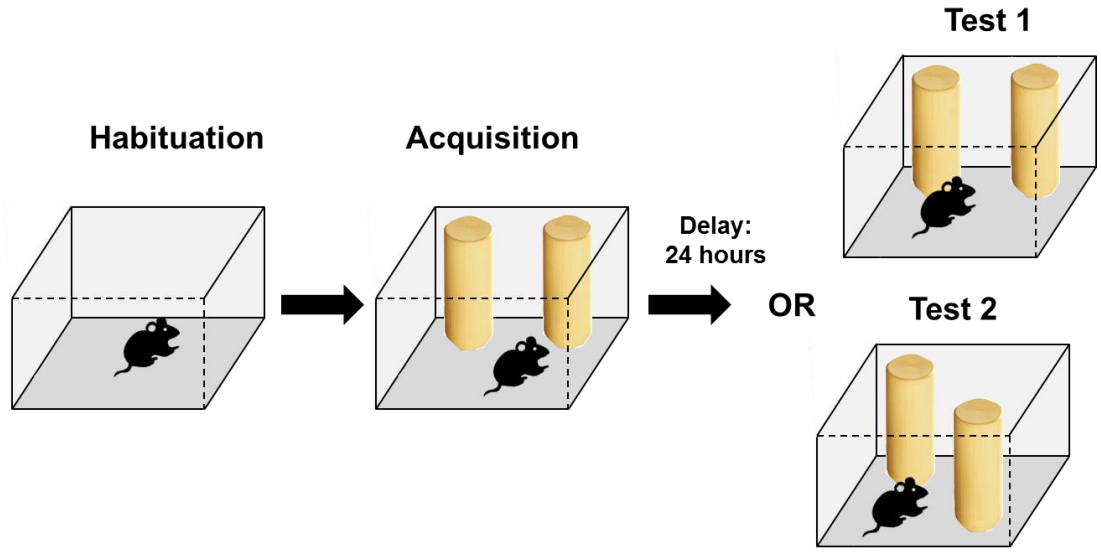

Figure 3.2Summary of Novel Object Location paradigm. Schematic summarising the arena set up for novel object location task during the habituation, acquisition, and test phases. A 10 minute habituation phase (4 sessions) is followed by acquisition phase with two identical objects in specific locations (D_{f1}, D_{f2} or E_{f1}, E_{f2}). 24 hours after acquisition mice where either tested with the objects in the same locations (D_{f1}, D_{f2} or E_{f1}, E_{f2}), or with one object moved to a new location (D_{f1}, D_n or E_{f1}, E_n)**.**

3.2.6. Statistical Analysis

All data were analysed using SPSS 23 (SPSS, USA). All data were checked for normality using the Shapiro-Wilkes test and appropriate analyses used. For the acquisition and test phases of the NOR and NOL, frequency and time spent exploring objects and locomotor indices, and the main measure of memory, the recognition index RI, were analysed using independent samples t-tests with between-subjects factor of GENOTYPE (*Ehmt1*$^{D6cre/+}$ or *Ehmt1*$^{fl/+}$) if normally distributed. Data not normally distributed were analysed using non-parametric between-subjects Mann-Whitney U test for GENOTYPE differences. To evaluate if novel object or location recognition differed from chance, separate within-subject t-tests (or non-parametric Mann-Whitney U) to calculate difference from chance (0.5) for each group [*Ehmt1*$^{D6cre/+}$ or *Ehmt1*$^{fl/+}$] for the 30 minutes, 24 hours after acquisition [NOR], and Novel and Familiar contexts [NOL].

Habituation data, cumulative time spent moving, total distance moved, percentage of time spent in each quarter of the arena, and frequency entering each half of the arena (arena subdivisions described above), for both novel object recognition and location tasks were analysed using repeated measures ANOVA with between-subjects factor of GENOTYPE and within subject factor of SESSION. These measurements together make up the locomotor indices measured throughout both tasks. Mauchly's test of sphericity of the covariance matrix was applied. Huynh–Feldt corrections were applied as necessary for data that violated sphericity, and adjusted degrees of freedom are provided. Data presented in this chapter was corrected for multiple comparisons using Benjamini-Hochberg FDR with a q-value of 0.05, and adjusted p-values are presented in text.

3.3. Results

3.3.1. Novel object Recognition

Both short- and long-term object recognition memory abilities of the behavioural cohort were assessed in NOR with 30 minute and 24 hour retention intervals.

As expected, when tested after a 30 minutes delay, both *Ehmt1*$^{fl/+}$ and *Ehmt1*$^{D6cre/+}$ mice showed an increased preference for the novel object compared to the familiar object and explored the novel object significantly above chance (Figure 3.3A, ***Ehmt1***$^{fl/+}$: t_{19}=4.045, p=0.007, ***Ehmt1***$^{D6cre/+}$: t_{16}=3.366, p=0.017). Although, the RI for *Ehmt1*$^{fl/+}$ mice was greater than for the *Ehmt1*$^{D6cre/+}$ mice, there was no significant group difference for this measure (t_{35}=0.581, p=0.747). Therefore, both groups of mice made more approaches and spent longer exploring the novel object than the familiar object (Table 3.2), and there were no differences between the two groups for either of these measures: novel (approaches: t_{35}=-0.631, p=0.747 and duration: t_{35}=-1.897 p=0.128) and familiar: (approaches: t_{35}= 1.93, p=0.78 and duration: t_{35}= -0.578, p= 0.747). Thus, with a 30 minutes delay, both *Ehmt1*$^{fl/+}$ and *Ehmt1*$^{D6cre/+}$ mice showed robust memory function.

However, when tested 24 hours after acquisition there was dissociation between the two groups in their ability to discriminate the novel and familiar objects. *Ehmt1*$^{fl/+}$ mice showed retention of a preference for the novel object compared to familiar object, exploring it significantly above chance (t_{19}=4.838, p=0.001). In contrast, *Ehmt1*$^{D6cre/+}$ mice showed no preference for the novel object

(t_{16}=-2.374, p=0.0757). These effects were not a result of altered novel object exploration, as there were no group differences in the frequency (t_{35}=0.465, p=0.796) or time spent (t_{35}= 0.503. p=0.782) exploring the novel object (Table 3.2) but were a result of increased approaches (t_{35}= 3.04 p=0.0178) and time spent (t_{35}= 3.44, p=0.0105) exploring the familiar object by *Ehmt1*$^{D6cre/+}$ mice.

Thus, *Ehmt1*$^{D6cre/+}$ mice demonstrate an apparent delay-dependent reduction in memory for objects in comparison to *Ehmt1*$^{fl/+}$ mice. This was not due to differential exploration of objects during acquisition (Figure 3.3B), suggesting normal learning of familiar objects. Both groups spent equivalent times exploring both acquisition objects (***A:*** t_{35}= -1.257, p= 0.217; ***A':*** t_{35}= 0.126, p= 0.901) and made an equivalent number of approaches to both acquisition objects (***A***: t_{35}= 1.367, p= 0.326; ***A'***: t_{35}= 0.960, p= 0.524).

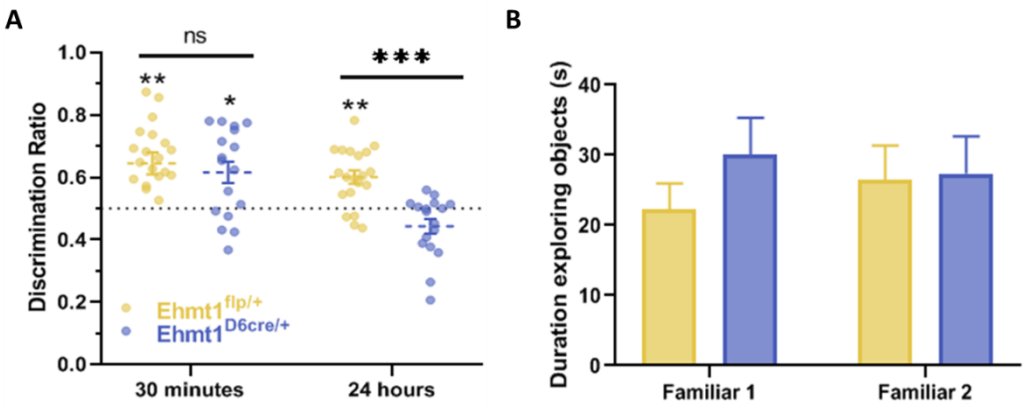

Figure 3.3 Novel Object Recognition Test and Acquisition A) Novel object recognition 30 minutes and 24 hours after acquisition: Both groups show a preference for the novel object 30 minutes after acquisition (intercept at 0.5, aka chance) with no difference between groups. However at 24 hour after acquisition, Ehmt1D6cre/+ mice no longer show a preference for the novel object suggesting impairment in long term recognition memory. **B)** Time spent exploring objects during acquisition: both groups explored either object equally during the acquisition phase, so impairment in long term recognition memory is not due to differential experience of objects by the Ehmt1D6cre/+ mice. Data presented as mean values with SEM * *P<0.05,* ** *P<0.01,* *** *P<0.001, ns nonsignificant. Ehmt1*$^{flp/+}$*: 20, Ehmt1*$^{D6cre/+}$*: 17.*

Table 3.2 Summary of frequency and duration spent exploring objects at 30 minutes and 24 hours after acquisition by genotype.

		30 minutes after acquisition		24 hours after acquisition	
Genotype	Parameter	Familiar Object	Novel Object	Familiar Object	Novel Object
Ehmt1$^{flp/+}$	Frequency exploring object	13.05 ±1.18	23.3 ± 1.71	9.8 ± 0.88	12 ± 0.88
	Duration exploring object (s)	18.73 ± 7.43	34.04 ± 2.74	9.38 ± 0.97	13.93 ± 1.45
Ehmt1$^{D6cre/+}$	Frequency exploring object	16.76 ± 1.56	21.82 ± 1.55	14.12 ± 1.12	12.76 ± 1.45
	Duration exploring object (s)	13.96 ± 1.88	26.38 ± 2.96	18.21 ± 2.38	15.2 ± 2.15

Secondary indices of locomotor activity showed that all of the animals habituated to the novel environment over the initial 5 sessions, with total distance moved (main effect of SESSION, $F_{3.273,\ 114.565}$= 32.97, p<0.001) significantly reduced across the sessions. However, *Ehmt1*$^{D6cre/+}$ mice moved a greater total distance (main effect of GENOTYPE, $F_{1,35}$=7.20, p=0.035) compared to their *Ehmt1*$^{fl/+}$ littermates (Figure 3.4A). There was no interaction between GENOTYPE x SESSION.

Interestingly whilst there was no difference in total distance moved by the final habituation session between groups ($t_{35=}$-1.333 p=0.33), there was an increase in locomotor activity in both *Ehmt1*$^{fl/+}$and *Ehmt1*$^{D6cre/+}$ mice (t_{35}=5.073, p<0.001, Figure 3.4B) indexed by the total distance moved in the acquisition phase. The addition of (novel) objects to the arena during acquisition had a differential effect on the total distance moved by each group, with *Ehmt1*$^{D6cre/+}$ mice moving significantly more compared to the *Ehmt1*$^{fl/+}$ mice (t_{35}= 2.873, p=0.025).

There were no differences in total distance moved between the *Ehmt1*$^{fl/+}$ and *Ehmt1*$^{D6cre/+}$ mice in the 30 minute test (Figure 3.4B, (t_{35}=1.319, p=0.344)). 24 hours after acquisition during the second test phase, *Ehmt1*$^{D6cre/+}$ mice once again

moved greater distance (t_{35}=3.413, p=0.01) compared to their *Ehmt1*$^{fl/+}$ littermates (Figure 3.4B).

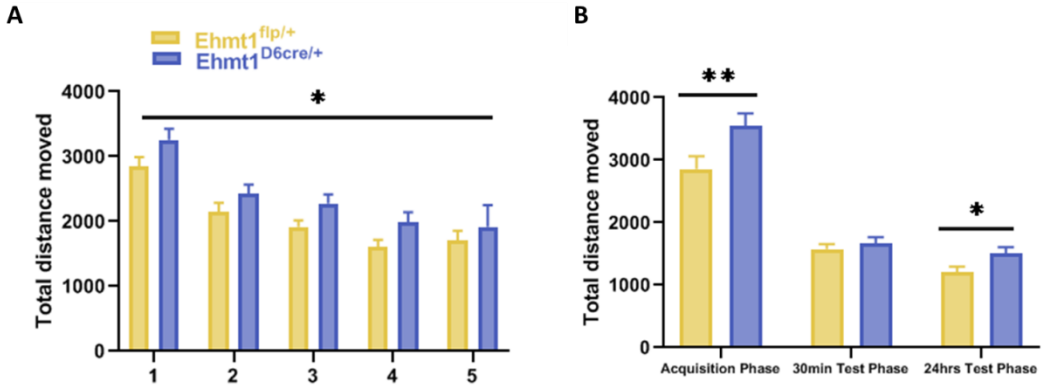

Figure 3.4Total Distanced Moved – NOR task A) Habituation: During the 5 day habituation phase, both groups reduced their total distanced moved between sessions however Ehmt1D6cre/+ mice were hyperactive compared to their Ehmt1fl/+ counterparts, until the last session where there was no difference between the groups. **B)** The addition of novelty in the form of the objects during acquisition leads to an increase in movement in both groups, with the Ehmt1D6cre/+ mice moving significantly more than their Ehmt1fl/+ counterparts. This difference was not seen 30 minutes after acquisition during the first test phase, however it remerges 24 hours after acquisition with the Ehmt1D6cre/+ move more than the Ehmt1fl/+ mice as reactivity to the environment. Data presented as mean values with SEM * *P<0.05, ** P<0.01. Ehmt1*$^{flp/+}$*: 20, Ehmt1*$^{D6cre/+}$*: 17.Ehmt1*$^{D6cre/+}$.

3.3.2. Novel Location memory

Spatial memory was assessed in *Ehmt1*$^{D6cre/+}$ mice using the novel object location paradigm. All mice underwent two tests with separate acquisitions, one where the location of the objects does not change, familiar; and where one object is moved to a different location, novel.

Animals were tested 24 hours after acquisition in both novel and familiar configurations (see methods for paradigm). In the familiar configuration both groups showed no preference for either object location as expected and explored both objects no different to chance (***Ehmt1***$^{fl/+}$ t_{19}=-0.286, p=0.87; ***Ehmt1***$^{D6cre/+}$ t_{16}=-0.706, p=0.74) (Figure 3.5A) There was no significant difference seen between groups (t_{35}= 0.362, p= 0.834). Therefore, there was no difference between the

groups in the number of approaches (***D*****$_{F1}$** $t_{27.574}$=0.231, p=0.873, ***D*****$_{F2}$** t_{35}=0.685, p=0.741) or duration spent exploring (***D*****$_{F1}$** t_{35}=1.209, p=0.389, ***D*****$_{F2}$** t_{35}=0.413, p=0.824) either familiar objects.

When tested under a novel configuration, where one object was placed in a novel location, both groups of mice showed no preference for the novel location (***Ehmt1*****$^{flp/+}$** t_{19}=2.275, p=0.0812, ***Ehmt1*****$^{D6cre/+}$**: t_{16}= 2.488, p=0.07) and explored it no differently to chance. There was no difference between the two groups in their preference 24 hours after acquisition (t_{35}= 0.634, p= 0.747). As expected, both *Ehmt1*$^{fl/+}$ and *Ehmt1*$^{D6cre/+}$ mice made more approaches to the object in the novel location compared to the familiar location and spent more time exploring the novel object (Table 3.3). However, there was no difference between the groups in the number of approaches made to either the familiar (***D*****$_{F}$** t_{35}= -1.905, p=0.065) or novel (***D*****$_{N}$** t_{35}= -1.561, p= 0.239) object locations. The same was found assessing the cumulative duration exploring the object locations (***D*****$_{F}$** t_{35}=0.115, p=0.909, ***D*****$_{N}$** t_{35}= -0.578 p= 0.747). These results show that 24 hours after acquisition both *Ehmt1*$^{D6cre/+}$ and *Ehmt1*$^{fl/+}$ mice display no preference for either object location, suggestive of forgetting the familiar object location.

This apparent forgetting was not due to differential exploration of the acquisition object locations by either group. During the acquisition phase for the novel configuration, both groups spent equivalent times exploring both acquisition objects and locations (***D*****$_{F1}$** t_{35}= -0.262, p= 0.87; ***D*****$_{F2}$** t_{35}= 0.262, p= 0.87) (Figure 3.5B) and made the similar number of approaches (***D*****$_{F1}$** t_{35}= 0.091, p= 0.928; ***D*****$_{F2}$** t_{35}= 0.243, p= 0.873). This was also seen in the acquisition step for the familiar

configuration, with no difference seen in duration spent exploring locations between groups (***D*** $_{F1:}$ U= 175 z=0.154, p=0.909; ***D*** $_{F2:}$ U=183 z= 0.401, p=0.834).

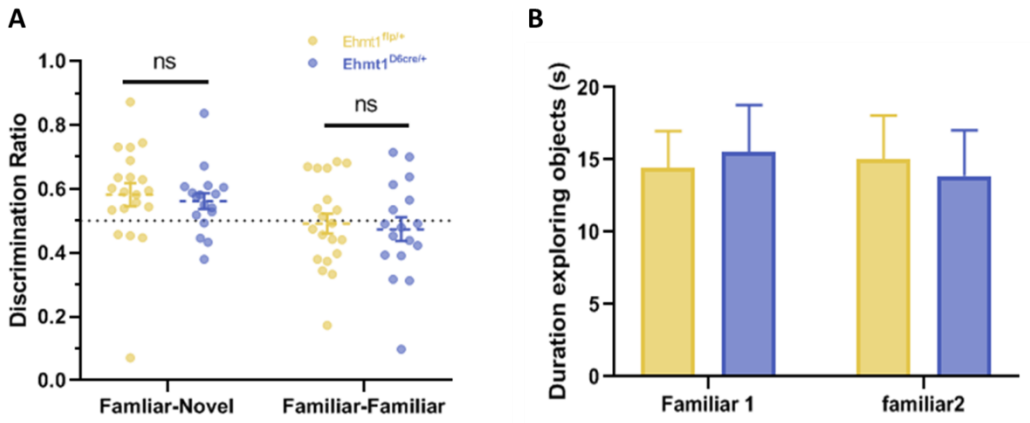

Figure 3.5 Novel Object Location Test and Acquisition. A) Novel object location: Both groups show no preference for the novel configuration 24 hours after acquisition (intercept at 0.5, aka chance). Both groups showed no preference to either object location in the familiar configuration 24 hours after acquisition, and explored both object locations equally**. B)** Time spent exploring objects during acquisition: both groups explored either object equally during the acquisition phase. Data presented as mean values with SEM. *Ehmt1*$^{flp/+}$ *: 20, Ehmt1*$^{D6cre/+}$ *: 17.Ehmt1*$^{D6cre/+.}$

Table 3.3 Summary of frequency and duration spent exploring object location at Novel and Familiar configuration tests 24 hours after acquisition by genotype.

		Familiar Test 24 hours after acquisition		Novel Test 24 hours after acquisition	
Genotype	Parameter	Familiar Object 1	Familiar Object 2	Familiar Object	Novel Object
Ehmt1$^{flp/+}$	Frequency exploring object	10.45 ± 0.59	9.40 ± 0.67	9.90 ± 0.99	11.80 ± 0.94
	Duration exploring object (s)	7.39 1.15	7.02 ± 0.84	10.82 ± 2.98	11.98 ± 1.40
Ehmt1$^{D6cre/+}$	Frequency exploring object	10.71 ± 0.94	10.12 ± 0.82	13.12 ± 1.42	14.47 ± 1.50
	Duration exploring object (s)	12.32 ± 4.22	7.60 ± 1.15	10.41 ± 1.59	13.32 ± 1.91

As in the object recognition task, secondary indices of locomotor activity were measured during the consecutive 4 days of habituation prior to the acquisition phases. Both groups show a comparable pattern of locomotor behaviour. However, here no habituation was seen across the 4 sessions; mice showed no reduction in total distance moved across the sessions (main effect of

SESSION, $F_{3,\ 105}$=3.216, p=0.072). This was not found to be different between groups, with both *Ehmt1*$^{D6cre/+}$ and *Ehmt1*$^{flp/+}$ mice travelling equivalent total distances across the sessions (main effect of GENOTYPE, $F_{1,\ 35}$=3.685, p=0.128). (Figure 3.6A). There was no interaction between GENOTYPE x SESSION.

Again there is an effect of novelty to locomotor activity of the mice. The addition of (novel) objects during both acquisition phases lead an increase in locomotor activity in both *Ehmt1*$^{flp/+}$ and *Ehmt1*$^{D6cre/+}$, measured in total distance moved ($Acquisition_{fam}$ t_{36}= -4.435, p<0.001; $Acquisition_{nov}$ t_{36}= -6.501 p<0.001) compared to their final habituation session. Whilst total distanced moved during the both test phases did not recapitulate the overall novelty-dependent increase in locomotion, the *Ehmt1*$^{D6cre/+}$ group were significantly more active compared to the *Ehmt1*$^{fl/+}$ group in total distance moved in both the familiar test phase ($Test_{fam}$ t_{35}= 3.347, p=0.01) and novel test phase ($Test_{nov}$ t_{35}= -3.692 p=0.007) 24 hours after their respective acquisition phase (Figure 3.6B).

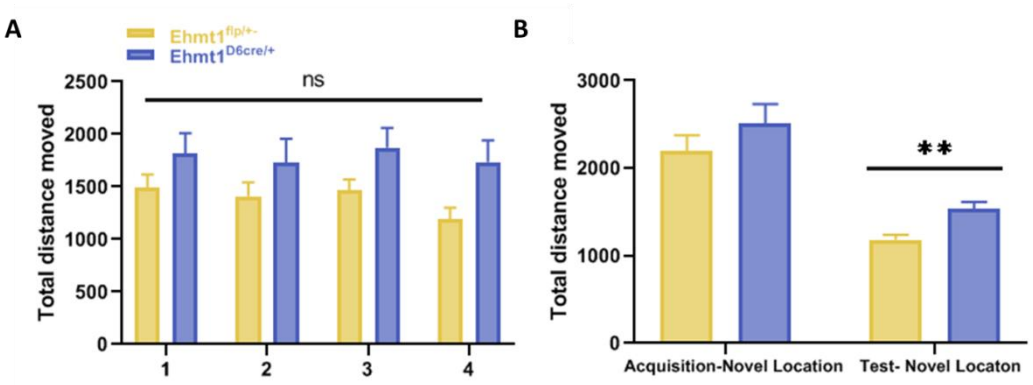

Figure 3.6 Total Distanced Moved – NOR task A) Habituation phase: during the 4 day habituation neither group reduced their locomotor activity, indexed by distance moved. **B)** the addition of novelty in the form of the objects during acquisition and also the change in object location during the novel context test lead to an increase in movement in both groups, with the Ehmt1D6cre/+ mice showing significantly higher locomotor activity, indexed by total distance moved, during the test phase compared to *Ehmt1*$^{flp/+}$ mice. Data presented as mean values with SEM ** *P<0.01, ns nonsignificant. Ehmt1*$^{flp/+}$*: 20, Ehmt1*$^{D6cre/+}$*: 17.Ehmt1*$^{D6cre/+.}$

3.4. Discussion

This chapter focussed on determining the role of *Ehmt1* haploinsufficiency on memory in the forebrain specific knockout mouse model. The role of *Ehmt1* in cognitive functions have been probed previously in spatial, object, and fear memory tasks leading to dissociable effects. *Ehmt1*$^{D6cre/+}$ mice showed reduced long term memory in the novel object recognition task, where a loss of preference for the novel object is seen at 24 hours after acquisition but not 30 minutes after acquisition. This is in contrast to the novel object location test, with both *Ehmt1*$^{flp/+}$ and *Ehmt1*$^{D6cre/+}$ mice showing a loss of preference by 24 hours in the novel configuration. Across both these tasks *Ehmt1*$^{D6cre/+}$ mice also showed increased locomotor activity. This appeared to a differential response to novelty.

Ehmt1$^{D6cre/+}$ underwent a novel object recognition paradigm that tested both their short (30 minute retention interval) and long (24 hour retention interval) term recognition memory. Both groups explored the novel object far greater than chance when tested at 30 minutes. Although absolute levels were reduced, *Ehmt1*$^{fl/+}$ control mice also explored the novel object far greater than chance when tested 24-hours after acquisition. Together these data suggest that in general the task was working as expected. In contrast, when tested 24-hours after acquisition *Ehmt1*$^{D6cre/+}$ mice showed no increased exploration of the novel object, suggesting an impairment of long term recognition memory. Importantly, this deficit is not confounded by difference in exploration during the acquisition phases for the tasks, suggesting that the deficit in recognition memory is not due to the *Ehmt1*$^{D6cre/+}$ mice experience either object differently. Interestingly, although at 30-minutes post-acquisition *Ehmt1*$^{D6cre/+}$ mice did show an increased exploration of

the novel object and a mean discrimination index equivalent to *Ehmt1*$^{fl/+}$ controls, the spread of data is far greater with six animals demonstrating chance or below chance discrimination index (all *Ehmt1*$^{fl/+}$ controls were above chance) (Figure 3.3). This implies that degradation of memory of the familiar object may be occurring soon after acquisition.

In contrast, when tested in the novel object location paradigm, *Ehmt1*$^{D6cre/+}$ mice and *Ehmt1*$^{fl/+}$ controls showed no differential impairment at 24 hours to the novel context, however due to both forgetting, differential retention can't be determined. This could be due to differential sensitivity of the two tasks (i.e. floor or ceiling effects). It is possible that there is a dissociation between deficits in declarative and spatial memory in *Ehmt1*$^{D6cre/+}$ mice, reflective the role of *Ehmt1* in memory circuitry established in the forebrain of the mice.

Novel object recognition has been attributed to the medial temporal lobe, specifically hippocampal and perirhinal cortex regions (Brown & Aggleton 2001). However, the role of the hippocampus in object recognition memory is not clear, with a number of studies supporting hippocampal involvement (Gaskin et al. 2003; Broadbent et al. 2004), and contradicted hippocampal involvement in object recognition (Aggleton et al. 2005; Barker & Warburton 2011). More widely accepted is the role of the perirhinal cortex on the formation and maintenance of recognition memory in a number of sensory domains; visuo-spatial, and tactile (Suzuki et al. 1993). Early gene activation imaging found a disassociation of the roles of the hippocampus and perirhinal cortex (Wan et al. 1999). *C-fos* was activated significantly more in the perirhinal cortex in the presence of novel objects, whereas the hippocampus, and specifically the CA1 region, had a greater

activation of *c-fos* in the presence of novel spatial displays. However the studies have found that the perirhinal cortex and hippocampus work together as part of singular circuit of memory to support object recognition memory (Mumby et al. 2002; Barker & Warburton 2011). In fact, a study has shown that the perirhinal cortex is sufficient for maintenance of object recognition memory in short term; however hippocampal involvement in necessary for longer term object recognition memory (Clark et al. 2000). Beyond this, the prefrontal cortex has also been linked to the recognition of novel objects, with lesions to the mPFC leading to impaired recognition memory (Bachevalier & Mishkin 1986; Meunier et al. 1997; Xiang & Brown 2004). Thus the overall integrity of the medial temporal lobe is important for normal performance in recognition memory, both object and location. However, this is contradicted in a study where bi- and uni-lateral lesioning of the perirhinal cortex and mPFC lead to differing results; a functional interaction of the mPFC and perirhinal cortex was necessary for object-in-place memory but not for object recognition memory (Barker et al. 2007).

Here, evidence of differential impairment in recognition memory via length of retention interval suggests long term memory circuits are specifically impaired in the *Ehmt1*$^{D6cre/+}$ mice. As mentioned above, evidence suggests hippocampal integrity is necessary for long term object recognition memory, which perhaps suggests a role of the *Ehmt1* in hippocampal functioning. Another study has found that antagonism of NMDA receptors in the perirhinal cortex specifically leads to an impairment in long term but not short term recognition memory (Barker et al. 2006), similar to what is seen in the *Ehmt1*$^{D6cre/+}$ mice. Interestingly, electrophysiological analysis of the *Ehmt1*$^{D6/cre+}$ mice shows comparable results to

Ehmt1$^{fl/+}$ mice that were administered ketamine, an NMDA antagonist; this was paired with a reduction of Grin1 protein expression. Regardless it appears that cortical systems of long term object memory are impaired in these mice.

Ehmt1$^{D6cre/+}$ mice show a specific impairment in object discrimination despite unknown, and possibly un-affected spatial memory performance. This is suggestive of a distinct role of *Ehmt1* in the neural circuitry of the prefrontal and perirhinal cortices for object recognition memory, and unimpaired hippocampal functioning. However this is in direct contradiction to studies showing specific hippocampal dysfunction in the *Ehmt1*$^{+/-}$ mouse model. Balemans et al. (2010) found reduced dendritic arborisations and mature spine density in CA1 pyramidal neurons, as well as reduced mEPSCs in these neurons. This was associated with memory deficits in both object recognition (at 10 and 80 minute retention interval but not 40 minutes) and in object location memory at 60 minute retention interval. This result is likely due to the different retention intervals used in each study; a shorter retention interval would be an interesting follow-up in assessing the role of temporal recency to object location memory in *Ehmt1*$^{D6cre/+}$ mice. Likely, the arguably more vital role of the hippocampus in novel object location would reveal an impairment in the *Ehmt1*$^{D6cre/+}$ much earlier than 24 hours. However this may not be the case. There may also be supporting, parallel circuitry that remain unimpaired in our forebrain specific knockout of *Ehmt1* compared to previous work in the full heterozygous mouse model. One such circuitry involves the striatum. In this knockout, *Ehmt1* expression remains unaffected in striatal circuits, of which forms of navigational memory are reliant upon.

Studies have shown the striatum is important for processing landmark-based spatial learning (Doeller et al. 2008), in which the location of an object is determined by the position of another object or landmark. This is in contrast to the role of the hippocampus in making boundary-based judgements on object locations. Arguably, both these types of judgements are made in parallel to determine object location recognition; it may be possible that an unimpaired striatum is sufficient to make object location discrimination. Interestingly a study found that diminishing dopamine everywhere bar the dorsal striatum was sufficient to rescue a number of behavioural phenotypes including spatial memory (Darvas and Palmiter 2009). It could very well be that *Ehmt1* forebrain specific haploinsufficiency is insufficient to cause impairment in object location memory under the current paradigm used, and further probing of performance in navigational tasks such as the Morris water maze, or increasing demand on memory reserves may lead to impairment.

In addition to deficits in declarative memory at 24-hours, the *Ehmt1*$^{D6cre/+}$ mice also showed increased locomotor activity at key points throughout both memory tasks that seemed to co-occur with novelty, either environmental or object. This contrasts with the specific locomotor activity task in chapter 2 where *Ehmt1*$^{D6cre/+}$ mice animals showed no baseline differences in their locomotion. Furthermore, this also corresponds with previous behavioural experiments conducted in these mice, where they spent more time in the novel location during the Novel Place Preference task as well as moved a greater total distance within the outer zone of the open field task (Davis B, unpublished).

Ehmt1$^{D6cre/+}$ mice also appear to have habituation deficits as a part of this novelty induced hyperactivity. Interestingly habituation is considered an important mechanism in learning and memory and is considered a form sensory gating and a basic form of learning (Schmid et al. 2014). Habituation has been attributed to various regions in the brain, notably the hippocampus and prefrontal cortex, where these regions are key to the speedy habituation to novel contexts in humans (Yamaguchi et al. 2004). Increasing novelty has been shown to lead to depreciating activation of hippocampal networks in fMRI in humans (Murty et al. 2013), suggesting normal functioning hippocampus adjust to the presence of novelty and thus decreased vigilance in humans. Interestingly, patients suffering from schizophrenia show deficit in habituation in both the hippocampus and visual cortex, paired with an inability to differentiate old and novel images in the hippocampus (Williams et al. 2013). Thus a lack of habituation may be telling when coupled with previous sensorimotor gating deficits seen in Chapter 2.

3.5. Conclusion

Ehmt1$^{D6cre/+}$ mice show specific and highly delineated phenotypes in their learning and memory. The forebrain specific knockout mouse model shows impairment in longer term recognition memory and not in short term object recognition memory; although the spread of the data may indicate some degradation of object memory soon after acquisition. Moreover, *Ehmt1*$^{D6cre/+}$ mice do not show a discernible deficit in longer term object location memory however a shorter retention interval is necessary. This dissociation differs to that seen in the full heterozygous knockout mouse model and allows for delineation in the possible neural substrates affected by the haploinsufficiency of *Ehmt1* in the forebrain. This mouse model also shows an interesting novelty induced hyperactivity not seen in other baseline activity tasks such as the LMA. This suggests impaired learning of context as well possible deficits in forms of sensory filtering.

Chapter 4 *Ehmt1* in Adult Hippocampal Neurogenesis

4.1. Introduction

Previously believed to be restricted to development, the creation of neurons starts around embryonic day 8 and is now known to persist into adulthood in humans (Ehninger & Kempermann 2008a; Ming & Song 2011; Kempermann et al. 2018). However, adult neurogenesis is canonically restricted to two main regions of the brain; the sub-ventricular zone, and the sub-granular zone (Ming & Song 2011). The former gives rise to neuroblasts that radially migrate to the olfactory bulb and differentiate into interneurons (Yamaguchi et al. 2000; Lledo et al. 2008; Ming & Song 2011). This neurogenic region is far more involved in species in which olfaction is a more notable and important aspect in their behaviour, such as rodents. In fact, neurogenesis in the olfactory bulb is hardly detectable in the relatively less development olfactory system of humans (Bergmann et al. 2015). In contrast, the subgranular zone of the hippocampus is widely studied in human adult neurogenesis due to its importance in memory and executive functioning (Eriksson et al. 1998; Bergmann et al. 2015; Kempermann et al. 2018).

4.1.1. Functional Neuroanatomy of the Dentate Gyrus

Adult hippocampal neurogenesis takes place specifically in the subgranular zone of the dentate gyrus. The subgranular zone generates granule cells, the key excitatory neuron of the dentate gyrus (David & Pierre 2006; Ehninger & Kempermann 2008b; Ehninger & Kempermann 2008a). These cells migrate upward from the subgranular zone into the granule cell layer and form dendritic arbors that project to the molecular layer of the dentate. The molecular layer also

contains local interneurons and projections coming from layer II of the entorhinal cortex (David & Pierre 2006; Amaral et al. 2007). In fact the dentate gyrus is the major connection point of the unidirectional connections from the entorhinal cortex to the hippocampus known as the perforant pathway (Suzuki et al. 1993). The dentate gyrus must therefore play an important role in processing the sensory information from the cortex in memory formation (Kesner 2007).

The dentate gyrus is subdivided into the functionally distinct suprapyramidal and infrapyramidal blades. The suprapyramidal blade consists of region of the granule cell layer that lies between the CA3 and CA1 fields, whilst the infrapyramidal blade is found opposite (Gallitano et al. 2016). The hippocampus can also be specified through its dorso-ventral and septo-temporal axes. Generally, the anterior (dorsal or septal) hippocampus is preferentially involved in learning and memory, whilst the posterior (ventral or temporal) hippocampus is involved inaffective behaviours including anxiety (Snyder et al. 2009; Jinno 2011). Higher levels of new born cells in adulthood are found in anterior hippocampus and specifically in the infrapyramidal blade compared to the posterior hippocampus and suprapyramidal blade of the dentate gyrus (Snyder et al. 2009). The blades also show distinct involvement in behaviour, with the suprapyramidal blade new born neurons are more involved in spatial learning, pattern separation and are preferentially targeted by chronic stress, whereas the infrapyramidal blade has not been found to be involved in many hippocampal related behaviours and has generally lower experience related activity (Snyder et al. 2009; Schmidt et al. 2012; Lieberwirth et al. 2016; Alves et al. 2018). All evidence points towards a remarkably heterogeneous dentate gyrus neuroanatomical structure and

connectivity in which new born granule cells play important and region specific roles.

4.1.2. Epigenetics and Adult hippocampal neurogenesis

Various genetic and epigenetic mechanisms have been associated with adult hippocampal neurogenesis and its regulation. These include transcription factors such as Pax6, Sox, and bHLH factors (Hodge & Hevner 2011), histone deactylases including HDAC1, and histone methyltranferases such as Ehmt1, G9a, and Mll (Lunyak & Rosenfeld 2005; Sun et al. 2011; Levitt & Veenstra-VanderWeele 2015; Hsieh & Zhao 2016; Yao et al. 2016). It is accepted that a highly complex cross talk of these intrinsic factors, along with extrinsic environmental factors, control neurogenesis through the modulation of the different stages of the process. The cell type progression of neural stem cells to mature granule cells involves highly regulated changes in the expression of these intrinsic factors and therefore a perturbation in the expression of one of these factors would thus lead to an impairment in the process of adult hippocampal neurogenesis.

4.1.3. Behavioural impact of adult hippocampal neurogenesis

In the previous chapters, *Ehmt1*$^{D6cre/+}$ mice showed a specific impairment memory and sensorimotor gating, suggestive of an impairment in hippocampal circuitry involved in these two processes. Adult neurogenesis has been linked to both of these phenotypes and thus impairment of this particular process may play a role in the pathology of the haploinsufficiency of *Ehmt1.*

As previously mentioned, adult hippocampal neurogenesis is involved in the formation of memory. It has been confidently attributed to spatial memory, in object location memory, and navigational spatial memory (Snyder et al. 2005;

Snyder et al. 2012; Lieberwirth et al. 2016). In fact inhibiting the neurogenesis process through irradiation impairs the performance of rats in the Morris water maze task (Snyder et al. 2005). It is also attributed to the processing of object recognition memory, although this is less clear. Studies suggest hippocampal integrity and adult hippocampal neurogenesis is involved with recognition memory in a temporally specific manner (Brown & Aggleton 2001).

An important memory formation process that involves neurogenesis is pattern separation. This is refers to the act of separating distinct but similar memory representations. Recollecting memory depends heavily on pattern separation when episodic memory representations bear heavy similarity to one another. The hippocampus, and specifically dentate gyrus, is considered a gateway for pivotal sensory information for the accurate formation of memories (Kesner 2007; Schmidt et al. 2012). In fact adult born granule cells carry out pattern separation and evidence shows a preferential incorporation of recently born adult granule cells for pattern separation in the mouse (Nakashiba et al. 2012). Several experiments have shown adult hipoocampal neurogenesis impacting discrimination power in pattern separation behavioural paradigms in rodents models, including a *Ehmt1*$^{+/-}$ mouse model (Benevento et al. 2017; França et al. 2017).

Neurogenesis has also been associated with sensorimotor gating, and specifically pre-pulse inhibition (PPI), its operational measure. Multiple animal models of developmental genes demonstrate a co-morbidity of neurogenesis and PPI deficits including DISC1, and BDNF (Clapcote et al. 2007; Manning & van den Buuse 2013; Osumi et al. 2015). Due to these associative findings, steps have

been taken to understand the role of neurogenesis in sensorimotor gating. Inhibition of neurogenesis during a critical postnatal period of mouse development leads to PPI deficits in a mouse model (Osumi et al. 2015). This attribution of the functional consequence of neurogenesis may also be region specific with evidence that PPI regulation takes place in the ventral hippocampus (Swerdlow et al. 2004; Snyder et al. 2009), and perhaps neurogenesis in this region are involved in this regulation.

4.1.4. Neurogenesis in neurodevelopmental disorders

It is not a surprise that adult hippocampal neurogenesis has been implicated in a number of neurodevelopmental (Chen et al. 2014; Gigek et al. 2015; Levitt & Veenstra-VanderWeele 2015; Allegra & Caleo 2017; Gilbert & Man 2017) , psychiatric (Osumi et al. 2015; Kang et al. 2016), and neurodegenerative disorders. A large number of autism genes have been implicated in neurogenesis including *LIS1, MECP2, FMR1,*and *PTEN* (Tsujimura et al. 2009; Levitt & Veenstra-VanderWeele 2015; Gilbert & Man 2017). Many of these genes are also implicated in various other neurodevelopmental disorders including intellectual disability and developmental delay. This is suggestive of a common group of genes involved in common endophenotypes in neurodevelopmental disorders. Adult neurogenesis has also been implicated in psychiatric disorders such as schizophrenia and depression. There is vast literature implicating impaired neurogenesis in depression with mechanistic and drug therapy studies. Various antidepressants stimulate adult hippocampal neurogenesis and enact neurogenesis dependant behavioural effects, including imipramine and fluoxetine (Sahay & Hen 2007; Levitt & Veenstra-VanderWeele 2015). Stress resiliency and

anxiety, aspects of depression, are also heavily associated with adult neurogenesis (Snyder et al. 2009; Alves et al. 2018).

Due to the association of adult hippocampal neurogenesis to previously identified behavioural phenotypes in *Ehmt1*$^{D6cre/+}$ mice, as well as the identified role of *Ehmt1*/*G9a* on the progression of cells through the neurogenesis process, it is possible that haploinsufficiency of *Ehmt1* causes an impairment in adult hippocampal neurogenesis. This chapter will investigate the proliferative and neurogenic capacity of *Ehmt1*$^{D6cre/+}$ mice *in vivo*.

4.1.5. Aims

- To assess the effect of *Ehmt1* haploinsufficiency on adult hippocampal neurogenesis in vivo through both short and long BrdU pulse-chase experiment paradigms.

4.2. Methodology

4.2.1. Animals

Experimental animals were generated through breeding *Ehmt1*$^{fl/fl}$ mice with D6-Cre heterozygous mice leading to forebrain specific deletion mouse model (***Ehmt1***$^{D6cre/+}$). ***Ehmt1***$^{fl/+}$ littermates were used as WT controls. Mixed genotype litters were housed together in groups of 3-5 animals per cage. Both female and male mice were used for immunohistochemistry in this chapter. All animals were housed under standard 12hr light – dark cycles, in temperature and humidity controlled environments. Cohort used for short term proliferation consisted of 9 *Ehmt1*$^{D6cre/+}$ and 11 *Ehmt1*$^{flp/+}$ mice. The cohort used for long term survival single BrdU-pulse chase paradigm consisted of 8 *Ehmt1*$^{D6cre/+}$ and 9 *Ehmt1*$^{flp/+}$ mice. The initial pilot BrdU cohort consisted of 3 animals for each genotype.

4.2.2. BrdU injection and Perfusion

BrdU was administered at 8 weeks (12 weeks for the pilot experiment) of age. Mice were given an intraperitoneal injection of 50mg/kg BrdU (Sigma-Aldrich, B5002) in PBS (10mg/ml). Tissue was collected at either 4 hours after injection or 4 weeks after injection for the different paradigms. Mice were terminally anaesthetised with an intraperitoneal injection of Euthatal (200mg/ml, Boehringer Ingelheim) at 150mg/kg and transcardially perfused. First the thorax was opened and the ribcage separated to expose the heart. A perfusion cannula was then inserted into the right ventricle and a small puncture was introduced into the left atrium. An infusion of phosphate-

buffered saline (PBS) was first introduced into the circulatory system to flush out blood before infusing with 4% Paraformaldehyde(Sigma-Aldrich, P6148) in PBS. Brains were then dissected out whole and placed in 4% PFA in PBS for fixation until ready for sectioning; clipping of tails were taken and placed in -20°C degrees for genotyping.

4.2.3. Tissue Processing

For preparation for sectioning, the brains were removed from the fixative and submerged into 30% sucrose solution until the samples had "sunk", indicating enough absorption of solution for cryoprotection. The samples were then positioned in OCT (Tissue-Tek) in correct orientation for coronal sectioning and frozen and stored in -80C to be sectioned. Samples were sectioned into 40um sections using a cryostat, and sections were collected free-floating into 12 well plates filled with ethylene-glycol cryoprotectant. Sections were stored at -20°C in cryoprotectant until used for immunohistochemistry.

4.2.4. Immunohistochemistry

Prior to carrying out immunohistochemistry, the tissue sections were first washed 3 x 30 minutes in PBS to wash out the cryoprotectant. Appropriate wells were selected for each sample for every 6^{th} section across the length of the dentate gyrus (every 10^{th} in the pilot study). To allow for anti-BrdU antibody to access DNA incorporated BrdU, a DNA denaturing step was required. Tissues were incubated in pre-warmed 2M HCl for 30 minutes at 37C. Sections were then blocked in 3% donkey serum in 0.1%

PBST for 2 hours at room temperature. Sections were subsequently incubated in primary antibodies diluted in 0.2% donkey serum in 0.1% PBST overnight at 4°C (mouse anti-BrdU BD Biosciences 1:200, rabbit anti-Ki67 ABCAM 1:1000 / rabbit anti-NeuN ABCAM 1:500) (Table B. 1).

The next day, sections were washed 3 x 30 minutes in 0.2% donkey serum in 0.1% PBST before being incubated in the secondary antibodies diluted in 0.2% donkey serum in 0.1% PBST for 2 hours in the dark at room temperature (Alexa Fluor® 488 Donkey α-mouse; Alexa Fluor® 647 Donkey α-rabbit; 1:1000) (Table B. 1). Sections were then washed once in PBS before nuclei were stained with DAPI (0.5 µg/ml, 1:200) in PBS for 5 minutes. Sections were washed once more in PBS mounting. Tissue sections were carefully mounted onto microscope slides and sealed with coverslips using Flouromount G.

4.2.1. Imaging and Counting

Tissue sections mounted onto microscope slides were imaged on an upright Leica DM600b fluorescence microscope. The dentate gyrus was tile scan imaged and images stitched together. The micrographs were then used for cells counts in ImageJ. Using the Cell counter plugin, total DAPI cells positive for BrdU or Ki67 were counted in the short pulse proliferation paradigm. In the survival pulse-chase paradigm, total numbers of DAPI cells positive for BrdU in the DG was counted and proportion of $BrdU^+$ cells expressing NeuN were analysed.

4.2.2. Statistical Analysis

All data were analysed using SPSS 23 (SPSS, USA). When analysing group differences in proliferation, independent two tailed t-tests were performed. Two-way ANOVA was used when analysing group differences between the proliferation and survival paradigms. A between-subject factors of GENOTYPE, and PROTOCOL was used.

4.3. Results

4.3.1. Pilot study to evaluate proliferation *in vivo*

A pilot study was first conducted on a smaller sample of 3 mice per genotype. Mice were injected with BrdU and brains collected 4 hours after injection. This single short single pulse and chase of BrdU will allow for analysis of adult hippocampal neurogenesis, and specifically the proliferation levels in the mice. Tissue was stained for both BrdU and Ki67, an intracellular marker for proliferation (Figure 4.1).

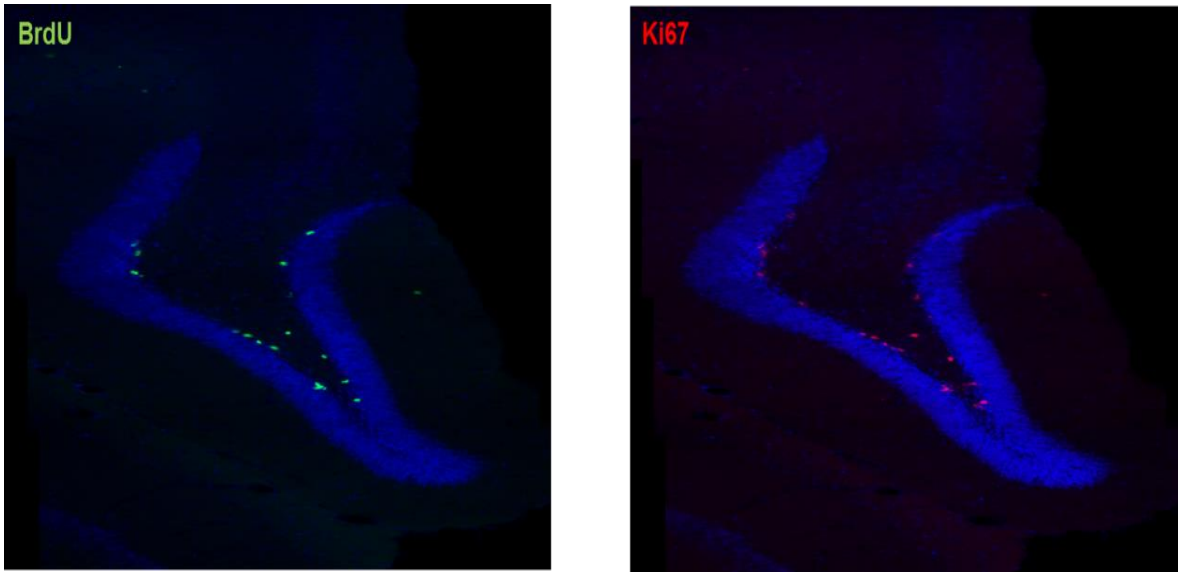

Figure 4.1 In vivo proliferation assay 4 hours following injection with BrdU. Brains were sectioned across the length of the dentate gyrus and stained for proliferative markers BrdU and Ki67. DAPI cells positive for BrdU and Ki67 was manually counted.

The initial pilot study showed no significant differences between BrdU and Ki67 labelled cells in *Ehmt1*$^{D6cre/+}$ and *Ehmt1*$^{flp/+}$ mice. However, this was unsurprising given the low "N". Nevertheless, *Ehmt1*$^{D6cre/+}$ mice had overall larger number of cells stained for either marker. *Ehmt1*$^{flp/+}$ mice had an average of 136 cells positive for BrdU (Figure 4.2), compared to *Ehmt1*$^{D6cre/+}$ mice with 146.7 cells (t_4= -1.543, p= 0.198) (Figure 4.4A).

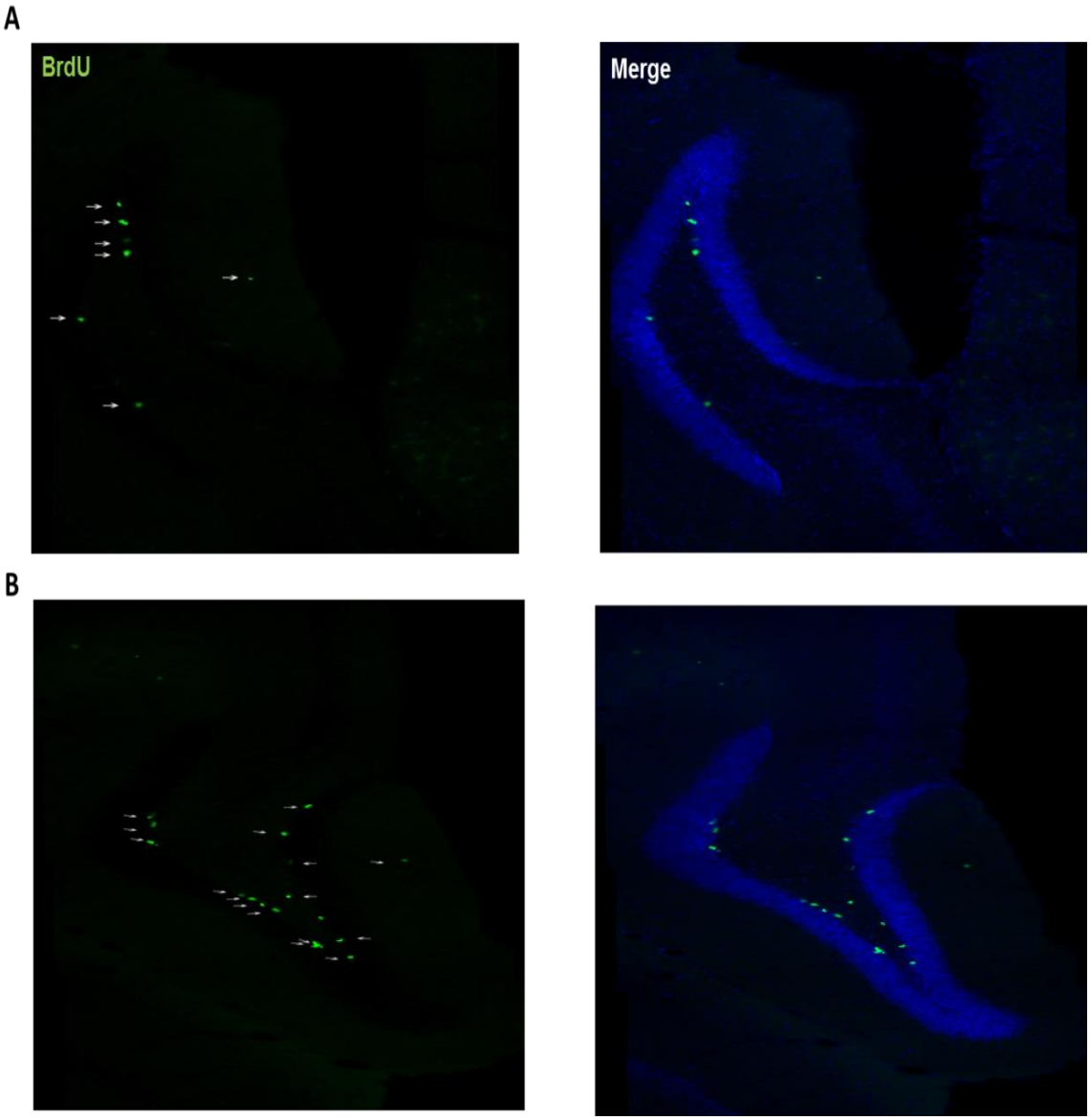

Figure 4.2 BrdU positive cells 4 hours after injection. Sections were immunolabeled for BrdU which incorporates into DNA during the S phase of a cell's cycle**. A)** *Ehmt1*$^{flp/+}$ show a robust incorporation of BrdU in the dentate gyrus. **B)** *Ehmt1*$^{D6cre/+}$ dentate gyrus shows a nonsignificant increase in number of cells expressing BrdU.

Ehmt1$^{D6cre/+}$ also had a higher mean number of Ki67 positive cells (Figure 4.3) at 318.3, whilst *Ehmt1*$^{flp/+}$ mice had an average of 269 cells positive for Ki67 (t_4= -1.464, p= 0.217) (Figure 4.4B).

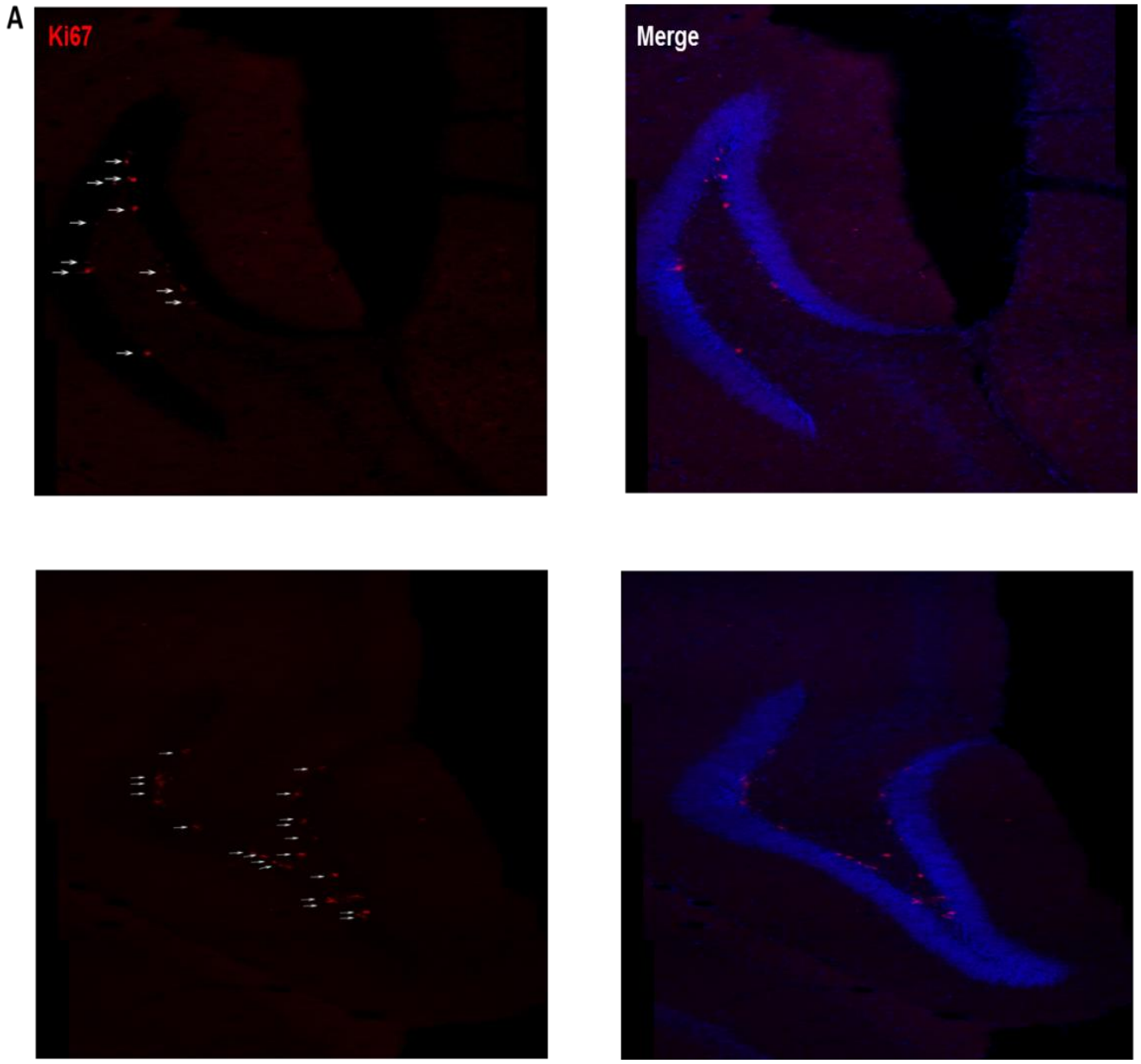

Figure 4.3 Ki67 positive cells 4 hours after injection. Sections were labelled for Ki67, an endogenous marker for proliferation, expressed during most of the mitotic phase of the cell cycle. A) *Ehmt1*$^{flp/+}$ showed positive expression of Ki67 in cells in the subgranular zone of the dentate gyrus. B) *Ehmt1*$^{D6cre/+}$ subgranular zone shows a robust but nonsignificant increase in the mean number of cells expressing Ki67 compared to *Ehmt1*$^{flp/+}$.

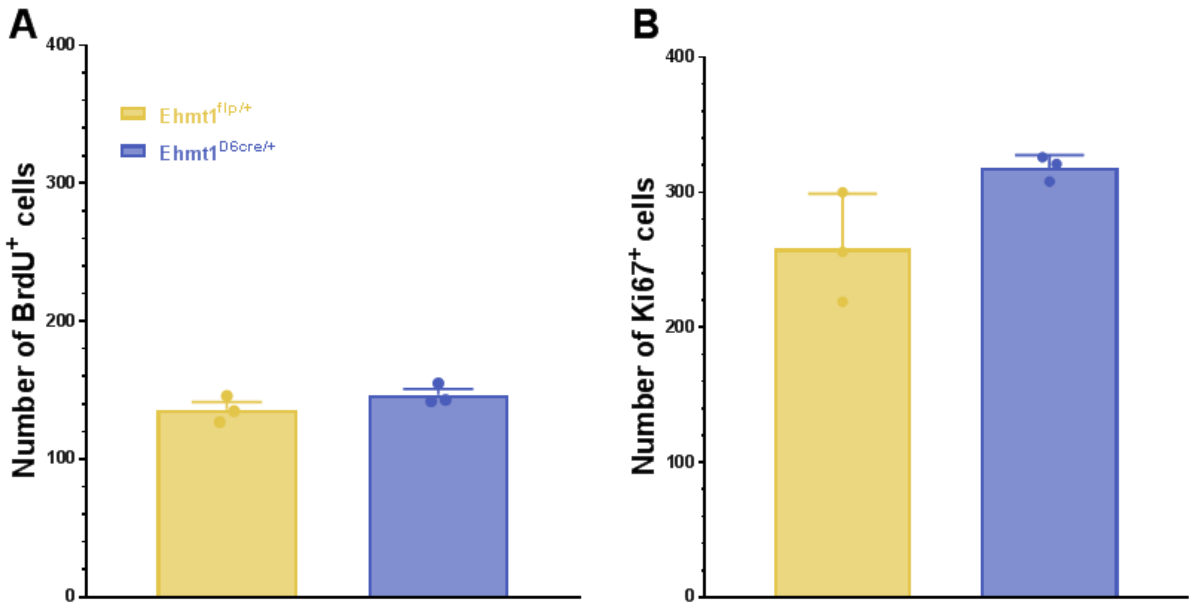

Figure 4.4in vivo Proliferation Pilot study. Numbers of BrdU and Ki67 positive cells across the length of the dentate gyrus in 5 sections were counted. **A)** There was no significant difference in BrdU positive cells between Ehmt1$^{flp/+}$ and Ehmt1$^{D6cre/+}$ mice. **B)** Ehmt1$^{D6cre/+}$ cells had a higher number of cells expressing the proliferative marker Ki67 compared to Ehmt1$^{flp/+}$, but this was not significant.

Consequently, the pilot study proved the experiment to be methodologically valid to measure proliferation differences between genotypes. The experiment was then repeated with a larger sample size and increased section sampling for more accuracy. A separate longer pulse-chase experimental interval of 4 weeks after injection was also implemented to analyse the progression of these cells in the dentate gyrus.

4.3.2. Increased in vivo proliferation in *Ehmt1*$^{D6cre/+}$ mice

Sections from samples collected after 4 hours of injection of BrdU showed an increase in proliferation. The number of BrdU$^+$ cells was significantly increased in the *Ehmt1*$^{D6cre/+}$ brains compared to the *Ehmt1*$^{flp/+}$ samples (t_{18}= -6.198, p <0.001) with a mean number of 465 BrdU$^+$ cells in the *Ehmt1*$^{D6cre/+}$ and 360 cells in the *Ehmt1*$^{flp/+}$ brains

(Figure 4.5A). This increase was also seen in the number of positive Ki67^{+} cells (t_{18}= -5.505, p<0.001) with *Ehmt1*$^{D6cre/+}$ sections having an average of 714 Ki67^{+} cells compared to *Ehmt1*$^{flp/+}$ sections, with a lesser 595 cells (Figure 4.5B).

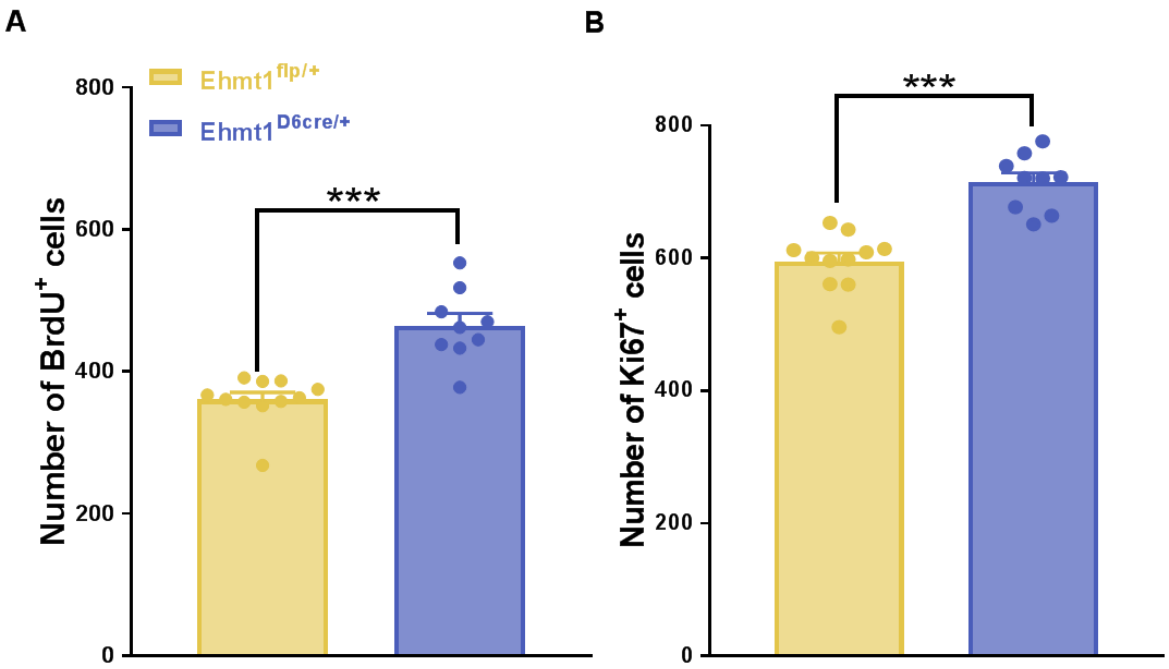

Figure 4.5 *in vivo* Proliferation main study *Ehmt1*$^{D6cre/+}$ dentate gyrus had increased proliferation compared to *Ehmt1*$^{flp/+}$. **A)** *Ehmt1*$^{D6cre/+}$ mice has a higher number of BrdU^{+} cells compared to *Ehmt1*$^{flp/+}$ mice. **B)** *Ehmt1*$^{D6cre/+}$ mice has a higher number of the proliferative marker KI67^{+} cells compared to Ehmt1$^{flp/+}$ mice.

4.3.3. *Ehmt1*$^{D6cre/+}$ does not affect adult hippocampal neurogenesis

The longer pulse-chase paradigm involved a single pulse injection of BrdU, followed by a chase period of 4 weeks. After 4 weeks, tissue was collected. *Ehmt1*$^{D6cre/+}$ and *Ehmt1*$^{flp/+}$ brains had comparable number of Brdu^{+} cells in the dentate gyrus with an average of 251 and 253 BrdU retaining cells respectively (t_{15}= 0.148, 0.885) (Figure 4.6A). To analyse the proportion of BrdU cells that have matured into neurons, sections were co-immunolabelled with NeuN, a neuronal marker first expressed in early mature neurons (Figure 4.7). The number of BrdU^{+} positive cells that were

also NeuN$^+$ was counted and a ratio calculated. Genotype did not have an impact in the proportion of BrdU$^+$/NeuN$^+$ cells in the mice's dentate gyri, with *Ehmt1*$^{D6cre/+}$ and *Ehmt1*$^{flp/+}$ mice having similar proportion of colocalised staining for the markers (t_{15}= -0.507, 0.623) (Figure 4.6B).

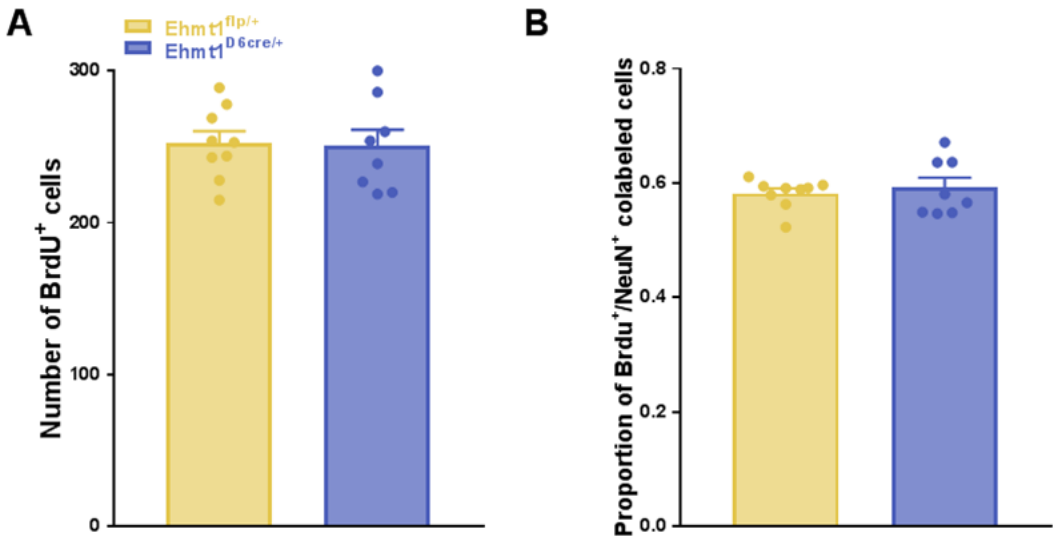

Figure 4.6 4 week single pulse-chase BrdU assay. After 4 week chase period, brains were sectioned and for BrdU and NeuN, and the ratios NeuN neuronal marker was compared to total number of BrdU$^+$ cells stained. **A)** Ehmt1D6cre/+ and Ehmt1$^{flp/+}$ mice had comparable number of BrdU retaining cells 4 weeks after injection. **B)** *Ehmt1*$^{D6cre/+}$ and *Ehmt1*$^{flp/+}$ BrdU$^+$ cells in the dentate gyrus had a comparable proportion co-localising with NeuN.

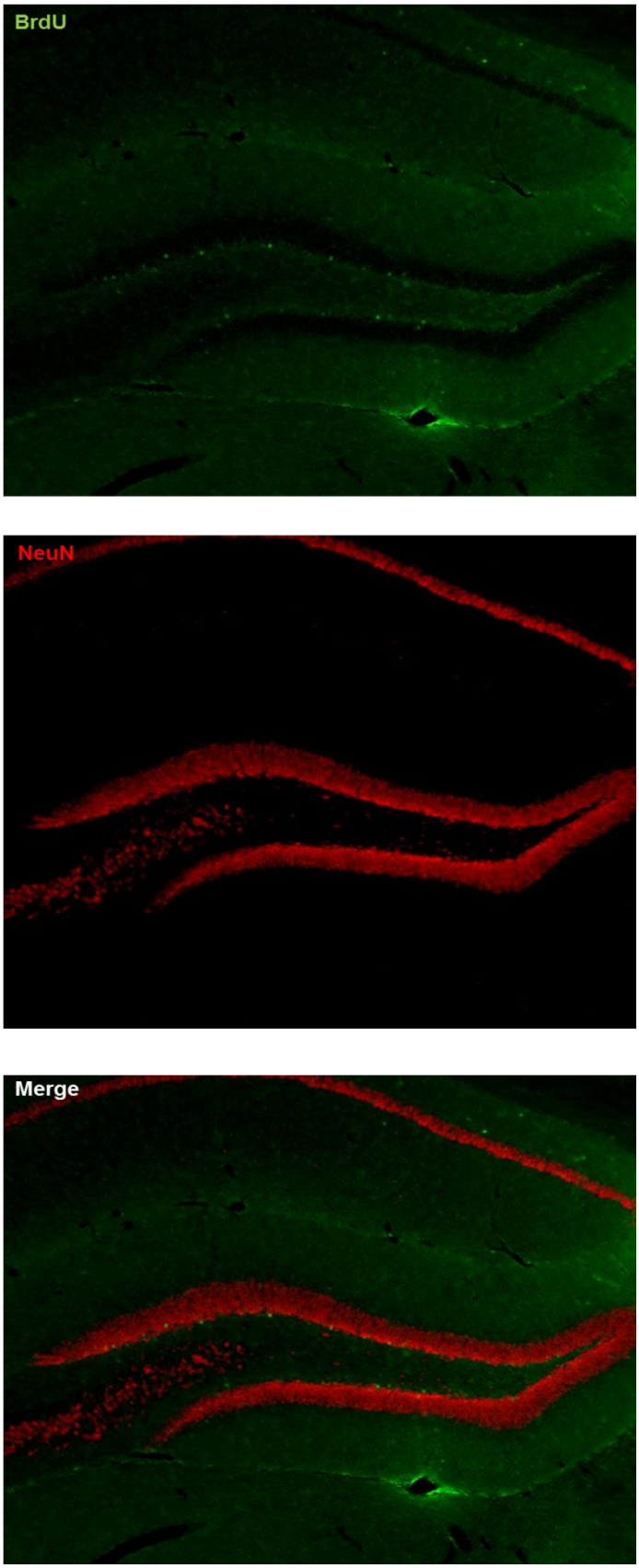

Figure 4.7 Example of BrdU/NeuN immunolabeling. Cells were stained for BrdU and NeuN, and ratio of BrdU positive cells that are NeuN positive were counted to analyse the number of cells that incorportated BrdU that matured into neurons during the 4 week chase period.

4.3.4. No differences in number of BrdU retaining cells between *Ehmt1*$^{D6cre/+}$ and *Ehmt1*$^{flp/+}$ mice

In order to analyse the effects of genotype on the survival of BrdU positive cells, two-way ANOVA was utilised. Here “short” is used to refer to the 4 hour long pulse-chase, whereas “long” refers to the 4 week long pulse-chase BrdU paradigm. Comparing the number of the BrdU$^+$ cells between the two pulse chase durations can allow us to infer whether *Ehmt1* may affect the survival rate of newborn cells. This analysis showed a statistically significant interaction between genotype of the mice and pulse-chase duration for number of BrdU retaining cells ($F_{1, 33}$ = 19.83, p < 0.001, partial η^2 = 0.375), thus one of the variables is impacted by the other variable. Due to the interaction, simple main effects were assessed for each variable at each level.

When analysing the simple main effects of each genotype across each chase period there is a statistical difference in the mean number of BrdU retaining cells within both *Ehmt1*$^{D6cre/+}$ mice ($F_{1, 33}$ = 149.791, p < 0.001, partial η2 = 0.819) and *Ehmt1*$^{flp/+}$ mice ($F_{1, 33}$ = 44.534, p < 0.001, partial η2 = 0.574) taken at 4 hours and 4 weeks after injection (Figure 4.8).

Next, the simple main effects of chase-pulse duration were analysed. Here the genotype of the mice had a significant effect on mean number of BrdU retaining cells in samples taken 4 hours after injection ($F_{1,33}$ = 41.454, p < 0.001, partial η^2 = 0.557), with a statically significance difference in the mean of BrdU$^+$ cells between *Ehmt1*$^{D6cre/+}$ and *Ehmt1*$^{flp/+}$. This difference in the mean is not recapitulated at 4 weeks after injection ($F_{1,33}$ = 0.012, p = 0.913),

and the number of BrdU retaining cells was comparable between genotypes after this pulse-chase duration (Figure 4.8).

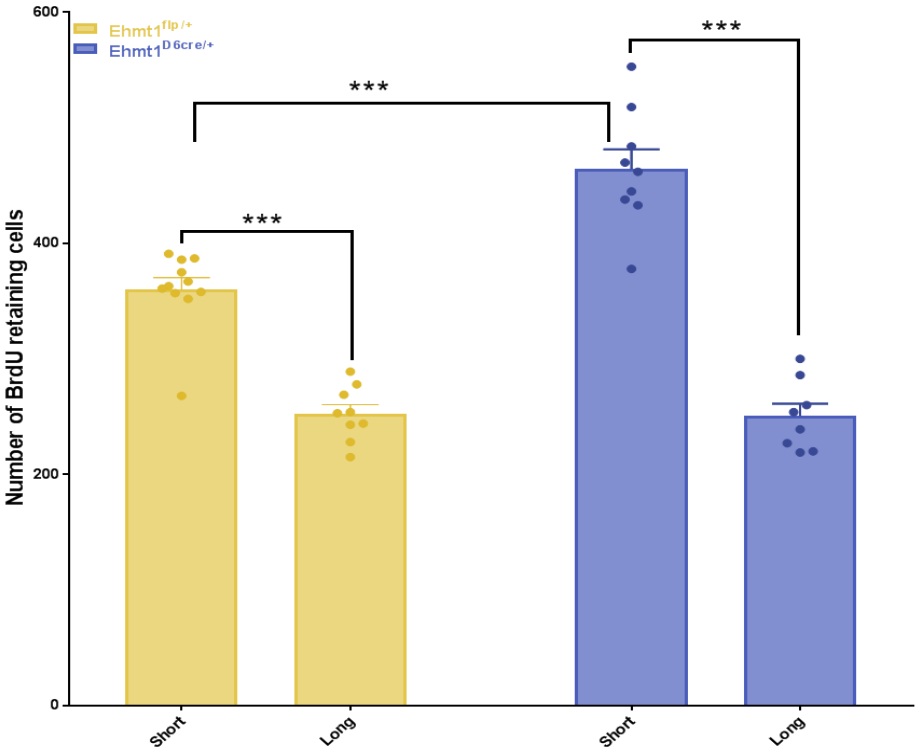

Figure 4.8 Differences in number BrdU retaining cells in short and long pulse-chase paradigms. When analysing the mean number of BrdU retaining cells in the dentate gyrus of *Ehmt1*$^{D6cre/+}$ and *Ehmt1*$^{flp/+}$ mice either 4 hours or 4 weeks after injection, we see there is a significant decrease within genotype in number of BrdU^{+} cells with a long 4 week chase period, compared to the short 4 hours. There is a difference between genotype mean number of BrdU retaining cells during the short pulse-chase duration, but this difference is not seen in samples from the long pulse-chase paradigm.

4.4. Discussion

Here, I examined whether haploinsufficiency of *Ehmt1* altered adult neurogenesis in the hippocampus *in vivo*. *Ehmt1*$^{D6cre/+}$ mice showed a significant increase in new cell production in the hippocampus, with an increase in the proportion of cells labelled for both BrdU and Ki67 compared to *Ehmt1*$^{flp/+}$ control hippocampus following a short 4-hour pulse-chase BrdU paradigm. In contrast, a longer 4-week pulse-chase BrdU experiment revealed no difference in the proportion of BrdU^{+} retaining cells and the proportion of NeuN^{+} (a neuronal marker) cells, nor in the proportion of BrdU retaining cells expressing NeuN, between *Ehmt1*$^{D6cre/+}$ and control mice. Together, these data suggest that although there is an increase in proliferation in *Ehmt1*$^{D6cre/+}$ mice, but that this does not necessarily lead to increased neurogenesis *in vivo.*

An increase in the number BrdU^{+} cells and cells positive for the proliferation marker Ki67 in *Ehmt1*$^{D6cre/+}$ mice relative to controls following a 4-hour BrdU chase experiment is indicative of greater proliferation. Overall, there was a significant reduction in number of BrdU retaining cells in samples that had a 4 week chase period compared to samples taken 4 hours after BrdU pulse. The number of BrdU^{+} cells decrease rapidly over time and stabilises by 4 weeks in the mouse, with the number of BrdU^{+} cells at 4 weeks comparable to the number of BrdU retaining cells at 11 months after last injection (Kempermann et al. 2003). This general reduction in BrdU^{+} cells between the early and 4 week time-points is expected during the progression of neurogenesis. However, at this latter stage any difference between *Ehmt1*$^{D6cre/+}$ and control mice in the number of BrdU^{+} cells had dissapeared.

Therefore, whilst *Ehmt1*$^{D6cre/+}$ mice have an increased proliferative activity in the adult dentate gyrus, this does not necessarily lead to increased adult hippocampal neurogenesis. Moreover, evidence suggests that these new born neurons are electrophysiologically indistinguishable from older neurons (van Praag et al. 2002). Therefore probing survival of BrdU-positive cells after a 4 week chase period provides an accurate assessment of the neurogenic phenotype of the *Ehmt1*$^{D6cre/+}$ mouse model.

In this chapter I examined adult hippocampal neurogenesis as a possible neural mechanism underlying the sensorimotor gating and memory deficits seen in earlier chapters, as well as the cognitive deficits found in other *Ehmt1* haploinsufficiency mouse models. The results presented in this chapter do not directly suggest an impairment in number of neurons born as a cause for the behavioural phenotypes outlined in previous chapters. Nevertheless I did not probe the impact, phenotype, and functioning of neurons born in *Ehmt1*$^{D6cre/+}$, therefore it is possible that other factors such as the incorporation and connectivity of these neurons are impacted by *Ehmt1* haploinsufficiency.

A recent study found an improved pattern separation in *Ehmt1* haploinsufficient mouse model compared to wildtype. This difference was linked to increased adult hippocampal neurogenesis in the model (Benevento et al. 2017). However, this study probed proliferation only and therefore there is no evidence these increased proliferation lead to increased neurogenesis. This is due to various factors including BrdU^{+} cells entering gliogenesis, or undergoing apoptosis during the process. Here the phenotype of increased

proliferation but not neurogenesis could be due to a preference for gliogenesis or vascular changes. However because there is no difference in raw $BrdU^+$ cell numbers after 4 week chase period, it is more credible that the increased number of proliferative cells in the short single pulse-chase experiment are lost through cell death by 4 weeks' time. Therefore this imbalance seen in proliferation may be homeostatically restored. Or specifically, the changes are due to specific impairment in the regulatory systems involved in proliferation, whilst the regulation of cells leaving proliferation and entering the differentiation process in neurogenesis remains intact. However, a maintained increase in proliferation and subsequent loss of these new born cells marked with BrdU may lead to deteriorated neurogenic capacity in older age, with reduction in the proliferative niche. Assessing the proliferative and neurogenic capacity of older *Ehmt1*$^{D6cre/+}$ mice will help further understanding of *Ehmt1* on hippocampal neurogenesis across the lifetime.

These findings are interesting in regards to the behavioural findings in the previous chapters. Memory phenotypes and neurogenesis phenotypes often coincide in literature. Often, it is a reduction of new born neurons that are linked to learning and memory deficits. Here I show that the long term object memory deficits are associated with a transient increase in proliferation in the dentate gyrus. This is suggestive of the a pleiotropic role of *Ehmt1*, and perhaps linking not just a deficit in new born neurons but rather homeostasis of hippocampal neurogenesis to normal cognitive functioning.

This imbalance in proliferation is likely due to the tight epigenetic regulation of proliferation and differentiation markers which have been associated with Ehmt1/G9a (Lunyak & Rosenfeld 2005; Fiszbein et al. 2016; Deimling et al. 2017), along with numerous other epigenetic regulators. This impairment of regulation of cell cycle markers, regardless of directionality, has been attributed as a possible model for neurodevelopmental disorders and autism (Chen et al. 2014; Gigek et al. 2015). Genes including FMR1 and MECP2, associated with Fragile X intellectual disability and Rett Syndrome respectively, have been found to lead to increased proliferation but stunted neurogenesis (Smrt et al. 2007; Tsujimura et al. 2009; Peschansky et al. 2016). NRXN1, associated with autism (Onay et al. 2016), schizophrenia (Kirov et al. 2009), and developmental delay (Zeng et al. 2013), impacted differentiation of neural precursors.

To fully understand the impact of *Ehmt1*$^{D6cre/+}$ on adult hippocampal neurogenesis, further probing is needed. Although there is no difference in base neurogenesis between the genotypes, it would be interesting to see how that fares when comparing BrdU^{+} cells in the suprapyramidal versus infrapyramidal blades, or anterior versus posterior hippocampus. This may delineate in a manner that would have functional consequences to explain the behavioural and cognitive deficits. The increase in proliferation may be due to either a general misregulation of proliferation across all proliferative neural precursor cell types or in a specific increase in one cell type during the process of neurogenesis.

4.5. Conclusions

This chapter focussed on an *in vivo* analysis of *Ehmt1's* role in proliferation and neurogenesis of adult hippocampal cells. *Ehmt1*$^{D6cre/+}$ mice appear to have a temporary neurogenesis phenotype. *Ehmt1*$^{D6cre/+}$ hippocampi have an increased proliferative rate compared to *Ehmt1*$^{flp/+}$ cells. This is seen in an increase in BrdU and Ki67 positive cells in the sub-granular zone of the dentate gyrus. When analysing survival of proliferative cells 4 weeks after incorporation of BrdU, this increased number of BrdU positive cells are no longer found. In fact *Ehmt1*$^{D6cre/+}$ has a comparable levels of BrdU positive cells in the dentate gyrus 4 weeks following BrdU injection. The mice also had comparable level of BrdU positive cells co-labelling for NeuN, a marker for mature neurons. This apparent lack of survival of the larger number of cells labelled early on in the neurogenic track is suggestive of possible increased cell death, or impairment in the process of proliferation, whilst differentiation remains normal.

Chapter 5 In Vitro Analysis of Hippocampal cells

5.1. Introduction

In chapter 4, I analysed the proliferation and neurogenesis of *Ehmt1*$^{D6cre/+}$ mice *in vivo*. These findings showed an apparent increase in proliferation in number of labelled cells after a 4 hour short pulse BrdU experiment in *Ehmt1*$^{D6cre/+}$ mice compared to *Ehmt1*$^{flp/+}$. This increase in labelled cells is not found in mice taken 1 month after initial injection. In order to more extensively probe the phenotype of the hippocampal cells, this chapter focusses on an *in vitro* analysis.

Using *in vitro* methods for cell culture allows for a much simpler analysis of cell types compared to *in vivo*. Here we can further probe the role of *Ehmt1* on the proliferation, differentiation and survival of postnatal hippocampal neural precursor cells. Hippocampal cells are isolated at P7, allowing for the extraction and analysis of NPCs that are closest to the behaviour adult hippocampal NPCs whilst maintaining a high enough yield for experimentation. In this chapter the *in vitro* methods allow us to analyse the effect of *Ehmt1* deficiency on the cell type ratios and the neurogenic developmental track.

It is first necessary to determine whether this proliferation phenotype can be validated *in vitro*. Proliferation assays using cell synthesis incorporation of a label, e.g. BrdU, *in vitro* is a highly accurate and reliable method for extrapolating relative proliferation rates in cell cultures. This

process is similar to the method *in vivo* and allows for reliable comparison across the methods.

5.1.1. *Ehmt1* and *G9a* in Cellular fate specificity

It is generally accepted that increased histone methylation and repressive marks are vital for differentiation and lineage specificity (Wu & Sun 2006; Jobe & Zhao 2017). The histone modification H3K9me2, generally regarded as transcription silencer, plays a role in this cellular commitment. It has been linked to the differentiation and specification of cells in blood, brain, and germline (Chen et al. 2012; Zylicz et al. 2015; Fiszbein et al. 2016; Olsen et al. 2016; Deimling et al. 2017).

Ehmt1 is necessary for normal early development, with homozygous knockout of the gene leading to embryonic lethality, suggesting a role of this gene in the progression and specification of cells (Tachibana et al. 2005). Furthermore, knocking out the related protein *G9a*, leads to impaired retinoic acid induced differentiation *in vitro* (Tachibana et al. 2002; Feldman et al. 2006; Epsztejn-Litman et al. 2008). This is due to the reduction in H3k9me2 marks necessary for prolonged repression of the chromatin in lineage specification and differentiation; *G9a*, and more specifically the E10 included isoform of *G9a* is necessary to promote neuronal differentiation and reinforces cellular specificity and commitment (Fiszbein et al. 2016). This is further exemplified in the fact the *Ehmt1*, and specifically its ability to recognise and bind to H3k9 methylation, was found to be important for silencing of genes involved in pluripotency in response to retinoic acid (Nan

Liu et al. 2015). This evidence shows that *Ehmt1* plays a significant role in the differentiation of NPCs into neurons.

Some of *Ehmt1*/*G9a*'s role in fate specification occurs with the recruitment of the proteins to the RE1-silencing transcription factor (REST) complex (Roopra et al. 2004; Chen et al. 2012). REST is necessary for the coordinating temporal development of the cortex (Ballas et al. 2005; Lunyak & Rosenfeld 2005), and deletion of REST causes impaired repression of pluripotent genes, and is specifically important for the maintenance and subsequent differentiation of type 1 radial glial cells (Soldati et al. 2012).

5.1.2. Neuronal differentiation in hippocampal neurogenesis

In the adult mouse hippocampus, there are a number of cell types within the neurogenic niche of the subgranular zone of the dentate gyrus which together maintains normal levels of adult neurogenesis (Ehninger & Kempermann 2008a; Ehninger & Kempermann 2008b). The first cell type in the neurogenic development track is the type 1 precursor cell. These cells, also referred to as radial glial cells due to their characteristic morphology, are the beginning of adult neurogenesis in the hippocampus (Yamaguchi et al. 2000; Ehninger & Kempermann 2008a; Berg et al. 2018). Type 1 precursor cells maintain a degree of stem cell abilities in which they self-renew allowing for the maintenance of the neurogenic capacity of the hippocampus (Kriegstein & Alvarez-Buylla 2009). Type 1 cells express a number of markers including Glial fibrillary acidic protein (GFAP), Nestin, and sex determining region y-box 2(Sox2) (Yamaguchi et al. 2000; Kriegstein &

Alvarez-Buylla 2009; Kempermann 2016). These cells are also generally quiescent, and divide rather limitedly. However, they are able to asymmetrically divide to give rise to type 2 intermediate precursor cells that are highly mitotic (Filippov et al. 2003; Fukuda et al. 2003; Steiner et al. 2006).

Type 2 intermediate precursor cells can be further delineated to type 2a, and type 2b cells. Type 2a cells maintain expression of the glial marker GFAP but have lost morphological characteristics of type 1 cells (Kempermann et al. 2018). This sets them apart from type 2b precursor cells in which GFAP is no longer expressed and instead neuron markers including neuronal migration protein doublecortin (DCX) and transcription factor Neurogenic differentiation 1 (NeuroD1) are expressed alongside Nestin (Steiner et al. 2006; Kempermann et al. 2018). In this cell type the expression of these markers provide evidence of an increased neuronal specificity not seen in type 1 and type 2a cells. These cells can further asymmetrically divide to type 3 cells (Brandt et al. 2003; Brown et al. 2003).

Type 3 cells are considered low proliferative and lose expression of Nestin but maintain expression of neuron-specific markers DCX and NeuroD among others (Brandt et al. 2003; Brown et al. 2003). These cells go through cell cycle exit and become newly postmitotic neurons (Brandt et al. 2003; Jessberger et al. 2005; Kempermann et al. 2018). These new born neurons express DCX and NeuN among other neuronal markers and go through an early phase of maturation and survival before becoming incorporated as mature neurons in the dentate gyrus (Ehninger & Kempermann 2008a).

The process of advancing through precursor cells types is necessary for the formation of neurons in adult hippocampal neurogenesis and it is this process has been found to go awry in a number of neurological disorders including intellectual disabilities such as Rett and Fragile X syndromes (Pons-Espinal et al. 2013; Allegra & Caleo 2017).

There is a large scientific literature linking functions of various genes linked to intellectual disabilities to the process of adult hippocampal neurogenesis. Deficiency of Ophn-1, linked to X-linked intellectual disability, leads to a significant decrease in survival and maturation of new born neurons in the hippocampus (Khelfaoui et al. 2007; Allegra et al. 2017). FMR4, a long on-coding RNA impacted in Fragile X syndrome, promotes neural precursor proliferation and impairment could therefore contribute to the intellectual disability phenotype of Fragile X syndrome (Peschansky et al. 2016). MeCP2, a gene in which mutations within it is known to cause Rett syndrome, has been linked to both cellular specification of neural precursor cells (Tsujimura et al. 2009), as well as the neuronal maturation of new born post-mitotic neurons (Kishi & Macklis 2004; Smrt et al. 2007).

Due to the known role of *Ehmt1*/*G9a* on cellular specificity and differentiation, and the interesting short term phenotype discovered in chapter 4, it is possible that haploinsufficiency of *Ehmt1* causes an imbalance in progenitor sub types and an impairment in the process of neurogenesis, and specifically the switch between proliferation and differentiation. This chapter will investigate whether there are changes to the process of neurogenesis *in vitro.*

5.1.3. Aims

- To validate *in vivo* findings of increased proliferation *in vitro*
- To assess whether *Ehmt1* deficiency affects the neural lineage pathway of hippocampal NPCs *in vitro*.

5.2. Methodology

5.2.1. Generation of Primary Hippocampal cell cultures

All cultures used in this chapter were generated from P7 pups hippocampal cells isolated in separation, and were maintained in serum-free conditions for 5 days (Figure 5.1). Tissue for genotyping was taken during isolation, and cells were maintained blind to genotype.

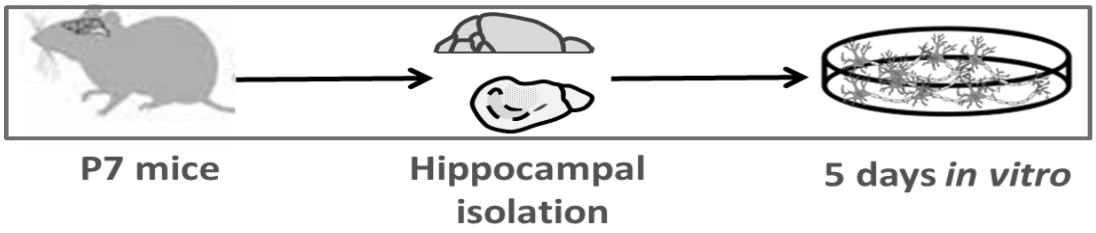

Figure 5.1 Summary of *in vitro* experimentation. Mice were culled at P7, brains were removed from the skull and hippocampi carefully isolated. The tissue was then dissociated and cells were released and then plated on coverslips coated in poly-L-lysine and laminin. The cells were maintained in a serum free medium with growth factors until day 5 *in vitro*, at which point cells underwent the different experiments discussed below.

5.2.1.1. Tissue culture coating

Tissue culture plastic-ware was prepared prior to the isolation. 13mm glass autoclaved coverslips were placed into 24-well plates for individually isolated hippocampal samples. Each well was coated with 350µl of poly-L-lysine (50µg/ml, PLL, Sigma) for 2 hours and incubated at 37˚C. The poly-L-lysine was then removed and the wells washed in sterilised PBS and left to dry for approximately one hour, and 350µl of laminin (10µg/ml, Sigma) in PBS for cell adherence to the glass coverslips. Wells were incubated at 37˚C overnight. On the day of isolations, the laminin was removed and wells washed in PBS once and allowed to dry fully before cell plating.

5.2.1.2. Tissue isolation protocol

7 day old pups from mixed genotype litters were culled by cervical dislocation and decapitated, heads were sprayed with 70% ethanol. Skulls were carefully folded back and their brains removed. The hippocampi of each pup was dissected out carefully, and placed into petri dishes containing cold PBS and were immediately proceeded to the next step. Tissue from each pup was also taken for post-mortem genotyping.

5.2.1.3. Tissue dissociation and cell release

Individual samples were placed on the stage of a Mcilwain Tissue Chopper set to 400µm and were chopped in order to aid tissue dissociation and cell density. Tissue was then immediately transferred into a papain enzymatic disassociation solution for digestion. The solution was made up of pre-filtered Papain (2µl/ml, Sigma) prepared in pre-warmed standard culture medium (Neurobasal A [NBA; Life Technologies], 2% b27 [Life Technologies], 1% Antibiotic [ABX, Life Technologies] and 0.25% Glutamax™ [Life Technologies]). Tissue sections were incubated at 37˚C in the papain solution for 30 minutes.

After the 30 minutes, the tissue was removed from the papain and added to 500µl of prewarmed standard culture medium. The solution was then mechanically triturated to further dissociated cells before being placed on top of an Optiprep (Stemcell Technologies) density gradient in a 1.5ml Eppendorf tube. Optiprep was used to fractionate cells by flotation through a density barrier. The density gradient was made by a carefully layering (to avoid mixing) of 250µl of 10% Optiprep in NBA/BS27/Glutamax medium on

top of a 20% optiprep solution in order to form a clean interface. The gradient was then centrifuged for 15 minutes at 600rcf.

After the centrifugation step, the cell fraction was suspended at the interface and was pipetted up and resuspended in 500µl of fresh standard culture medium in a 1.5 ml Eppendorf tube. The solution was then centrifuged at 250rcf for 5 minutes, pelleting the cell into the bottom of the tube. The supernatant was carefully aspirated and the pellet resuspended in fresh 500µl of standard culture medium ready for cell counting and plating.

Density of cells per ml was calculated using a haemocytometer and cells were further diluted in standard culture medium appropriately to plate at a concentration of $1x10^5$ cells per ml.

5.2.1.4. Cell maintenance

Cells were plated at 500µl per well in the previously prepared and coated 24 well plates at a total cell concentration of $5x10^4$ cells. Cells were then incubated at 37˚C incubator kept at 5% CO_2 and 9% O_2. Two hours after plating, all standard medium was aspirated to remove dead cells that did not adhere to the plate. Wells were then replaced with standard culture medium of NBA/B27/Glutamax supplemented with growth factors: 20ng/ml Epidermal growth factor (EGF, Sigma), and 20ng/ml Fibroblast growth factor (FGF-2, Sigma) to promote survival and growth of cultures. Partial medium change occurs on day 3 *in vitro*, where half the medium with growth factors were replenished. Cells were taken for experiments at 5 DIV.

5.2.2. Primary cell culture assays

5.2.2.1. Proliferation

In vitro proliferation levels were assayed at 5 DIV. 6 hours prior to fixation standard culture medium with growth factors was removed and replaced with 10 µM BrdU in standard medium labelling solution. The cells were then returned into the incubator. During the 6 hours cells were able to incorporate BrdU into their DNA during synthesis. After 6 hours, medium was aspirated and wells washed once with PBS. Cells were then fixed with 50ul of 4% paraformaldehyde (PFA, Sigma) and stained for BrdU (BD Biosciences, 1:250) and Ki67 (Abcam, 1:1000) as markers for proliferation (Table B. 1).

5.2.2.2. Cell phenotype

Cell type phenotypes of primary hippocampal cell cultures were assayed in 5 DIV cell cultures. At DIV 5, standard culture medium was removed and wells were washed once in PBS. Cells were then fixed and stained for neuronal lineage markers: GFAP (ThermoFisher, 1:1000), Nestin (Milipore, 1:500), and Doublecortin (Santa Cruz Biotech, 1:500) for an accurate snapshot of cell type ratios. All nuclei were stained with DAPI (Table B. 1).

5.2.2.3. Caspase induced cell death and cellular stress response

Cell type phenotypes of primary hippocampal cell cultures were assayed in 5 DIV cell cultures. For baseline cell death, standard culture medium was removed and wells were washed once in PBS. Cells were then fixed with 500ul 4% PFA for 30 minutes at 4C and stained for activated

caspase-3, alongside neuronal lineage markers GFAP and Nestin. To assay the cells response to stress, 5DIV all media was aspirated, and replenished with growth-factor and B27 free NBA/Abx/Glutamax media for 8 hours. Cells were then fixed and stained as described for baseline cell death assay (Table B. 1).

5.2.3. Immunocytochemistry

After cells were fixed in 4% PFA for 30 minutes at 4C, they were washed times in PBS and then blocked for 30 minutes at room temperature with 5% Donkey serum and 0.1% triton-X in PBS. The solution was then aspirated and replaced with primary antibodies at 250ul/well in 0.1% PBS-Triton-X overnight at 4C. Cells were then washed three times in PBS before incubated in appropriate secondary antibodies [Alexa Fluor® 488 Donkey α-mouse; Alexa Fluor® 555 Donkey α-rat; Alexa Fluor® 647 Donkey α-rabbit] in 250ul/well 01% PBS-T for two hours in the dark. The antibodies were then removed and cells washed once in PBS before counterstained in DAPI in dH2O for 5 minutes away from light. Coverslips were removed from the wells and mounted face down onto slides in Flouromount-G (Table B. 1).

5.2.4. Imaging and Counting

Coverslips mounted onto microscope slides were imaged on an upright Leica DM600b fluorescence microscope. 8 fields per coverslip were randomly sampled and imaged. The micrographs were then used for cells counts in ImageJ. Total DAPI cells were counted and proportion of cells expressing different stained markers relative to total cells were analysed.

5.2.5. Statistical Analysis

All data were analysed using SPSS 23 (SPSS, USA). When analysing group differences in proliferation and phenotype assays, independent two tailed t-tests were performed. ANOVA was used when analysing caspase induced cell death and cellular stress response with a between subject actor of GENOTYPE, and a within subject factor of PROTOCOL to compare cells that underwent starvation protocol against cells from the same pup that were plated for baseline caspase cell counts.

5.3. Results

In vitro Validation of *in vivo* increase in proliferation

Ehmt1$^{flp/+}$ and *Ehmt1*$^{D6cre/+}$ primary hippocampal cultures were established, and the *in vitro* rate of proliferation as measured at DIV 5. BrdU was incorporated 6 hours prior to fixation. Immunocytochemistry was preformed and cells were labelled for BrdU and Ki67 expression for the identification of proliferating cells (Figure 5.2).

There was no difference in total number of cells counted between genotypes (t_{14}=-0.588, p=0.566), with both *Ehmt1*$^{flp/+}$ and *Ehmt1*$^{D6cre/+}$ cultures have similar number of DAPI stained nuclei (Figure 5.3A).

There was however a significant difference in the ratio of DAPI cells that were also BrdU^{+} or Ki67^{+} cells in the cultures. A higher ratio of DAPI stained cells in *Ehmt1*$^{D6cre/+}$ cultures also expressed both BrdU (Figure 5.3B) and Ki67 (Figure 5.3C) compared to *Ehmt1*$^{flp/+}$ cultures (BrdU [t_{13}=-3.905, p=0.002], Ki67 [t_{14}=-6.794, p<0.001]).

This increase in *in vitro* proliferation of *Ehmt1*$^{D6cre/+}$ hippocampal cells replicates previously discussed changes in *in vivo* adult hippocampal proliferation in *Ehmt1*$^{D6cre/+}$ mice (Chapter 4).

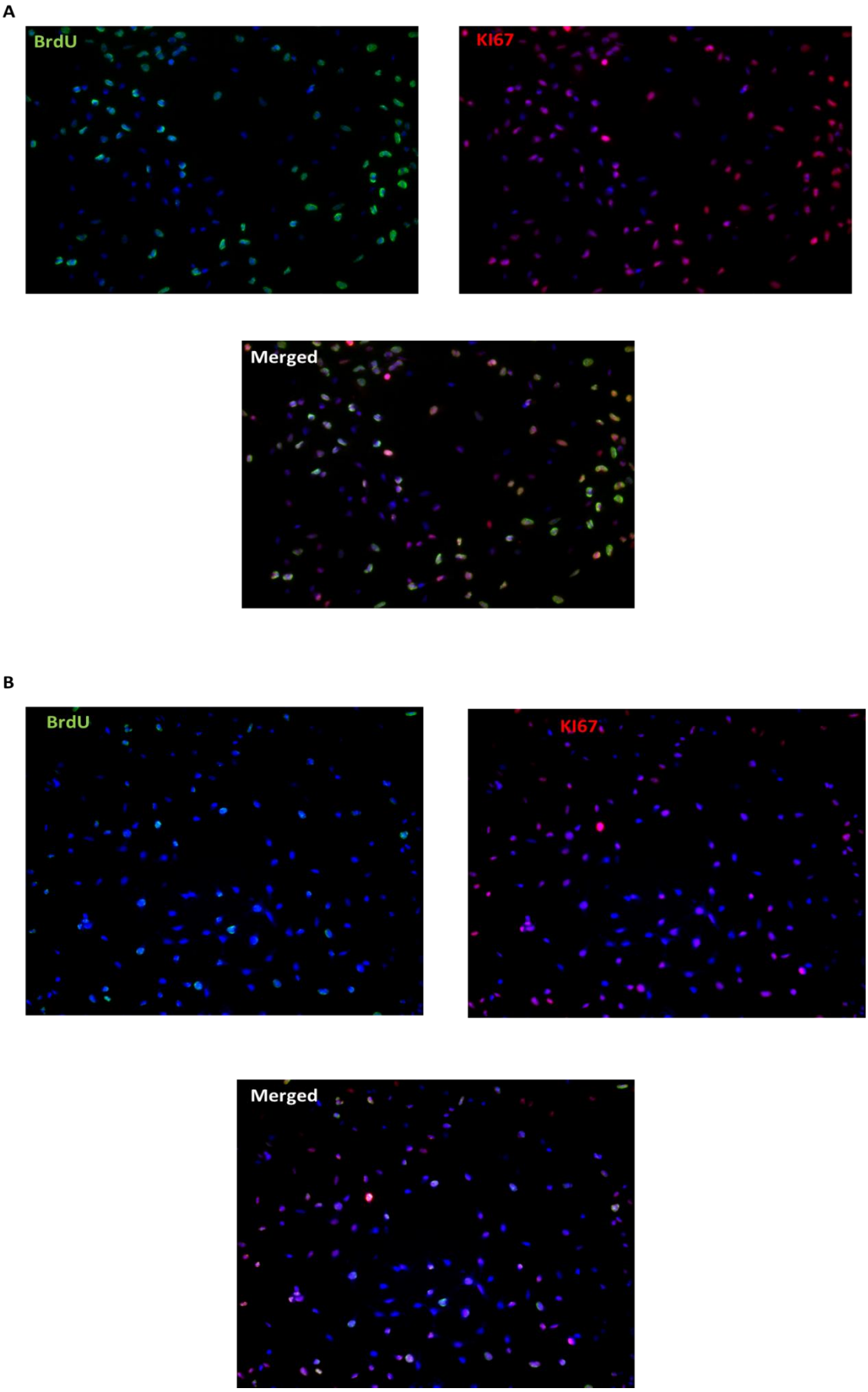

Figure 5.2 *in vitro* proliferation assay. At day 5 *in vitro* cell cultures were incubated with standard medium incorporated with BrdU for 6 hours, after which cells were fixed and stained for proliferative markers BrdU and Ki67. **A)** *Ehmt1*$^{D6cre/+}$ cell cultures showed robust incorporation of BrdU and expression of Ki67. **B)** *Ehmt1*$^{flp/+}$ hippocampal cells showed incorporation of BrdU and expression of Ki67 but to a lesser extent.

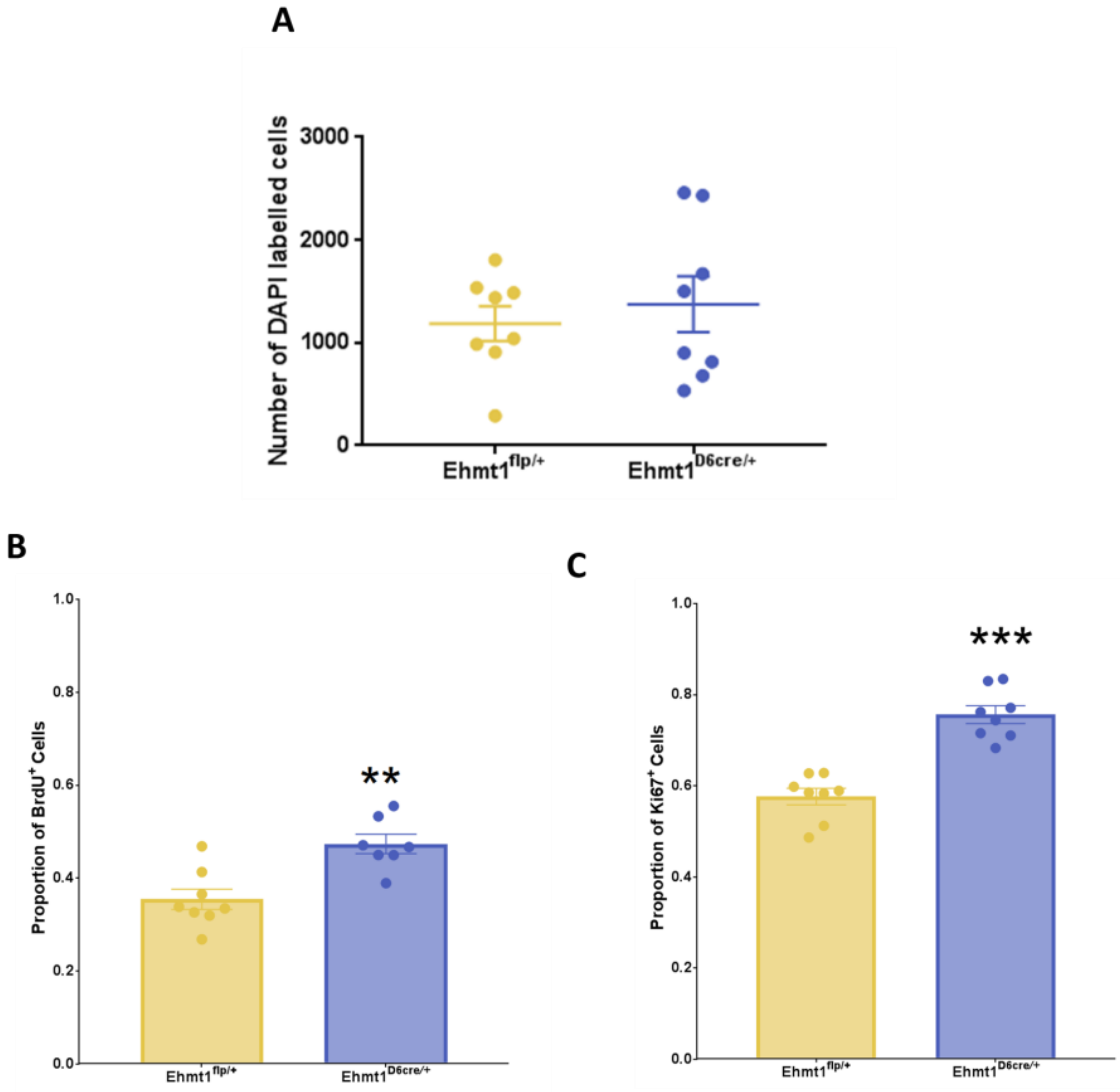

Figure 5.3 *Ehmt1*$^{D6cre/+}$ primary hippocampal cell cultures are more proliferative compared to *Ehmt1*$^{flp/+}$ cell cultures. A) After 6 hours of incubation with BrdU, cells were ficed and stained for BrdU and Ki67, and the ratios of these markers were compared to total number of cells stained. There was no difference between *Ehmt1*$^{D6cre/+}$ and *Ehmt1*$^{flp/+}$ cultures in total number of DAPI stained cells. **B)** *Ehmt1*$^{D6cre/+}$ cells had a higher ratio of BrdU^{+} cells compared to *Ehmt1*$^{flp/+}$ cells. **C)** *Ehmt1*$^{D6cre/+}$ cells had a higher ratio of cells expressing the proliferative marker Ki67 compared to *Ehmt1*$^{flp/+}$ cells.

Ehmt1$^{D6cre/+}$ leads to a dual phenotypic shift in neurogenic lineage proportions

To determine what these differences in proliferation mean in terms of cell type ratios, the phenotype of the cells were investigated. The cells were fixed at DIV 5 and co-stained for neural differentiation markers GFAP,

Nestin, and DCX. Cells co-expressing GFAP and Nestin are classified as radial-glia like type1 and intermediate type2a neural precursors, where Nestin positive cells, not expressing GFAP are classified as a subset of non-GFAP expressing type 2a intermediate prescursors. Nestin and DCX colocalised cells are classified as the more neuronally restricted type 2b transient amplifying precursors, and DCX positive only cells describe cells that are either minimally proliferative type 3 cells, or very early postmitotic neurons. Therefore costaining of these 3 markers of differentiation allows for an extensive snapshot of the phenotype of the primary cell cultures (Figure 5.4).

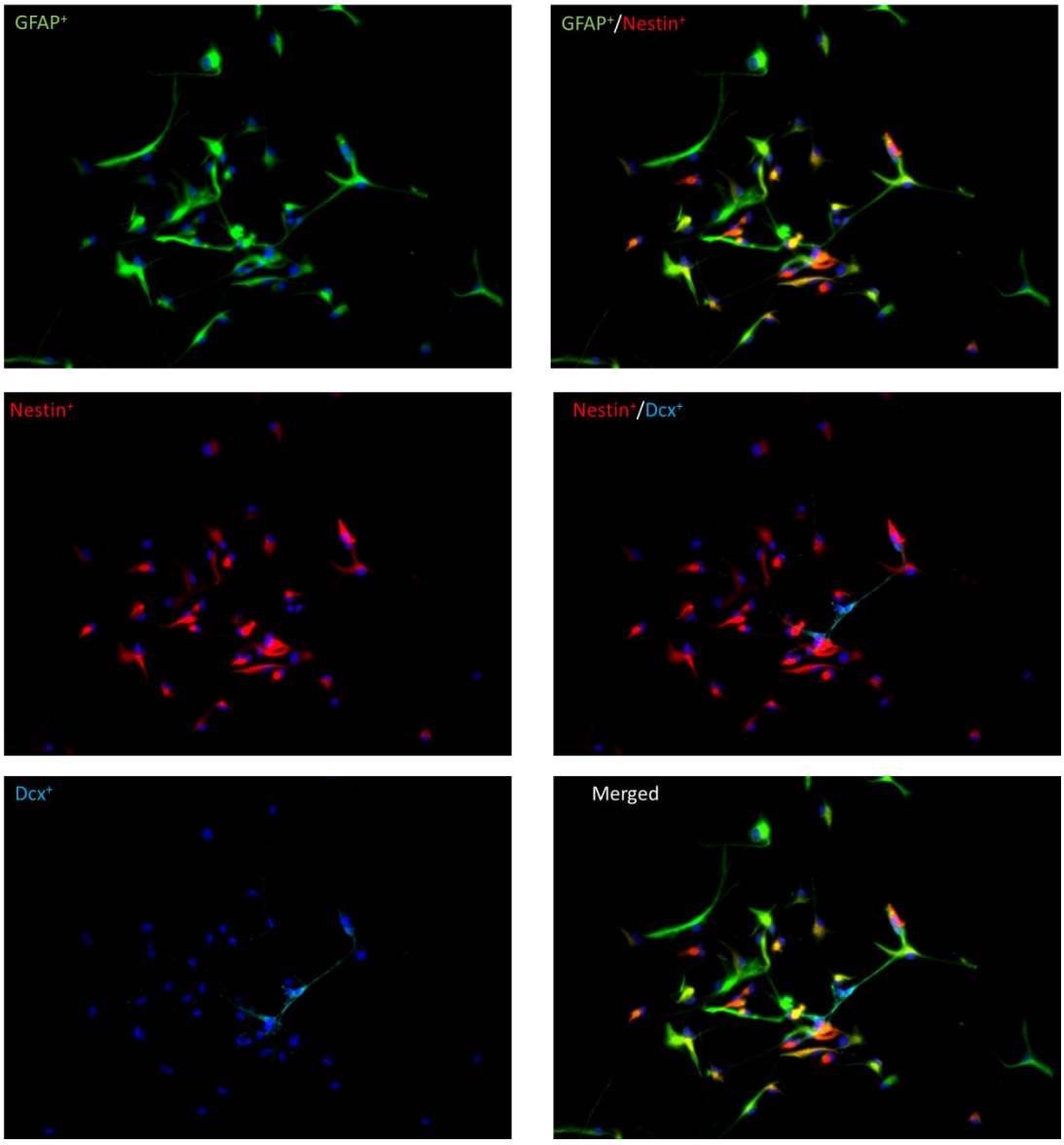

Figure 5.4 Example of Cellular phenotype counting. Cells were stained for GFAP, Nestin and Dcx allowing for an accurate snapshot of the developmental stages of the cell culture to be analysed. $GFAP^+$ only cells are considered glial cells, whilst $GFAP^+/Nestin^+$, $Nestin^+$, $Nestin^+/Dcx^+$, and Dcx^+ cells label the various progenitor subtypes in the process of neurogenesis.

There was a no significant difference in ratio of $DAPI^+$ cells that were also $GFAP^+$, marking astrocytes between the two genotypes (t_{10}=1.689, p=0.122). However when looking at the combination of markers for neural differentiation, there is a significant increase in the proportion of $Nestin^+/GFAP^+$ cells in *Ehmt1*$^{D6cre/+}$ cultures compared to *Ehmt1*$^{flp/+}$ cultures

(t_{10}=-2.409, p=0.037), suggestive of an increase in early proliferative type 1 and type 2a neural precursors (Figure 5.5). This genotype difference disappears when analysing the proportion of type 2a Nestin^{+} cells (t_{10}=0.516, p=0.617) and type 3 Nestin$^{+/}$DCX^{+} cells (t_{10}=0.885, p=0.397).

A genotype difference re-emerges when the proportion of early post-mitotic neurons labelled with DCX. *Ehmt1*$^{flp/+}$ cultures had significantly higher proportion of DAPI stained cells that also expressed DCX compared to *Ehmt1*$^{D6cre/+}$ cultures (t_{10}=3.2, p=0.009), suggesting a decrease in postmitotic neurons in the *Ehmt1*$^{D6cre/+}$ cultures (Figure 5.5).

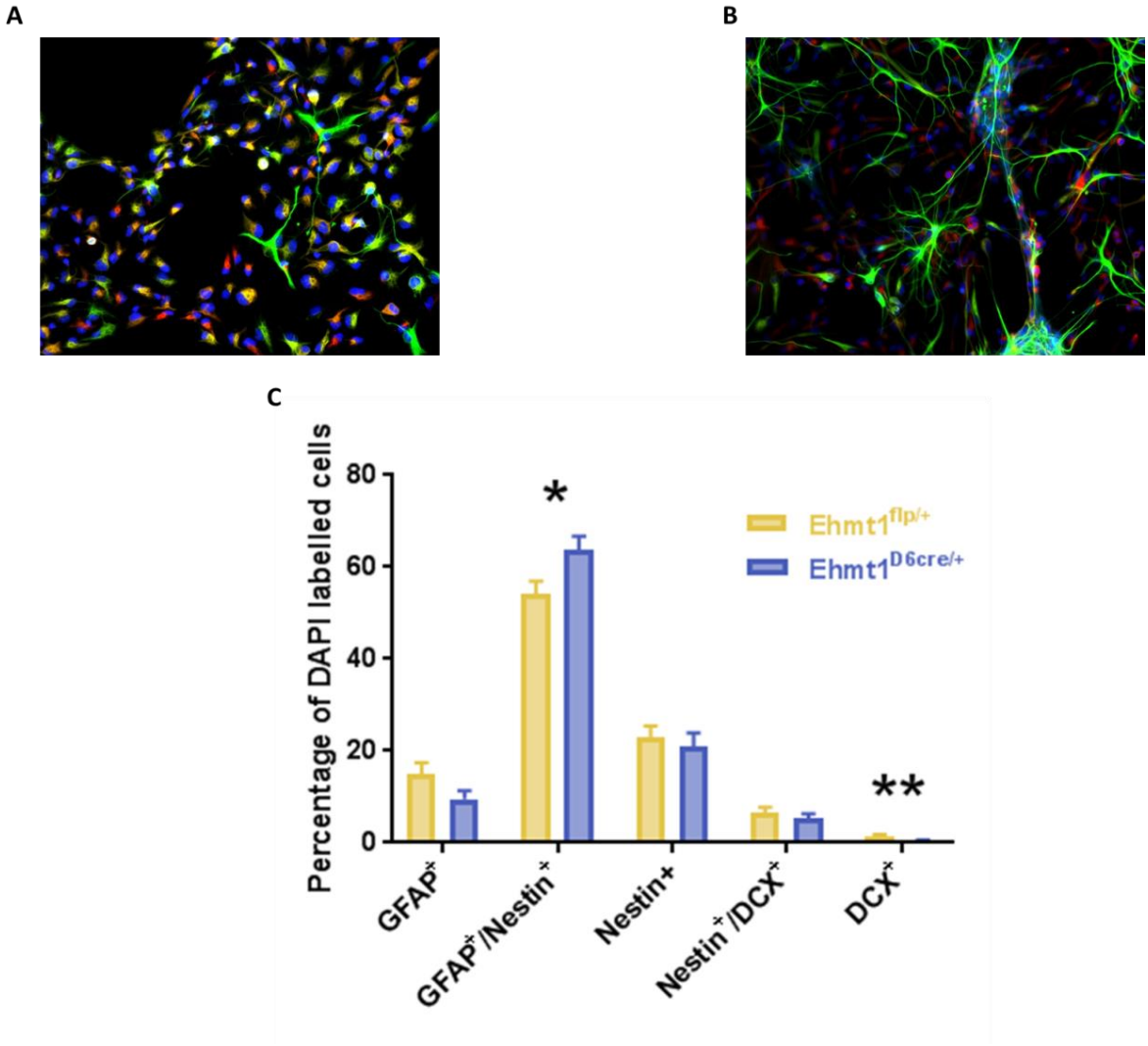

Figure 5.5 *Ehmt1*$^{D6cre/+}$ cells show a phenotypic shift in cellular subtypes. A) A representative image from a *Ehmt1*$^{D6cre/+}$ cell culture. **B)** A representative image from a *Ehmt1*$^{flp/+}$ cell culture **C)** *Ehmt1*$^{D6cre/+}$ hippocampal cell cultures have an increased number of GFAP+/Nestin+ type 1 cells. However despite having more early progenitor cells , *Ehmt1*$^{D6cre/+}$ culture have significantly less Dcx expressing cells, suggesting reduced number of late progenitor and immature neurons compared to *Ehmt1*$^{flp/+}$ cell cultures.

Ehmt1$^{D6cre/+}$ does not affect baseline cell survival or cells resiliency *in vitro*

In order to identify possible cause for the decrease in post mitotic neurons despite the increase in both proliferation and presence of transient

amplifying precursors in *Ehmt1*$^{D6cre/+}$ cultures, baseline cell survival was measured using activated capase-3 as a marker for cell death, and co-stained with Nestin and GFAP to identify any possible cell type specific changes (Figure 5.6A). To determine whether *Ehmt1* deficiency leads to a decrease of cellular resiliency, cultures were also stained for activated caspase-3 after 6 hour long serum-starvation stress protocol (Figure 5.6B).

Virtually all cells stained for caspase-3 in both protocols co-expressed both Nestin and GFAP, marking type 1 and type 2a precursor cells. No differences in proportion of activated capase-3 stained cells in baseline survival cultures, with both *Ehmt1*$^{D6cre/+}$ and *Ehmt1*$^{flp/+}$ cultures having a similar amount of cell death (*Ehmt1*$^{D6cre/+}$ mean=0.116, *Ehmt1*$^{flp/+}$ mean=0.125). There was a significant increase in proportion of cells stained for activated caspase-3 in cultures that underwent serum-starvation protocol compared to baseline (*Ehmt1*$^{D6cre/+}$ mean=0.291, *Ehmt1*$^{flp/+}$ mean=0.280) ($F_{1,18}$=151.511, p<0.001). *Ehmt1*$^{D6cre/+}$ cells did not have a divergent effect to the starvation protocol, with no effect of GENOTYPE x PROTOCOL ($F_{1,18}$=0.589, P=0.453). There was no effect of GENOTYPE ($F_{1,18}$=.014, p=0.909), with both *Ehmt1*$^{D6cre/+}$ and *Ehmt1*$^{flp/+}$ cell cultures having similar expression of activated caspase-3 (Figure 5.7).

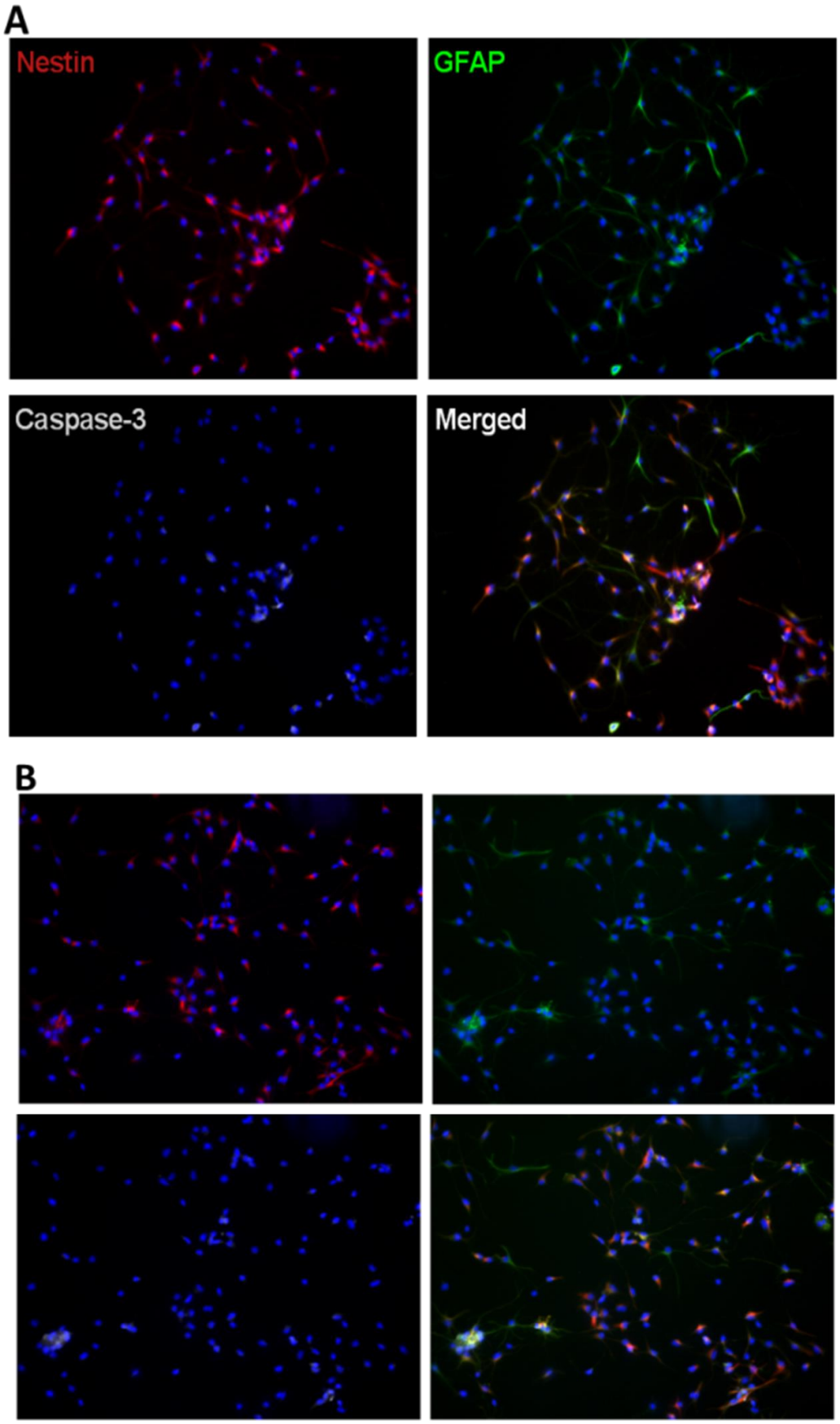

Figure 5.6 Example of Caspase-3 staining with Nestin and GFAP. A) Baseline: cells were taken at DIV 5 and stained for activated caspase-3 and neural markers GFAP and Nestin. **B)** Stressed protocol: Cells were starved for 6 hours before fixed and stained as described. Images show increased staining for caspase-3 in stressed protocol compared to baseline, and thus this is a successful protocol for inducing cell death.

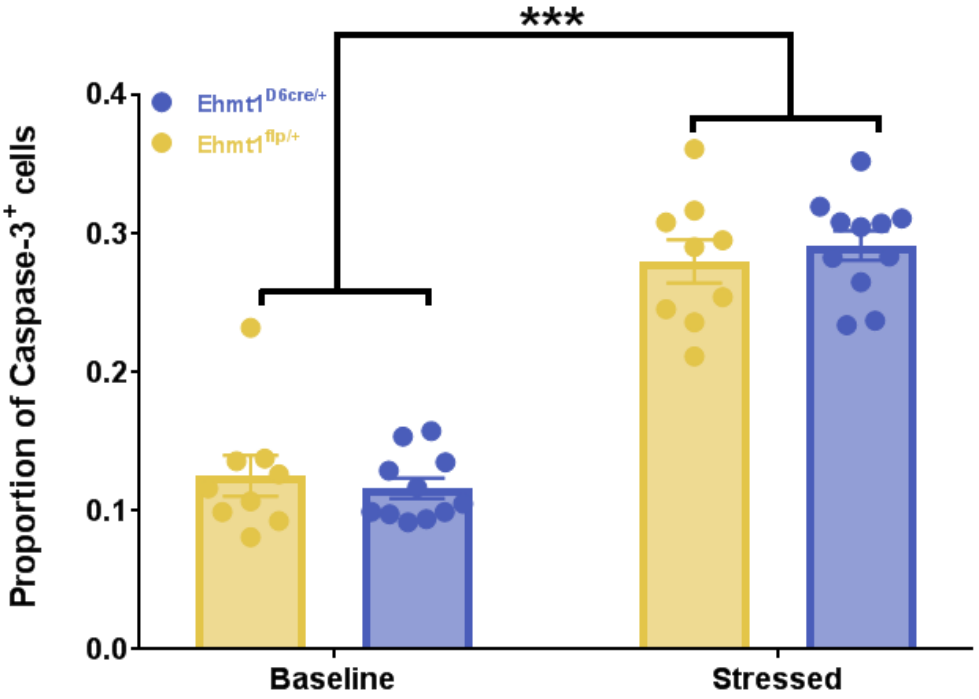

Figure 5.7 *Ehmt1*$^{D6cre/+}$ cells have normal baseline and stressed-induced cell death. *Ehmt1*$^{D6cre/+}$ and *Ehmt1*$^{flp/+}$ cells were measured for both their baseline capase-3 expression and the caspase-3 expression after undergoing a starvation protocol. *Ehmt1*$^{D6cre/+}$ cells showed normal baseline cell survival compared to *Ehmt1*$^{flp/+}$ cells. After undergoing the starvation protocol, caspase-3 expression increased significantly for both groups, however there was no differential effect in cellular resilience in either genotype.

5.4. Discussion

In vitro analysis of *Ehmt1*$^{D6cre/+}$ hippocampal cells show a similar proliferation phenotype as seen *in vivo*, with a significant increase in proportion of cells labelled for both BrdU and Ki67 compared to *Ehmt1*$^{flp/+}$ hippocampal cells. Coupling this with the *in vivo* results shows a definitive increase in proliferative capacity in adult and postnatal hippocampal cells.

Ehmt1$^{D6cre/+}$ cells also show an increase in the number of Nestin^{+}/GFAP^{+} positive cells. This suggests an increase in specifically early proliferative type 1 and type 2a neural precursors. Conversely, *Ehmt1*$^{D6cre/+}$ cells showed a decrease in number of cells staining for DCX, marking late progenitor type 3 cells and early post-mitotic neurons. This is suggestive of a lack of development through the neurogenic track, and the increase in proliferation therefore does not necessarily conclude an increase in neurons *in vitro*.

To further analyse why there is a two pronged phenotype impairment in the *Ehmt1*$^{D6cre/+}$ cell culture, I probed whether there is an increase in cell death occurring In *Ehmt1*$^{D6cre/+}$ cells during the neurogenic track. Interestingly, there was no difference seen in the number of cells staining for activated caspase-3, a marker for apoptosis, between genotypes. This remained true when looking at cell types that stained for caspase-3, with virtually all caspase-3 cells in all cultures were also labelled as Nestin^{+}/GFAP^{+} type 1 and type 2a cells.

Cells were also plated as replicates, allowing for different wells isolated from the same animal to be used in a nutrient serum starvation protocol. This

allowed for the analysis of whether specific cell types in *Ehmt1*$^{D6cre/+}$ cell cultures were more prone to an apoptotic response to cellular stress to account for the phenotypic cell type differences between genotypes. After 6 hours in serum starvation protocol, there was a significant increase in activated capsase-3 labelled cells compared to cells that did not undergo starvation, however there was no difference between genotypes in terms of number of caspase-3 labelled cells or proportion of cells labelled Nestin/GFAP.

The starvation protocol included the removal of growth factors and b27- a nutrient supplement necessary for normal and healthy survival of the cells. Cells are generally able to reduce their energy consumption to survive the starvation, however cells that are less resilient to this form of stress will show an increase in apoptotic activity (Caro-Maldonado & Muñoz-Pinedo, 2011). The process to isolate, dissociate and plate cells involves drastic mechanical stress under normal circumstances and leads to a large amount of cell death at plating, thus mechanical stress during isolation could account for difference in DIV5 cellular phenotypes. However as mimicking the mechanical stress after plating would not be possible, this starvation protocol was chosen as a proxy to stress the cells. In this case, there is no differences in cell death in starvation stress, however it may not be possible to conclude that mechanical stress during isolation is not involved but it could be argued that the *Ehmt1*$^{D6cre/+}$ cells do not appear less resilient to stressful environments compared to *Ehmt1*$^{flp/+}$ cells *in vitro*.

Haploinsufficiency of *Ehmt1* leads to an increase in proliferation, which can be explained by the increase in type 1 progenitors. *Ehmt1*$^{D6cre/+}$ mice therefore have a larger neurogenic/progenitor pool and thus a higher proliferative capacity compared to *Ehmt1*$^{flp/+}$ mice. This increase in proliferation however does not correlate with an increase in newborn neurons in culture. This lack of later stage progenitors and new born neurons are neither associated with increased cell death or reduced cellular resiliency in the *Ehmt1*$^{D6cre/+}$ cell cultures. This provides more evidence towards *Ehmt1's* role in the epigenetic switch between cellular proliferation and differentiation.

Various studies have shown that cellular proliferation and differentiation involves specific, local and highly differential changes to epigenetic repression versus just a global reduction of repression (see: Wu & Sun 2006; Hsieh and Zhao 2016; Yao et al. 2016; Jobe & Zhao 2017) . This is also true for *Ehmt1; Ehmt1/G9a* have been previously associated with the necessary silencing of temporally regulated genes, including proliferative genes, for the development of neurons (Mozzetta et al. 2014). Their epigenetic mark H3K9me2 has been found to have a dynamic presence in neural development as well (Lienert et al. 2011).

Ehmt1's known involvement in neural development is often associated with REST and Polycomb (PRC2) repressive complexes which *Ehmt1/G9a* connect with during development (Ballas et al. 2005; Mozzetta et al. 2014). Both these repressive complexes are found to be important in neuronal development, and specifically in the temporal regulation of genes. REST acts as a scaffold for a number of regulatory enzymes that are recruited to gene

regulation; Ehmt1/*G9a* are recruited to REST and silence target genes (Roopra et al. 2004). REST has been found have a multistage effect in neurogenesis; REST expression is reduced dramatically during stem cell to progenitor transitioning while remaining bound to RE1 sites of target genes primed for expression (Ballas et al. 2005). Upon further differentiation REST unbinds said targets to allow of the expression of genes associated with differentiation (Ballas et al. 2005). This adds to the evidence that differential levels of REST and thus by association *Ehmt1*/*G9a* are necessary for timely coordinating regulation in neurogenesis. Altering expression of these proteins will thus have a differential effect on cells at different stages of neurogenesis as seen in this chapter.

5.5. Conclusions

This chapter focussed on an *in vitro* analysis of *Ehmt1's* role in proliferation and neuronal fate specificity in postnatal hippocampal cells. *Ehmt1*$^{D6cre/+}$ cells show a highly specific neurogenesis phenotype. *Ehmt1*$^{D6cre/+}$ cells have an increased proliferative rate compared to *Ehmt1*$^{flp/+}$ cells. This is associated with an increase in type 1 neural progenitors in the cultures. When analysing the ratio of cell subtypes in the culture, whilst *Ehmt1*$^{D6cre/+}$ cells show an increase in type 1 progenitors, this difference doesn't remain across other neural subtypes. In fact *Ehmt1*$^{D6cre/+}$ has a significant reduction in Dcx^{+}. These cells are either late type 3 progenitor cells, or new born immature neurons in the culture. This apparent lack of progression of early progenitor cells to neurons in *Ehmt1*$^{D6cre/+}$ cell cultures is not associated with any increase in apoptotic activity or decreased cellular resilience to external stress.

This chapter sets out evidence of *Ehmt1's* importance in the dynamic epigenetic regulation of neurogenesis and cell fate specificity using *in vitro* analysis.

Chapter 6 **Retrospective analysis of RNA-Seq data**

6.1. Introduction

Ehmt1's role as an epigenetic regulator represents an important aspect in neurodevelopment and cognition (Shinkai & Tachibana 2011). So far this thesis investigated the role of *Ehmt1* through a forebrain specific haploinsufficient mouse model. This allowed for the assessment and identification of phenotypes associated with *Ehmt1* dysfunction as it relates to cognition, executive functioning and cellular specificity. However to better understand *Ehmt1's* role in gene expression regulation, transcriptomic and epigenomic analyses are required. One such analysis is RNA-Seq, a high through-put method for measuring RNA transcript abundance in tissues and cells. This allows for an unbiased quantification of genes affected by *Ehmt1* dysfunction, and could help pin point biological relevant processes resulting in the endophenotypes observed in previous chapters.

6.1.1. Previous Gene expression analyses of *Ehmt1*

RNA analysis has been used to assess *Ehmt1* reduction in a number of publications. One of the first analyses investigating RNA changes in *Ehmt1* reduction was in the *Ehmt1*$^{camk2a\text{-}cre}$ mouse model conducted using a microarray analysis (Schaefer et al. 2009). This was conducted as a microarray analysis. Comparison of WT and knockdown tissue (striatum, hippocampus, cortex, and hypothalamus) found both a collection of genes marking deficiency of *Ehmt1* across all brain regions, as well as region specific gene expression changes, showing *Ehmt1* has a region specific and

likely a cell type specific function. They also found an upregulation of non-neuronal genes making up a robust portion of the deregulated genes, such as genes expressed in the development of skeletal systems.

Chen et al. (2014) also analysed the molecular consequences of haploinsufficiency of *EHMT1* by a number of next generation sequencing techniques, including RNA-Seq. In human derived fetal brain cells (FBCs), they used shRNA to generate stable *EHMT1* knockdown cell lines. Despite *EHMT1* being regarded as a gene repressor, the study found 409 genes with increased expression patterns and 318 genes with decreased expression, suggestive of ***EHMT1's*** much wider impact. This is corroborated with enrichment seen in processes of development including cellular differentiation.

Recently, Iacano et al. (2018) also used RNA-Seq, combined with ChIP-seq and Bisulfite-Seq, to provide a developmental track of *Ehmt1* haploinsufficiency dependent gene expression changes from postnatal day 1 to 30 in the *Ehmt1*$^{+/-}$ mouse model.

6.1.2. Dataset background

This chapter will be retrospectively analysing the RNA-Seq data available from Benevento et al. (2016) for enrichment in disorders. These authors used primary neuronal cell cultures from E18 rat to conduct analysis of shRNA mediated *Ehmt1* knockdown. In combination, they also examined the effect of TTX (Tetrodotoxin) incubation. TTX, Tetrodotoxin, is a sodium channel blocker that inhibits action potential initiation in neurons triggering synaptic upscaling in networks through the trafficking of receptors to the

post-synaptic membrane in order to return excitatory postsynaptic potentials back to normal levels (Chowdhury & Hell 2018). Although the transcriptional machinery necessary for synaptic upscaling is generally unknown, here the authors demonstrated that *Ehmt1* is necessary for synaptic upscaling through the H3K9me2 repression of BDNF expression (Benevento et al. 2016).

This dataset was chosen as the disruption of homeostatic plasticity is a common pathology across neurodevelopmental disorders including autism spectrum disorders, intellectual disabilities, schizophrenia, and Fragile X Syndrome (Mohn et al. 1999; Südhof 2008; Gao et al. 2010; Jakawich et al. 2010; Soden & Chen 2010; Blackman et al. 2012; Sarti et al. 2013; Wondolowski & Dickman 2013; Della Sala & Pizzorusso 2014). The role of *Ehmt1* in synaptic scaling could therefore explain the role of *Ehmt1* in executive function and cognitive deficits. This also allows for the linking of epigenetic regulation to more developed frameworks of pathology such as 'synaptopathies' of neurodevelopmental disorders. Retrospective mining of this publically available data, using both the non-TTX changes and TTX-related changes, for enrichment in processes and pathways as well as associated disorders can therefore help unearth translatable, cross-species processes and genes in the pathways involved in the development of phenotypes associated with *Ehmt1* haploinsufficiency.

6.1.3. Aims

- To validate the quality and variation in the chosen dataset.
- To analyse functional and phenotype enrichment of gene-sets.
- To analyse enrichment for key neurodevelopmental disorders.

6.2. Methodology

6.2.1. Dataset

This chapter retrospectively analysed publically available data set published in Benevento et al. 2016. The RNA-Seq data was collected on E18 primary cortical neuronal rat cultures. Briefly, the cell cultures were transfected with shRNAs to significantly reduce *Ehmt1* expression by 50% at DIV 0 to create shRNA-treated cells. At DIV 11, both WT and shRNA-transfected cultures were either incubated with TTX for 48 hours for TTX-conditioning, or kept as baseline.

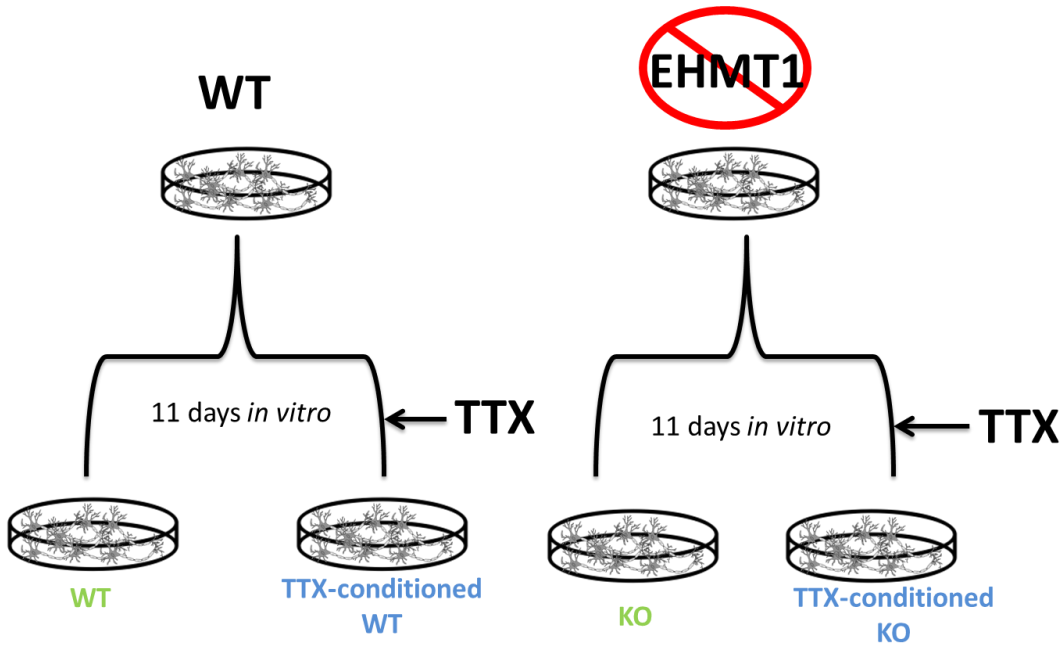

Figure 6.1 Schematic of sample prep. Rat embryonic day 18 cortical neurons were cultured *in vivo;* 6 wells were treated with shRNA, knocking down *Ehmt1* expression on DIV0, whilst 6 were maintained as WT cell cultures. At DIV11, 3 cultures from each WT and ShRNA-transfected cultures were incubated with TTX for 48 hours to induce synaptic upscaling. RNA-seq analysis was done on WT, KO, TTX-conditioned WT, and TTX-conditioned KO cell cultures. WT and KO transcriptomes were compared to find baseline differences in gene expression. TTX-conditioned WT and KO transcriptomes were compared to find conditioned gene expression changes.

Total RNA was treated with ribo-Zero rRNA removal kit. Depleted RNA was resuspended in RNase free water. The RNA-Seq library was prepared with KAPA Hyper prep kit. The libraries were sequenced on the illumina HiSeq, yielding at least 40 million single-end reads per sample. The RNA-Seq libraries were mapped to the rat gnome and read count calculated before DEseq2 was used for differential expression analysis. RNA-Seq data is available on GEO at: GSE68960.

6.2.2. Data validation and Gene Set Selection

Using the excel tables available on GEO, the normalized read counts were independently inputted into Deseq2 for all the samples to verify p-values and calculating log fold changes. This chapter focused on two main pairwise comparisons:

1) The data labelled as “Startpoint_wt_shrna_VS_wt” for the effect of shRNA silencing of *Ehmt1* on neurons; this data is referred to as baseline changes here.

2) The data labelled as “Endpoint_ttx_shrna_VS_ttx” for the effect of shRNA silencing of *Ehmt1* on the TTX incubated samples, this data is labelled as TTX-conditioned changes.

Briefly, “Wt_ttx” and “shrna_ttx” data files were also validated to check for the strength TTX-conditioning in WT samples and transduced samples. These data underwent evaluation for sample and group variation based on treatment or condition.

For human disease enrichment, Differentially expressed genes found in “endpoint” TTX-conditioned samples were compared to “startpoint” baseline samples, and all genes uniquely effected by shRNA silencing of *Ehmt1* after TTX-conditioning were taken as a separate third gene-set labelled “unique”.

6.2.3. Functional Enrichment Analyses

6.2.3.1. Gene Ontology Enrichment

Gene ontology enrichment analyses on each gene-set were performed using the Database for Annotation, Visualization and Integrated Discovery (DAVID) (https://david.ncifcrf.gov/) against a background of all expressed genes in RNA-Seq datasets in *Rattus norvegicus* genome. Enrichment of GO terms was corrected for multiple testing by the Benjamini-Hochberg method with adjusted *p*-values presented in the chapter.

6.2.3.2. MGI Mamallian Phenotype Enrichment

For phenotypic enrichment analysis of phenotypes of associated with mouse mutants, the standardized by Mouse Genome Informatics mammalian phentyope database is used. Specifically, the gene-sets were converted one-to-one human protein coding homologs, and then the human genes were compared against the background gene-set for MGI phenotype using locally developed MGI list containing entrez ids of human protein coding genes that are annotated to mouse phenotypes. A contingency table was made and odd ratio calculated before fisher’s exact test was performed. The significant phenotypic terms corrected by Benjamini-Hochberg’s method for multiple testing.

6.2.4. Gene Set Enrichment Analysis

6.2.4.1. De novo mutations enrichment analysis

Genes associated with *de novo* mutations for schizophrenia, autism, and intellectual disability were compiled from Fromer et al. 2014 for gene set enrichment analysis. In order to model enrichment of *de novo* mutations within the gene sets, *dnenrich* was used. It allows for one-sided pathway enrichment and recurrence analysis, using a binomial distribution to calculate p-value for observed hits per gene-set.

6.2.4.2. De novo SNV analysis

6.2.4.2.A SNV data

Enrichment of *de novo* SNV from autism and schizophrenia patients in the gene sets was tested using a modified Denovolyzer statistical framework as described in Samocha et al. 2014. Here a scaled Poisson distribution analysis was used. Using gene mutation rates provided in Ware et al. 2015, as well as in frame insertion and deletion mutation rates calculated using DDD study methods.

6.2.4.3. Schizophrenia CNV enrichment analysis

6.2.19.1.A CNV studies

Schizophrenia patient CNVs used for the analysis were compiled the following data sets: the International Schizophrenia Consortium (3395 cases, 3185 controls), the Molecular Genetics of Schizophrenia (2215 cases, 2556 controls) study and CLOZUK (6307 cases, 10 675 controls) as used in Clifton et al. 2017. These CNV data sets were annotated with the genes spanning

CNVs. Analyses were performed on CNVs at least 100 kb in size and covered by at least 15 probes, to optimise CNV calling reliability.

6.2.19.1.B Logistic Regression Analysis

Baseline, TTX-conditioned and Unique gene sets underwent enrichment analysis for schizophrenia case CNVs. Using the following covariates: CNV study, chip, CNV size (in kb) and total number of genes hit by the CNV, case status was regressed against overlapping genes for each gene set in a two-tailed analysis.

6.3. Results

6.3.1. Basic evaluation of RNA-Seq data quality

Since the quality of RNA-Seq data can vary, the quality of the publically available RNA-Seq datasets were assessed. First, the Benevento et al. (2016) gene sets used here were validated using deseq-normalised gene expression counts available. Genes corresponding with a deseq p-value of <0.05 were taken for gene set analysis.

Systematic evaluation of the RNA-Seq data using principal component analysis on four key gene expression analyses was conducted. When analysing gene expression pattern of individual samples from baseline WT and shRNA treated cultures, the use of short hairpin RNA to silence *Ehmt1* was enough to adequately separate samples based on gene expression variation (Figure 6.2A).

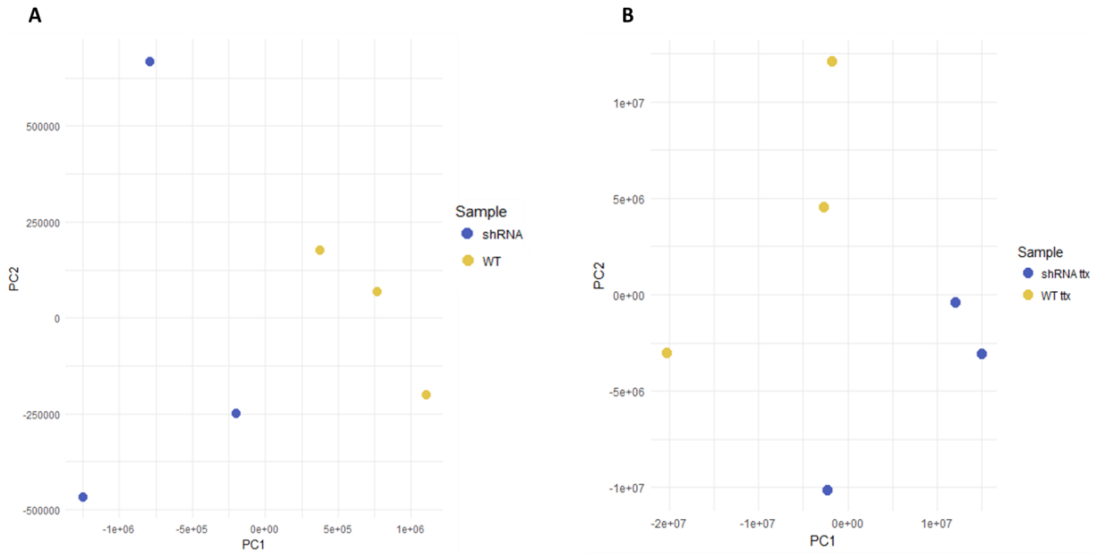

Figure 6.2 PCA plots of baseline and TTX-conditioned samples. A) WT and shRNA treated unconditioned baseline samples plotted on principle components from normalised count gene expression data. **B)** WT and shRNA treated TTX-conditioned samples. Both plots show that samples adequately separate based on shRNA treatment. TTX-conditioning shows specific gene expression characteristics where both shRNA treatment and TTX-conditioning are a driving force of variation in samples.

However when plotting principal components of unconditioned and TTX-conditioned WT or shRNA treated samples, the effect of TTX incubation on gene expression, presented as normalised counts, was not sufficient to cluster samples by condition (Figure 6.3) and thus the effect of TTX on gene expression within sample groups was not a large driving force of variation between treated and untreated cultures.

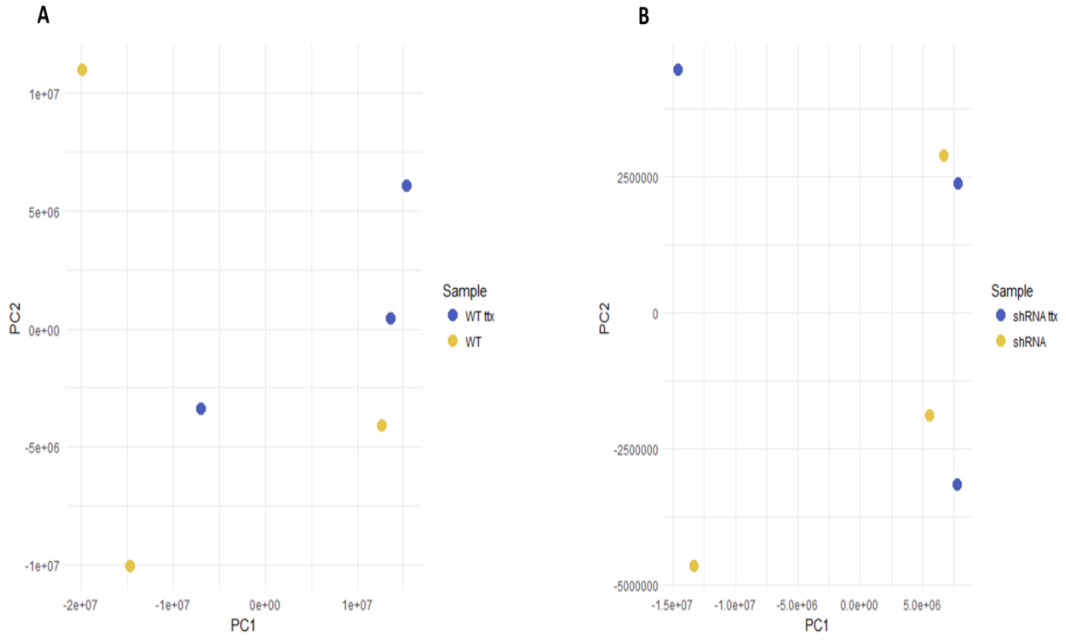

Figure 6.3 PCA plots of baseline versus TTX-conditioned samples. A) WT unconditioned and TTX-conditioned samples plotted on principle components from normalised count gene expression data . **B)** shRNA treated unconditioned and TTX-conditioned samples. Both plots show that TTX-conditioning shows variable, nonspecific gene expression characteristics where TTX-conditioning is not the driving force of variation in samples.

Despite this, the effect of TTX between WT and shRNA treated cultures showed suitable variation between groups, suggesting shRNA treatment and TTX-conditioning interact to effect the gene expression profile, distinct from WT cultures (Figure 6.2)

In fact when looking at the top 500 most variable genes in WT and shRNA treated cultures that underwent TTX- conditioning with a heatmap and dendogram, WT and shRNA treated by group sample, suggestive of highest degree of similarity within samples in the same conditions (Figure 6.4).

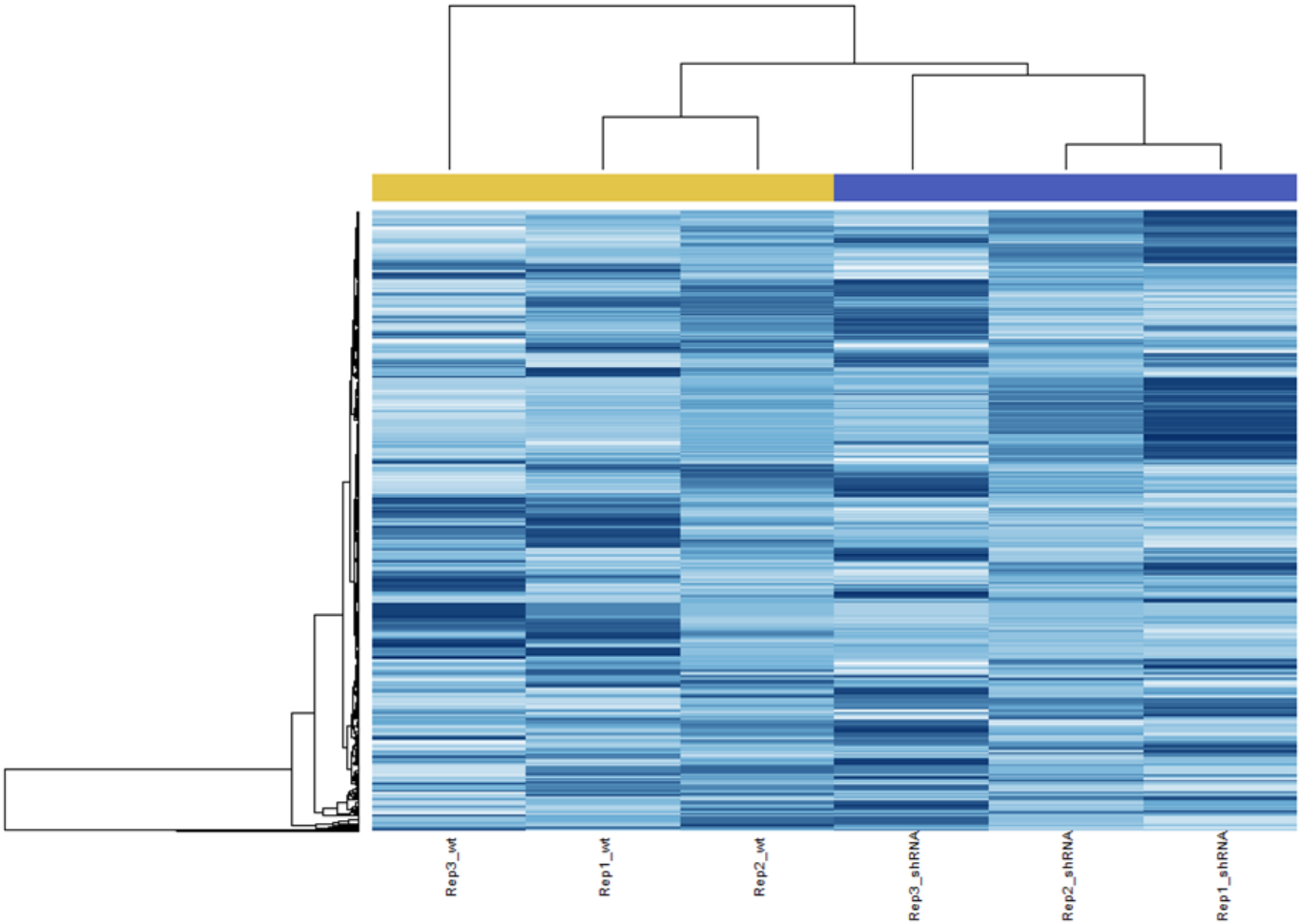

Figure 6.4 Hierarchical clustering and heatmap of TTX-conditioned samples. WT and shRNA treated cell cultures that underwent TTX incubation clustered by group when looking at the top 500 most variable genes. Thus the top genes responsible for the variation cluster together as both shRNA treatment and TTX-conditioning affect gene expression. Yellow samples are WT TTX treated samples,whilst blue samples indicate shRNA TTX treated samples.

6.3.2. Functional Enrichment Analysis

The differentially expressed genes in unconditioned shRNA treated cells compared to WT cells were taken as one gene set referred to baseline changes. Differentially expressed genes in TTX-conditioned shRNA treated cells compared to TTX-conditioned WT cells were taken as the second gene set of interest, and referred to as conditioned changes.

Gene ontology enrichment analysis was performed on these two gene sets to gain insight into the functional properties of genes differentially regulated between both WT and shRNA treated cultures at both baseline and after TTX-conditioning. At baseline, all differentially expressed genes enriched 20 functional groups after FDR adjustment (Table 6.1), including focal adhesion (p= 2.01e-10), driven by downregulated genes (Table C. 1 Gene Ontology Enrichment of differentially DOWNREGULATED genes of baseline WT versus shRNA treated cultures.Table C. 1), protein binding (p= 2.32e-07) that is driven by differentially upregulated genes (Table C. 2), and substantia nigra development (p= 1.32e-05), that does not appear to be driven by up- or down- regulated genes.

Table 6.1 Gene Ontology Enrichment of differentially expressed genes of baseline WT versus shRNA treated cultures.

Term	PValue	Fold Enrichment	FDR
GO:0005925 focal adhesion	2.01E-10	3.253404	2.85E-07
Phosphoprotein	3.93E-10	1.530608	5.28E-07
rno03010:Ribosome	1.04E-09	4.487357	1.35E-06
GO:0043025 neuronal cell body	5.53E-09	2.684058	7.85E-06
GO:0005515 protein binding	2.32E-07	1.774549	3.49E-04
Synapse	2.73E-07	3.178056	3.67E-04
GO:0070062 extracellular exosome	3.21E-07	1.54592	4.56E-04
Methylation	5.59E-07	2.55438	7.51E-04
Cell junction	6.75E-07	2.575622	9.08E-04
Lipoprotein	1.28E-06	2.506011	0.001713
IPR009030:Insulin-like growth factor binding protein, N-terminal	1.32E-06	4.454044	0.002128
Cytoplasm	1.83E-06	1.556061	0.002462
GO:0043209 myelin sheath	2.13E-06	3.54127	0.00302
Ribosomal protein	2.85E-06	3.13904	0.003827
Glycoprotein	4.27E-06	1.577159	0.00574
GO:0031012 extracellular matrix	4.60E-06	3.043341	0.006529
Acetylation	8.42E-06	1.622279	0.011309
GO:0021762 substantia nigra development	1.32E-05	6.765046	0.023215
Cell projection	1.34E-05	2.535273	0.018007
GO:0030054 cell junction	3.44E-05	2.356734	0.048822

In the TTX-conditioned gene set the differentially expressed genes enriched 39 functional groups after FDR adjustment, 16 of which were also found to be enriched in the baseline gene-set (Figure 6.5).

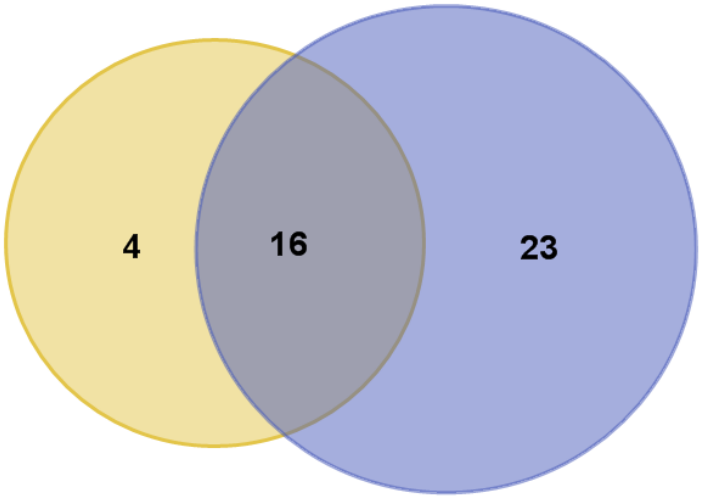

Figure 6.5 Overlap between enriched GO terms at baseline and after TTX-conditioning. Of the 20 enriched GO terms at baseline, 16 remained enriched at TTX-conditioned gene set. TTX-conditioned gene-set also were uniquely overrepresented in 23 other GO terms.

The 23 uniquely enriched in the TTX-conditioned WT vs shRNA differentially expressed gene-set included membrane (p=1.38e-11) and neuron projection (p= 6.03e-08) (Table 6.2). There was a number of processes and terms highly enriched in the differentially upregulated genes (Table C. 4) compared to the downregulated genes in the gene-set (Table C. 3), and contain a number of terms not seen in other gene groups. Differentially upregulated genes in the TTX-conditioned gene-set are statistically overrepresented in processes including response to cocaine (p=1.74e-05) and amphetamine (p2.77e-06), both of which have a relatively high fold enrichments (6.6, and 8.2 respectively) (Table C. 4).

Table 6.2 Gene Ontology Enrichment of differentially expressed genes of TTX-conditioned WT versus shRNA treated cultures.

Term	PValue	Fold Enrichment	FDR
Phosphoprotein	2.32E-30	1.736413118	3.16E-27
Cytoplasm	2.22E-18	1.773492393	3.03E-15
GO:0005737 cytoplasm	1.11E-17	1.425642686	1.63E-14
Methylation	6.55E-16	2.897840779	9.10E-13
GO:0005515 protein binding	8.43E-15	1.855287115	1.34E-11
Acetylation	4.69E-13	1.768001565	6.40E-10
Synapse	6.10E-12	3.132655367	8.32E-09
GO:0016020 membrane	1.38E-11	1.601549233	2.04E-08
GO:0043025 neuronal cell body	1.45E-11	2.401417196	2.13E-08
Cell junction	3.18E-11	2.550581671	4.34E-08
GO:0043209 myelin sheath	5.87E-11	3.538110433	8.67E-08
Alternative splicing	1.21E-10	1.990958896	1.65E-07
Ubl conjugation	1.28E-10	2.095872011	1.74E-07
GO:0030424 axon	1.33E-09	2.580275041	1.96E-06
Cytoskeleton	1.85E-09	2.269204011	2.53E-06
GO:0005925 focal adhesion	4.07E-09	2.444464368	6.02E-06
GO:0030426 growth cone	7.22E-09	3.578815502	1.07E-05
GO:0070062 extracellular exosome	2.55E-08	1.435742388	3.76E-05
GO:0043005 neuron projection	6.03E-08	2.323702265	8.90E-05
Lipoprotein	8.21E-08	2.201461076	1.12E-04
GO:0030054 cell junction	8.99E-08	2.271900707	1.33E-04
Glycoprotein	1.55E-07	1.487261213	2.11E-04
GO:0044822 poly(A) RNA binding	1.69E-07	1.684077491	2.69E-04
GO:0030425 dendrite	4.22E-07	2.088433449	6.23E-04
GO:0045202 synapse	7.50E-07	2.42281528	0.001107844
GO:0042552 myelination	8.42E-07	5.057978539	0.001545078
IPR009030:Insulin-like growth factor binding protein, N-terminal	8.90E-07	3.401428223	0.001503939
GO:0048709 oligodendrocyte differentiation	1.66E-06	5.636033229	0.003047829
Cell projection	4.04E-06	2.161539019	0.005507852
Nucleotide-binding	5.36E-06	1.552409361	0.007315787
GO:0043204 perikaryon	6.21E-06	2.941900639	0.009172886
GO:0043195 terminal bouton	7.64E-06	3.196252465	0.011278817
GO:0030027 lamellipodium	1.21E-05	2.828020615	0.017894019
Isopeptide bond	1.22E-05	1.957232596	0.016583378
RNA-binding	1.28E-05	2.243042071	0.017450419
GO:0005856 cytoskeleton	2.24E-05	2.349349767	0.033127725
GO:0007420 brain development	2.59E-05	2.163412603	0.047420318
GO:0005829 cytosol	2.99E-05	1.435872626	0.044079996
Cytoplasmic vesicle	3.51E-05	2.196625652	0.047836943

6.3.3. MGI Mammalian Phenotype Enrichment

In order to complement the gene ontology functional enrichment and to gain insight on phenotypes that could be translatable in *Ehmt1*$^{D6cre/+}$ mouse

model, the gene-sets of interest were analysed for enrichment using the MGI mammalian phenotype database.

When analysing all differentially expressed genes at baseline WT vs shRNA samples, we see enrichment in 4 mammalian phenotype terms (Table 6.3). This is driven primarily by the differentially upregulated genes, with an additional 6 mammalian phenotypes found to be enriched (Table C. 5). No enrichment was found when analysing the differentially downregulated genes. The enriched phenotypes are broadly categorised into three areas; anxiety and affect behaviour, synaptic transmission, and learning behaviour and deficits.

Table 6.3 MGI Mammalian phenotype enrichment of differentially expressed genes of baseline WT versus shRNA treated cultures.

MP Terms	P	FDR
MP:0003633_abnormal_nervous_system_physiology	1.14E-06	0.005146
MP:0014114_abnormal_cognition	5.19E-06	0.007801
MP:0002063_abnormal_learning/memory/conditioning	5.19E-06	0.007801
MP:0002572_abnormal_emotion/affect_behavior	3.58E-05	0.04039

The number of enriched phenotypes in differentially expressed genes from TTX-conditioned WT vs shRNA treated cultures was considerably higher at 42, with all 4 enriched phenotypes at baseline present. Again most phenotypes can be categorised into abnormal synaptic transmission; including abnormal post- and pre-synaptic currents, susceptibility to seizures, and long term potentiation; abnormal cognition; including a number of learning related phenotypes; and basic behaviour; including anxiety, locomotor activity, and startle reflex (Table 6.4). These are again mainly driven by the differentially upregulated genes (Table C. 6).

Interestingly, the differentially down regulated genes did have an enrichment in the TTX-conditioned gene-set, with 4 phenotype terms not seen in other gene sets, including abnormal long bone morphology (p=3.59e-05), and abnormal cell cycle (p=6.12e-07)(Table C. 7)

Table 6.4 MGI Mammalian phenotype enrichment of differentially expressed genes of TTX-conditioned WT versus shRNA treated cultures.

MP Terms	P	FDR
MP:0003635 abnormal synaptic transmission	1.10E-13	4.96E-10
MP:0002206 abnormal CNS synaptic transmission	3.77E-12	8.50E-09
MP:0003633 abnormal nervous system physiology	2.52E-10	3.78E-07
MP:0014114 abnormal cognition	3.25E-09	2.93E-06
MP:0002063 abnormal learning/memory/conditioning	3.25E-09	2.93E-06
MP:0002572 abnormal emotion/affect behaviour	3.89E-08	2.92E-05
MP:0002066 abnormal motor capabilities/coordination/movement	8.96E-07	0.000577
MP:0002065 abnormal fear/anxiety-related behaviour	1.04E-06	0.000585
MP:0002062 abnormal associative learning	1.41E-06	0.000705
MP:0001362 abnormal anxiety-related response	2.37E-06	0.001067
MP:0009745 abnormal behavioural response to xenobiotic	7.72E-06	0.002988
MP:0001968 abnormal touch/ nociception	7.96E-06	0.002988
MP:0004753 abnormal miniature excitatory postsynaptic currents	1.36E-05	0.004562
MP:0002067 abnormal sensory capabilities/reflexes/nociception	1.42E-05	0.004562
MP:0002064 seizures	2.66E-05	0.008
MP:0002557 abnormal social/conspecific interaction	5.39E-05	0.014884
MP:0001399 hyperactivity	5.61E-05	0.014884
MP:0001262 decreased body weight	6.42E-05	0.01522
MP:0012322 decreased total tissue mass	6.42E-05	0.01522
MP:0012349 increased susceptibility to induction of seizure by inducing agent	7.52E-05	0.016942
MP:0005451 abnormal body composition	8.08E-05	0.017332
MP:0004275 abnormal postnatal subventricular zone morphology	9.66E-05	0.018376
MP:0002272 abnormal nervous system electrophysiology	9.76E-05	0.018376
MP:0002945 abnormal inhibitory postsynaptic currents	0.000105	0.018376
MP:0001468 abnormal temporal memory	0.000106	0.018376
MP:0012315 impaired learning	0.000108	0.018376
MP:0001364 decreased anxiety-related response	0.00011	0.018376
MP:0001392 abnormal locomotor behaviour	0.00012	0.019256
MP:0000947 convulsive seizures	0.00013	0.019819
MP:0001488 increased startle reflex	0.000132	0.019819
MP:0001259 abnormal body weight	0.000138	0.020027
MP:0002910 abnormal excitatory postsynaptic currents	0.000156	0.02196
MP:0002906 increased susceptibility to pharmacologically induced seizures	0.000188	0.025711
MP:0001463 abnormal spatial learning	0.000199	0.02641
MP:0003313 abnormal locomotor activation	0.000213	0.027478
MP:0003491 abnormal voluntary movement	0.000223	0.027559
MP:0003360 abnormal depression-related behaviour	0.000226	0.027559
MP:0012321 abnormal total tissue mass	0.00027	0.03128
MP:0001473 reduced long term potentiation	0.000271	0.03128
MP:0001454 abnormal cued conditioning behaviour	0.000377	0.042482
MP:0002882 abnormal neuron morphology	0.000396	0.043524
MP:0002207 abnormal long term potentiation	0.000411	0.044117

6.3.4. Human disease enrichment

The gene-sets used were then converted to their one-to-one human homologs for enrichment analyses in human disorders. As we are interested in parsing the effect of uniquely impacted genes in *Ehmt1* deficient cells after TTX incubation to assess the role of *Ehmt1* knockdown in a synaptic and developmental event, a third gene set made of genes that are uniquely found deregulated in TTX-conditioned shRNA treated cell cultures , and not seen in baseline shRNA mediated changes. Baseline and TTX-conditioned gene-sets were compared and genes only found in the TTX-conditioned gene-set were referred to as the unique gene-set.

6.3.4.1. De novo rare mutations

Firstly, we looked for enrichment in the gene sets for *de novo* mutations in autism spectrum disorder, intellectual disability, and schizophrenia. The *Dnenrich* framework calculated enrichment for *de novo* non-synonymous mutations in the gene sets, and also for specifically loss-of-function mutations (nonsense, spice, and frameshift).

None of the gene-sets (baseline, TTX-conditioned, or unique) were enriched for genes hit by intellectual disability or schizophrenia nonsynonymous or loss-of-function *de novo* mutations (Table 6.5).

Overall differentially expressed genes at baseline were not enriched for autism *de novo* mutations (non-synonymous and/or loss-of-function). However, when analysed separately, the differentially *upregulated* genes were statistically overrepresented in genes hit by *de novo* nonsynonymous

mutations (p=0.016). This was not driven specifically by an enrichment in loss-of-function mutations specifically (p=0.261) (Table 6.5).

The differential expressed genes in TTX-conditioned gene-sets were enriched for genes with *de novo* nonsynonymous mutations in autism (p=0.016), and is primarily driven by the differentially upregulated genes (p=0.049) (Table 6.5) . All genes that were deregulated in TTX-conditioned gene set that were not also deregulated at baseline was isolated as a unique gene set; we see no significant enrichment of ASD *de novo* mutations (p=0.09) in this gene set, and no particular enhanced enrichment in either the up- or down-regulated genes (Table 6.5) (appendix table).

Table 6.5 Summary results of de novo mutation enrichment analysis by gene-set and associated disorders. NS: nonsynonymous, LOF: loss of function (subset of NS)

Gene sets		*De Novo* Mutations					
		Intellectual Disability		Autism		Schizophrenia	
		NS	LOF	NS	LOF	NS	LOF
Baseline							
	All	0.246		0.156	0.532	0.691	0.741
	Down	0.359	1	0.878	0.88	0.58	1
	Up	0.327	1	**0.015**	0.261	0.769	0.362
TTX-Conditioned							
	All	0.232	0.692	**0.015**	0.109	0.341	0.245
	Down	0.632	1	0.079	0.358	0.323	0.178
	Up	0.149	0.456	**0.048**	0.262	0.635	0.541
Unique							
	All	0.322	0.631	0.09	0.499	0.310	0.287
	Down	0.607	1	0.151	0.595	0.133	0.186
	Up	0.241	0.337	0.237	0.501	0.740	0.691

6.3.4.2. De Novo SNV enrichment analysis

Next the gene sets were analysed specifically for enrichment in genes hit by *de novo* nonsynonymous single nucleotide variants associated with autism and schizophrenia. Here again, loss-of-function mutations were also specified as a subcategory of non-synonymous SNVs. Again, none of the

gene-sets (baseline, TTX or unique) were enriched for genes containing non-synonymous and/or loss of function SNVs associated with schizophrenia. This was also true when the overall gene-sets were sub-divided into up- and down-regulated genes (Table 6.6).

Genes containing SNVs associated with autism were not enriched in baseline differentially expressed genes, although this was marginally non-significant SNVs (p=0.0571). When this gene-set was subdivided in up- or down-regulated genes, it was clear this was primarily driven by an enrichment for autism SNV gene hits in genes that are differentially up-regulated at baseline (p=0.0192).

Differentially expressed genes in the TTX-conditioned gene set were enriched for autism-associated SNVs (p=0.006). This enrichment was not specifically driven by either upregulated (p=0.0246) or downregulated genes (p=0.0297), with both sets enriched for ASD nonsynonymous *de novo* SNVs, but not loss-of-function SNVs specifically (Table 6.6). The uniquely deregulated gene-set were also overrepresented for *genes with de novo* ASD-associated SNVs (p=0.0221), but there was no enrichment seen in either up (p=0.0656) or downregulated genes (p=0.103) (Table 6.6).

Table 6.6 Autism and Schizophrenia *de novo* SNV enrichment analysis with observed and expected mutation rates. Pvalues are not corrected for multiple comparisons

		Autism SNVs								Schizophrenia SNVs							
		Nonsynonymous				Loss-of-Function				Nonsynonymous				Loss-of-Function			
Baseline		Obs	Exp	O/E	P val	Obs	Exp	O/E	P val	Obs	Exp	O/E	P val	Obs	Exp	O/E	P val
	all	30	21.9	1.369863	0.0571	3	2.6	1.153846	0.493	21	24.52179	0.856381	0.788487	4	3.547385	1.127591	0.473557
	up	19	11.1	1.711712	**0.0192**	2	1.2	1.666667	0.354	9	12.2815	0.732809	0.862566	3	1.648306	1.82005	0.229197
	down	11	10.8	1.018519	0.514	1	1.4	0.714286	0.753	12	12.24029	0.980369	0.565591	1	1.899079	0.526571	0.850294
Conditioned																	
	all	41	26.8	1.529851	**0.00638**	6	3.4	1.764706	0.127	30	29.83191	1.005635	0.512041	5	4.506082	1.109611	0.46905
	up	23	14.8	1.554054	**0.0297**	2	1.8	1.111111	0.55	15	16.50604	0.908758	0.677982	3	2.453685	1.222651	0.703065
	down	20	12.2	1.639344	**0.0246**	4	1.6	2.5	0.0746	15	13.64144	1.099591	0.391618	2	2.095311	0.954512	0.349102
Unique																	
	all	30	20	1.5	**0.0221**	3	2.6	1.153846	0.473	24	22.27694	1.077347	0.385149	4	3.418632	1.170059	0.445712
	up	14	8.8	1.590909	0.0656	1	1.1	0.909091	0.673	9	9.807254	0.917688	0.645065	1	1.490277	0.671016	0.77469
	down	16	11.2	1.428571	0.103	2	1.4	1.428571	0.424	15	12.47569	1.202338	0.272609	3	1.930649	1.553882	0.30456

6.3.4.3. Schizophrenia CNV enrichment analysis

We investigated whether our gene-sets of interest were enriched for genes hit by schizophrenia CNVs. There was no enrichment in baseline differentially expressed genes for schizophrenia patient CNVs (p=0.437) (Table 6.7). This was maintained when looking at both the up- and downregulated genes separately, as well as defining either deletion or duplication CNV gene hits (Figure 6.7).

However after TTX incubation, cells that were treated with shRNA had differentially expressed genes that are statistically overrepresented in genes hit by schizophrenia CNVs (p<0.001) (Table 6.7). This enrichment was driven by both the differentially upregulated (p=0.012) and downregulated (p=0.023) genes (Figure 6.7A). Statistical overrepresentation varied when defined as amongst genes hit by deletion CNVs or duplication CNVs. Whilst downregulated genes appeared to be primarily enriched for genes hit by deletion patient CNVs (p<0.001) (Figure 6.7B), upregulated genes were primarily enriched for genes hit by duplication CNVs (p<0.001), and were significantly depleted of genes hit by deletion CNVs, as indicated by the negative coefficient (p=0.045) (Figure 6.7C).

Genes that were uniquely deregulated in shRNA treated cells after TTX incubation were also enriched in patient CNVs (p<0.001). This effect was primarily driven by differentially upregulated genes (p<0.001), however enrichment was also seen in downregulated genes (p=0.037) (Table 6.7, Figure 6.8A). Again, downregulated genes were disproportionately overrepresented in deletion CNVs (p<0.001) (Figure 6.8B), whilst

upregulated genes were enriched for genes hit by patient duplication CNVs (p<0.001) (Figure 6.8C).

Table 6.7 P-value results summary for enrichment of Schizophrenia CNVs for each gene-set. +/- symbols indicate correlation coefficients from regression analysis.

		Schizophrenia CNVs		
Baseline		**all**	**deletions**	**duplications**
	all	0.458453616 -	0.437845124 +	0.311279336 -
	up	0.393057181 -	0.78499701 -	0.83705096 -
	down	0.840366435 -	0.144321653 +	0.266136747 -
Conditioned				
	all	**0.00081978 +**	0.931977296 -	**4.02712E-05 +**
	up	**0.011898431 +**	**0.044954642 -**	**1.9139E-06 +**
	down	**0.023350596 +**	**0.000704757 +**	0.963742815 +
Unique				
	all	**5.53732E-06 +**	0.466845818 +	**1.01301E-06 +**
	up	**0.000182033 +**	0.13424047 -	**1.1769E-08 +**
	down	**0.036553018 +**	**0.000545003 +**	0.786369888 -

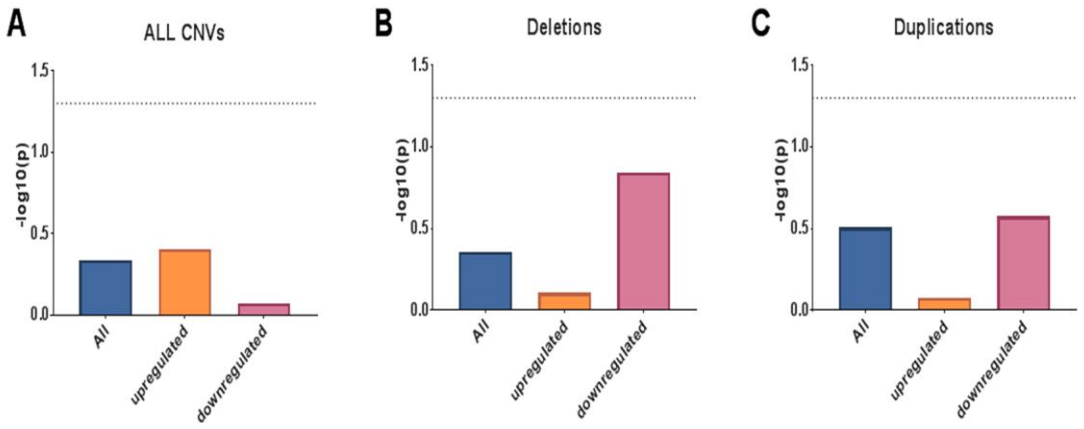

Figure 6.6 Baseline shRNA-treatment genes have no enrichment in copy number variants (CNVs) associated with schizophrenia. The baseline gene-set was sub-categorised into up- and down-regulated genes. No enrichement is seen when analysing **A)** All CNVs. This remains true when analysing either **B)** deletion CNVs or **C)** duplication CNVs. Data is represented in −log10(P-value) , dotted lines represent a p=0.05 threshold for statistical significance.

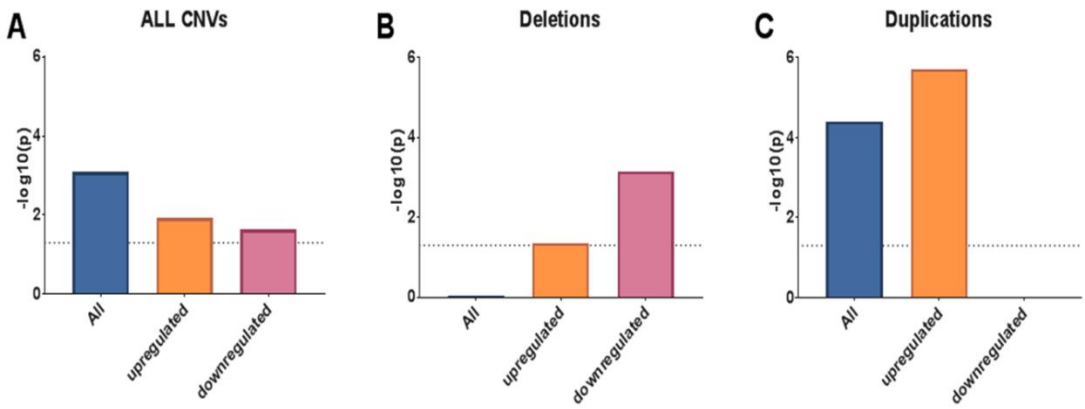

Figure 6.7 TTX-conditioned shRNA-treatment genes are enriched for copy number variants (CNVs) associated with schizophrenia. The gene-set was sub-categorised into up- and down-regulated genes**. A)** Enrichment is seen for All CNVs for both down and upregulated genes**. B)** Whilst both upregulated and downregulated genes were separately enriched for deletion CNVs, downregulated genes were mainly overrepresented in this category deletion CNVs **C)** duplication CNVs enrichment is seen in upregulated genes which drives the baseline gene-set's enrichment for duplication CNVs. Data is represented in −log10(P-value) , dotted lines represent a p=0.05 threshold for statistical significance.

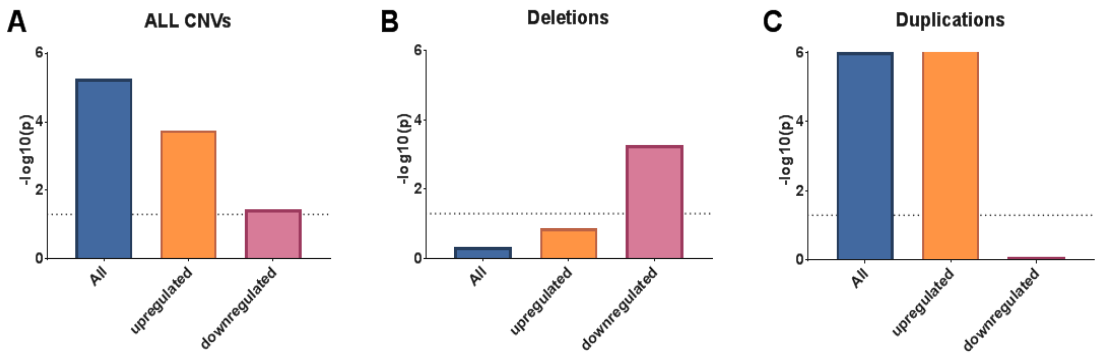

Figure 6.8 Uniquely TTX-conditioned differentially expressed genes are enriched for copy number variants (CNVs) associated with schizophrenia. The gene-set was sub-categorised into up- and down-regulated genes. **A)** Enrichment is seen for All CNVs for the geneset and both down and upregulated genes, but mainly driven by upregulated genes **B)** Downregulated genes were statistically overrepresented in deletion CNVs **C)** duplication CNVs enrichment is seen in upregulated genes which drives the baseline gene-set's enrichment for duplication CNVs. Data is represented in −log10(P-value) , dotted lines represent a p=0.05 threshold for statistical significance.

6.4. Discussion

The Benevento et al. (2016) publically available RNA-seq dataset was used to mine for potential biologically interesting enrichment in functional and phenotypic terms, as well as an association with human neurodevelopmental disorders: intellectual disability, autism, and schizophrenia.

This data-set was ideal in probing *Ehmt1's* role development and disease by identifying the functional and phenotypic relevance of genes deregulated by the gene's knockdown at baseline in neurons. Due to the known association of *Ehmt1* in a number of disorders, notably intellectual disability, but also autism and schizophrenia, the primary hypothesis was that there would be enrichment for genes associated with these disorders, particularly autism and intellectual disability, in this gene set. This dataset also allowed for the functionally relevant probing of the effect of *Ehmt1* deficiency during synaptic upscaling, a process necessary in normal learning, memory, and neurodevelopment *in vivo*. Benevento et al. (2016) proved knocking down *Ehmt1* directly disrupts this vital synaptic event, therefore the genes deregulated in this process due to *Ehmt1* knockdown were hypothesised to be involved in associated disorders, notably schizophrenia due to the high concordance of synaptic genes associated with the disorder, but also in ID and autism. Together this allowed for the possible identification of downstream targets and mechanisms in the pathology of *Ehmt1* deficiency.

Enrichment in functional GO terms was reserved at baseline, with only 20 terms enriched when assessing the whole gene-set. This number of GO terms enriched was significantly increased in TTX-conditioned genes, with 23

additional terms enriched in this gene-set. Interestingly, whilst at baseline, downregulated genes showed no enrichment for GO terms, TTX-conditioned down regulated genes were enriched for bone morphology terms. This is interesting due to the known increase in non-neuronal genes in neurons, including bone development and function. In fact *Ehmt1*$^{+/-}$ mice and children suffer from cranio-facial abnormalities due to abnormal bone growth (Balemans et al. 2014; Atik et al. 2015).

A similar pattern is seen when looking at enrichment for associated phenotypes in mutant mice. These terms can be summarised into impaired learning and cognitive functioning, affective/emotional behavioural deficits, and in the TTX-conditioned gene set, irregular bodyweight and locomotion. Interestingly, TTX-conditioning also saw an enrichment for cocaine and amphetamine response, and addiction, therefore disrupted synaptic upscaling pathways in *Ehmt1* deficient cells play a role in the drug responses of mutant mice (Benevento et al. 2015). We also see enrichment for terms involved in the phenotypes seen in other chapters including impaired sensorimotor gating, increased startle reflex, and impaired memory.

Baseline and TTX-conditioned *Ehmt1* deficiency-dependent gene expression changes as well as a list of shRNA dependent genes uniquely effected by TTX incubation were analysed for enrichment in genes hit by *de novo* mutations, SNVs, and CNVs in autism, schizophrenia and ID. The findings are summarised in the table below (Table 6.8).

Table 6.8 Summary of Human disorder enrichment analysis. P-values that are significant are in bold, p-values that are close to significance are underlined.

Samples		*De novo* mutations						*De novo* SNVs				CNVs		
		ID NS	ID LOF	ASD NS	ASD LOF	SCZ NS	SCZ LOF	ASD NS	ASD LOF	SCZ NS	SCZ LOF	All CNVs	Deletion CNVs	Duplication CNVs
Baseline														
	All	0.246	1	0.156	0.532	0.691	0.741	0.062	0.493	0.788	0.473	0.458	0.438	0.311
	Down	0.359	1	0.878	0.880	0.580	1	0.336	0.753	0.566	0.850	0.840	0.144	0.266
	Up	0.327	1	**0.015**	0.261	0.769	0.362	0.051	0.354	0.863	0.229	0.393	0.785	0.837
TTX-conditioned														
	All	0.232	0.692	**0.015**	0.109	0.341	0.245	**0.014**	0.127	0.512	0.469	**0.0008**	0.932	**4.02712E-05**
	Down	0.632	1	0.079	0.358	0.323	0.178	0.058	0.075	0.391	0.349	**0.0234**	**0.0007**	0.964
	Up	0.149	0.456	**0.048**	0.262	0.635	0.541	**0.035**	0.550	0.678	0.703	**0.0119**	**0.045**	**1.9139E-06**
Unique														
	All	0.322	0.631	0.499	0.310	0.287	0.322	**0.0221**	0.473	0.385	0.446	**5.53732E-06**	0.467	**1.01301E-06**
	Down	0.607	1	0.595	0.133	0.186	0.607	0.0656	0.673	0.645	0.775	**0.0366**	**0.0005**	0.786
	Up	0.241	0.337	0.501	0.740	0.691	0.241	0.103	0.424	0.272	0.305	**0.00018**	0.134	**1.1769E-08**

No enrichment was seen for intellectual disability *de novo* mutations. This is likely due to the smaller list of gene hits available, whilst autism and schizophrenia studies have been robust, the number of genes associated with *de novo* mutations in I.D. is smaller and often involve large regulatory genes such as *Ehmt1* itself (van Bokhoven 2011), as opposed to genes regulated by *Ehmt1*.

Autism *de novo* mutations and SNVs were enriched in upregulated genes at baseline. This was amplified after TTX-conditioning, with enrichment being seen for both autism SNVs and general *de novo* mutations when analysing the whole gene-set. The shRNA genes uniquely impacted by TTX maintained enrichment for autism *de novo* SNVs. This shows an interesting pattern whereby at baseline there is already an overrepresentation of deregulated genes associated with autism, and this number can be aggravated and enrichment increased with introducing the

process of synaptic upscaling; a process that is impaired in *Ehmt1* deficient cells. As previously stated impairment in homeostatic plasticity has been associated with autism (Wondolowski & Dickman 2013), and it could be that *Ehmt1* contributes to autism risk through this synaptic scaling impairment. This however would be partial as it would not account for the enrichment seen at baseline.

Enrichment for schizophrenia associated genes was only seen in analysis of CNV and not in SNV or other *de novo* mutations. This enrichment was also restricted to TTX-conditioned gene set, and reinforced by the unique gene-set which lists the uniquely TTX-dependent effects on *Ehmt1* deficient cells. This is likely due to a number of reasons, one being CNV analyses in schizophrenia are far more comprehensive, and only recent strides have been made to characterise SNV and in-del mutations in schizophrenia (Rees et al. 2012). CNVs, due to their size, also tend to hit far more genes, and thus the list is more robust. Enrichment in these genes being seen only after TTX treatment, and thus impaired synaptic upscaling once again suggests *Ehmt1's* role in the pathogenesis of schizophrenia to be one involving the impairment of the pathways of homeostatic plasticity. This is associated with the phenotype terms enriched, such as associative learning. Schizophrenia is highly enriched for associative learning genes, particularly those involved in extinction of fear learning/memory (Clifton et al. 2017). It has been found that homeostatic plasticity is necessary for extinction of memory (Mendez et al. 2018). This is of particular interest as *Ehmt1*$^{+/-}$ mouse model suffers from impaired fear extinction (Balemans et al. 2013). These lines of evidence suggest *Ehmt1* modulation of H3K9me2 is

necessary for homeostatic plasticity which in the hippocampus is needed for adequate fear memory extinction.

In terms of human development, it is widely agreed that synaptic scaling is a very important process for executive functioning, and adolescence is a crucial time point in which a large synaptic scaling takes place, along with the emergence of executive functions (Selemon 2013). The effect of stress, alcohol, and other environmental factors have been shown to be have enhanced detriment during this time point likely due to the large synaptic plasticity events taking place (Acheson et al. 1998; Arnsten & Shansky 2004). The continued haploinsufficiency of *Ehmt1* disrupts this process and downstream causes impairment into key executive functioning such as impulse control, and goal setting behaviour (Belin et al. 2008; Selemon 2013). Therefore it is likely that whilst a large amount of *Ehmt1* dysfunction can be attributed to the lack of expression embryonically, this sustained lack *Ehmt1* causes continued postnatal problems through adolescence and into adulthood. It could also explain the emergence of early onset psychosis in Kleefstra patients (Vermeulen et al. 2017).

Briefly, some genes of interest that drove some of the enrichment analyses can help cast understanding on the pathways and processes *Ehmt1* haploinsufficiency effects. These genes are notably important for development and are involved in cell positioning and migration, axonal guidance, and synapse formation. They are also individually associated with neurodevelopmental disorders; mainly intellectual disability syndromes.

Some of these genes identified here include Netrin (NTNG1); a gene expressed across the embryonic and perinatal CNS and is shown to be important for axonal guidance. It has been implicated in a number of disorders including Rett Syndrome and Schizophrenia (Fukasawa et al. 2004; Archer et al. 2006; Nectoux et al. 2007; Eastwood & Harrison 2008). Another gene implicated in the in these enrichment analyses is Reelin. Reelin, widely studied in both development and disorder, is highly expressed across the developing brain and is secreted by Cajal-Retzius cells during the formation of the cortex layers. It is critical for normal cell positioning and neuronal migration during development. Because of this it has been identified as associated in a number of developmental disorders, most notably lissencephaly, but also epilepsy, ID, autism, and schizophrenia (D'Arcangelo 2014). TBR1, a gene involved in intellectual disability and microcephaly with pontine and cerebellar hypoplasia or MICPCH syndrome, was also identified as a gene of interest in this analysis. This gene is critical for normal vertebrate embryonic development and is used as a marker for neuronal differentiation, particularly in marking the developmental lineage of glutamatergic neurons (Englund et al. 2005; Hevner 2007; Hadjivassiliou et al. 2010). Expressed across the cerebral cortex, hippocampus & olfactory bulb TBR1 has an important role in neuronal migration and axonal projection as well as the modulation of NMDA receptors in the hippocampus(Bedogni et al. 2010; Kwan et al. 2012). Lastly, KIRREL3 a gene associated with autosomal dominant non-syndromic intellectual disability was also identified. This gene is in expressed in embryonic and adult brain. It is highly implicated

in the synaptogenesis through interactions with synaptic protein CASK (Gerke et al. 2006; Ying F. Liu et al. 2015; Martin et al. 2015).

6.5. Conclusions

This chapter focussed on a retrospective enrichment analysis on *Ehmt1* deficiency related genes from a publically available RNA-Seq dataset. *No enrichment was seen in Ehmt1* deficiency related genes for intellectual disability *de novo* mutations. *Ehmt1* deficiency related genes do however show a baseline enrichment for genes hit by *de novo* mutations and SNVs associated with autism. This is increased after TTX incubation; initiating synaptic upscaling events in *Ehmt1* knockdown cells lead to an increase in statistical overrepresentation of autism genes. TTX-treated *Ehmt1* deficiency related genes were uniquely enriched for genes hit by patient CNVs of schizophrenia. These findings correlate with enrichment in molecular and behavioural endophenotypes in mice with associated genes.

This chapter sets out evidence of *Ehmt1's* role in the pathogenesis of neurodevelopmental disorders using publically available data to find biologically interesting points for further study.

Chapter 7 General Discussion

7.1. Overview

Epigenetics, such as post-translational histone modifications, coordinate dynamic changes to the chromatin leading to spatial and temporally specific gene regulation necessary for normal neurodevelopment. The role of epigenetics in neurodevelopment is wide-ranging, including neurogenesis, cellular specificity, synapse functioning, and network connectivity. Therefore it is anticipated that epigenetic modifiers may cast a deeper understanding in the pathogenesis of a number of neurodevelopmental disorders (NDDs).

Various neurodevelopmental disorders share commonalities amongst each other, and are often co-diagnosed with one another. This indicates that there are common pathways and genes vulnerable to disruption associated with these disorders. *EHMT1* is one such gene in which mutations and deletions of the gene has been associated with autism, schizophrenia, and intellectual disabilities such as Kleefstra syndrome. A number of studies have implemented models to gain an understanding of the role of *Ehmt1* in development and disorder. This includes the ubiquitous heterozygous *Ehmt1* mouse model, and the homozygous postnatal forebrain knockout model driven by *CamK2acre.* Whilst these models have led to a greater understanding of *Ehmt1* in the establishment of behavioural phenotypes, I utilised an embryonically deleted heterozygous forebrain specific knockout to better deconstruct the region specific role of *Ehmt1*, focussing on

hippocampal and cortical dependent cognitive behaviours associated with the neurodevelopmental disorders linked to *Ehmt1* dysfunction.

Table 6.9 Table recapitulating thesis aims and main findings

Aims	Main Findings
Assess the behavioural phenotype of the *Ehmt1*$^{D6cre/+}$ mouse model	• No anxiety phenotype • No deficits in locomotor activity and habituation • Age-related startle and sensorimotor gating deficit • Deficit in long term object recognition memory
Evaluate *in vivo* adult neurogenesis in *Ehmt1*$^{D6cre/+}$ hippocampus	• Increased proliferation in 4 hour pulse-chase paradigm • No evidence of increased neurogenesis in 4 week pulse-chase paradigm
Assess the *in vitro* phenotype of hippocampal cells from the *Ehmt1*$^{D6cre/+}$ mouse model	• *In vitro* replication of proliferation phenotype • Stalling phenotype in the progression of cells across neurogenic track • Reduced type3/immature neurons not due to increased apoptosis or reduced cellular resiliency
Mine publically available data for functional relevant biological points of interest for future research.	• Benevento et al. (2016) chosen for retrospective analysis for disease enrichment • *Ehmt1* deficient cells were enriched for genes linked to ASD • *Ehmt1* deficient cells undergoing synaptic upscaling were enriched for genes linked to the pathogenesis of schizophrenia.

7.2. *Ehmt1*$^{D6cre/+}$ displays distinct behavioural phenotypes compared to other mouse models

Ehmt1$^{D6cre/+}$ mouse model displayed behavioural phenotypes similar to, but subtly distinct from the previous mouse models. A leading motive for the current model was to avoid confounds of the deletion of *Ehmt1* in peripheral tissue. Lack of *Ehmt1* in other mouse models led to a reduction in locomotor activity and was in some cases associated with weight gain/obesity in mice (Schaefer et al. 2009; Balemans et al. 2010). Here, *Ehmt1*$^{D6cre/+}$ mice had no reduction in overall locomotor activity, opposing findings in the previous constitutive heterozygous and conditional hemi and homozygous mouse models. This suggests the restriction of *Ehmt1* heterozygous deletion to cells expressing *Dach1 (D6)* gene circumvents pathways involved in the pathogenesis of these phenotypes in other mouse models. The lack of an anxiety phenotype in *Ehmt1*$^{D6cre/+}$ mice can also be attributed to the lack of impairment in locomotor activity due to the exploratory nature of anxiety tasks such as EPM; whilst other models show increased anxiety, this may be confounded by the reduction in locomotor activity.

Ehmt1$^{D6cre/+}$ *and Ehmt1*$^{camK2acre/+}$/*Ehmt1*$^{camK2acre/camK2acre}$ mouse models share very similar patterns of deletion. Both are forebrain specific deletions, however *CamK2a* is also expressed in the striatum; therefore phenotypes associated with striatal dysfunction seen in that mouse model are not recapitulated here. This includes the lack of reduce palatability for a sweet food substance. In the food neophobia task, *Ehmt1*$^{D6cre/+}$ showed a normal preference for the condensed milk solution and no increased anxiety in

approaching the novel foodstuff, whilst the *Ehmt1*$^{camK2acre/+}$ had impaired palatability for a sucrose substance (Schaefer et al. 2009). These findings suggest *Ehmt1* plays an important role in motivation and reward circuitry in the striatum. It also suggests that the decreased goal oriented behaviour seen in Kleefstra patients (Kleefstra et al., 2006) may not be PFC and hippocampal dependent, but more striatal dependent. This is supported by the implication of *G9a* in cocaine dependence in mice and its role in striatal pathways (Maze et al. 2010).

These findings show distinct differences in the phenotype in *Ehmt1*$^{D6cre/+}$ mice compared to other mouse models of *Ehmt1* haploinsufficiency, pointing towards the specific and variable role of *Ehmt1* in different cell types and pathways of behaviour.

7.3. *Ehmt1*$^{D6cre/+}$ displays key translational psychiatric and NDD endophenotypes: a focus on the hippocampus

Interestingly, this mouse model was found to exhibit behaviour related to translational endophenotypes of neurodevelopmental disorders, namely an impairment in startle reactivity and sensorimotor gating, as well as memory deficits. An interesting aspect of the impairment of startle and prepulse inhibition seen in *Ehmt1*$^{D6cre/+}$ mice was the apparent emergence and deterioration with age. The emergence of startle reactivity deficits at an older age coincides with the known literature on the appearance of this phenotype in patients during the acute stage of psychosis, whilst impairments in PPI can already be seen during the prodormal phase (Quednow et al. 2008). This provides the first evidence of *Ehmt1*

haploinsufficiency in an animal model corroborating the growing literature on the regressive pathology of Kleefstra syndrome in human patients.

These mice also show a deficit in novel object recognition memory. This deficit emerges at 24 hours after acquisition pointing towards impairment of long term memory, increasing the evidence of *Ehmt1's* role in the process of consolidation and recall of memory. To further test whether these memory deficits are due to altered acquisition, retention, consolidation or retrieval, pharmacological interventions of *Ehmt1* function during a memory task would be necessary. Pre-/and post-acquisition and time sensitive effects of *Ehmt1* deletion can be used to tease apart effects of gene on novel object memory. H3K9me2 transiently mediates necessary changes in the chromatin during learning and memory processes. H3K9me2 is upregulated in CA1 region of the hippocampus 1 hour after associative and novel context learning phases, and is necessary for the repression of transcription in the process of consolidation (Gupta et al. 2010; Gupta-Agarwal et al. 2012b). In fact inhibiting *Ehmt1* in the CA1 region led to reduced 'freezing' 24 hours after fear conditioning learning, suggesting a loss in associative memory (Gupta-Agarwal et al. 2012b). Taken together, *Ehmt1* and its modification lead to subtle but important transient changes to the chromatin in a region specific manner during key stages of memory and learning. Therefore the deletion/reduction of *Ehmt1* in a number of neurodevelopmental disorders would lead to the impairment of these key processes that lead to the cognitive and executive function impairments commonly seen across diagnostic boundaries.

An interesting commonality between these translational endophenotypes is the evidence of the role of the hippocampus in their manifestation. Infusion and lesion studies investigating the role of various aspects of the hippocampus on behaviour found that disruption of the ventral hippocampus, and specifically GABAergic transmission, leads to decreased startle reactivity and disrupted prepulse inhibition (Bast et al. 2001; Daenen et al. 2003; Swerdlow et al. 2004). Sensorimotor gating deficits in animal models of neurodevelopmental and psychiatric disorders are often found alongside cognitive deficits included impaired memory. This is most likely due to the processes involved in information filtration necessary for normal sensorimotor gating being intertwined with the processes involved in learning and memory. The hippocampus has long been examined in the context of normal and impaired memory (Ergorul & Eichenbaum 2004). Specifically it has been linked to a number of processes of memory including the transition between short and long term memory, and the extinction of associative fear memory in numerous lesion, pharmacological, and animal model studies (Alonso et al. 2002; Vianna et al. 2004; Hartley et al. 2007; Ji & Maren 2007; Ji & Maren 2008; Jeneson et al. 2011).

Postnatal hippocampal neurogenesis has been linked to both memory and sensorimotor gating. There is a high association of neurogenesis and PPI deficits in animal models of psychiatric and neurodevelopmental disorders (Osumi et al. 2015). It would therefore not be overly speculative to assume a link between the two. Impairing neurogenesis has been also been found to cause object memory impairments. Interestingly, dorsal hippocampal neurogenesis is associated with learning and memory whilst

ventral hippocampal neurogenesis is associated with affective and mood behaviours (Jinno 2011); sensorimotor gating deficits are commonly seen in specific ventral hippocampal lesion and pharmacological studies (Swerdlow et al. 2004). *Ehmt1* haploinsufficiency might be causing differential gene expression changes across the dorso-ventral hippocampus corresponding to these phenotypes seen in the *Ehmt1*$^{D6cre/+}$ mouse model. To test this hypothesis, analysis of the BrdU and NeuN labelling changes across the dorso-ventral axis is necessary.

The constitutive *Ehmt1* heterozygous mouse model has recently been shown to have increased proliferation in the adult hippocampus. This increase was associated with impaired memory, but enhanced pattern separation (Benevento et al. 2017). The memory deficits were comparable to the deficits seen in the *Ehmt1*$^{D6cre/+}$ mouse model. Due to these findings, and corroborative literature, *in vivo* proliferation and neurogenesis was examined in my mouse model. Findings show a specific transient increase in BrdU^{+} cells i.e. increased proliferation, with no evidence of neurogenesis. This in part recapitulates what was seen in the *Ehmt1*$^{+/-}$ mouse model; however survival and neurogenesis was not measured in that model. This suggests that *Ehmt1*, and likely it's modification H3K9me2, transiently influences the process of neurogenesis through regulating genes involved in the activation of quiescent cells to enter the cell cycle and divide to create new cells, as well as the genes that push these cells through the developmental track to neurons. These are probably dynamically opposing and transient, and dynamic expression of H3K9me2 is involved in the switch between the two processes.

To better understand the *in vivo* phenotype of proliferation, *Ehmt1*$^{D6cre/+}$ hippocampal cells were cultured *in vitro* to assess the proliferation and neuronal fate specificity. The increase in proliferation was also seen *in vitro*. This is associated with an increase in type 1 neural progenitors in the cultures. This difference doesn't remain across other neural subtypes. In fact *Ehmt1*$^{D6cre/+}$ cultures have a significant reduction in cells that are either late type 3 progenitor cells, or new born immature neurons. This apparent lack of progression of early progenitor cells to neurons in *Ehmt1*$^{D6cre/+}$ cell cultures was not associated with any increase in baseline apoptotic activity or decreased cellular resilience to external stress. *Ehmt1* is most likely involved in the progression of the cells through the neurogenic track and knockdown of *Ehmt1* would therefore lead to a halting/slowing of the progression across the neurogenic track. This could eventually lead to a depletion of the neurogenic niche which may be a contributor to the regressive pathology of Kleefstra syndrome patients.

Findings presented in these chapters point towards specific behavioural phenotypes attributed to dysfunction in the formation and functioning of the hippocampus, in part related to the role *Ehmt1* plays on the formation of new born adult neurons in the dentate gyrus of the hippocampus.

7.4. *Ehmt1* knockdown effects genes and pathways vulnerable to neurodevelopmental disorders

The final chapter focussed on a retrospective enrichment analysis of *Ehmt1* deficiency related genes from a publically available RNA-Seq dataset linked to synaptic plasticity. *Ehmt1* deficiency related genes showed a baseline enrichment for genes hit by *de novo* mutations and SNVs associated with autism, with slight increases in enrichment after triggering synaptic upscaling events. The baseline enrichment is likely due to the involvement of important neurodevelopmental genes, and genes with high foetal brain expression, whilst the slight increase after TTX incubation capturing the addition of specific synaptic genes signal.

TTX-treated *Ehmt1* deficiency related genes were uniquely enriched for genes hit by patient CNVs of schizophrenia, pointing towards evidence that initiating synaptic upscaling events in *Ehmt1* knockdown cells leads to an increase in statistical overrepresentation of genes associated with schizophrenia, hitting genes represented in learning and memory. An interesting aspect of this enrichment is the seemingly biologically relevant signals seen; downregulated genes after triggering synaptic upscaling were specifically enriched for deletion CNVs, whilst upregulated genes were specifically enriched for duplication CNVs. These are suggestive of a common dosage dependent effect of *Ehmt1* knockdown related genes and genes associated with schizophrenia. This also falls in line with the emergence of psychosis in Kleefstra patients as well as the age-related onset of sensorimotor gating deficits seen in the $Ehmt1^{D6cre/+}$ mouse model.

The synaptic upscaling event used here is a form of synaptic plasticity. This has been shown by Benevento et al. (2017) and others to be impaired in *Ehmt1* knockdown neurons. This is a possible explanation for the role of *Ehmt1*/*G9a* in drug addiction, notably cocaine, due to the role of synaptic plasticity and *Bdnf* expression on reward, drug seeking, and vulnerability to relapsing (Schoenbaum et al. 2007). *Ehmt1*/*G9a* role in *Bdnf* regulation also effects protein synthesis dependent LTP (Sharma et al. 2016), a hebbian form of plasticity.

Taken together, all evidence point towards *Ehmt1* as a synaptic plasticity regulator, and reduction of *Ehmt1* leads to cognitive and behavioural deficits due to both early and postnatal changes to the formation and normal functioning of neurons in a region and cell type specific manner.

7.5. Limitations

Whilst this thesis was designed to minimise confounding factors, there are limitations to the study design. For instance the *Ehmt1*$^{D6cre/+}$ mouse group used were compared to *Ehmt1*$^{flp/+}$ mice acting as wild types, rather than pure WT mice. This was to minimise number of mice used, and to allow for efficient within cage littermate controls. Comparison to wild types would be preferable due to some evidence of other *flp/flp* mouse models carrying their own distinct phenotypes (Kwan 2002). However *Ehmt1*$^{flp/+}$ mice were found to behave within the constraints of normal behaving mice e.g. time spent in open versus closed arms, and short and long term object recognition. *Ehmt1*$^{flp/+}$ mice show no distinct outlier phenotypes suggesting

they provide an accurate representation of wild type for comparison with *Ehmt1*$^{D6cre/+}$ mice.

An interesting confound seen in the behavioural tasks was the increased locomotor activity in *Ehmt1*$^{D6cre/+}$ mice compared to *Ehmt1*$^{flp/+}$ mice. In most tasks this increased locomotion was found, although only surviving multiple corrections in the memory tasks. Heightened locomotion induced by novelty ad maintained locomotion even after habituation suggests a possibility that the mice are still being affected by the arena unlike the WT mice, and thus confounding object exploration results.

One major limitation of this study is the inability to properly quantify the level of haploinsufficiency in the mouse model. Although genotyping has shown deletion of one copy of the *Ehmt1*, I was unable to translate this deletion to reduction in protein or mRNA levels. qPCR analyses found that the haploinsufficiency levels were variable between each sample with no statistically significant reduction in the *Ehmt1*$^{D6cre/+}$ cohort. This is may be due to a feedback mechanism by Ehmt1/G9a with evidence pointing towards an ability to self-regulate. It could also be that because this *flp* is directed at exon 23, the shorter transcripts not affected by the deletion of the exon are affecting the ability to quantify the deletion. This variability in *Ehmt1* levels can also account for the greater spread of data in the *Ehmt1*$^{D6cre/+}$ mice in the novel object recognition task at 30 minutes after acquisition.

This thesis focussed on adult and postnatal neurogenesis, ideally characterisation of embryonic neurogenesis and brain development in this mouse model will discern whether the adult phenotype is a uniquely

postnatal feature of *Ehmt1* haploinsufficiency, or if *Ehmt1* knockdown also affects embryonic neurogenic processes.

Here the *in vitro* work was assessed at 5 DIV, this allowed for a fair snapshot of the cell culture neurogenic lineage to avoid losing early neuronal lineage markers. However to proper understand whether it is a stalling of progression phenotype or a slowing, culturing the cells until DIV 14 or DIV 20 would be necessary.

In Chapter 6, data used was from a rat cell culture experiment. These gene sets were then changed to both mouse and human protein coding homologous gene sets. This allowed for the enrichment analyses linked to mouse model phenotypes and human disease phenotypes. However due to the lack of some homologous genes between the species, data was lost at each stage. Whilst these genes may be important and are affected by *Ehmt1* reduction in the rat, this method of analysis meant not all genes can be translated to the human. Along with this, whether *Ehmt1* function and targets are conserved across evolution is not entirely known; therefore it is possible that some homologous genes are unreliable in understanding *EHMT1's* role in human disorder.

7.6. Future directions

Further behavioural characterisation of *Ehmt1* function is necessary to understand the forebrain specific role of *Ehmt1* in the mouse. Whilst two experiments were repeated at an older age to determine old age effects of Ehmt1 haploinsufficiency, Ehmt1 function as an early developmental gene means the analysis of behavioural output of adolescent mice. Determining

whether locomotor activity and memory deficits remain in adolescents or whether these deficits are specific to the mature neural circuitry will increase the current understanding of *Ehmt1*. More cognition driven behavioural tasks including pattern separation would help elucidate more specific pathways for *Ehmt1* function, particularly in linking the proliferative phenotype with the learning and memory behaviour, especially as pattern separation is widely accepted to preferentially use newborn neurons in the dentate gyrus. A more robust spatial memory task such as the Morris water maze will allow me to properly burden hippocampal dependent pathways to test whether *Ehmt1* haploinsufficiency in my mouse model has a leads to spatial memory impairment. Aside from pure behavioural analyses, experiments to assess the causality of the molecular phenotype on the behavioural phenotypes are necessary. Cells specific and timed reduction of *Ehmt1* in the hippocampus during behavioural assessment of memory would provide a better understanding of the correlation between these findings. Use of transgenic mice with techniques such as optogenetic simulation in tandem with spontaneous behavioural tasks can help specify behavioural findings to specific cell types and pathways.

To further probe the role of *Ehmt1* in the forebrain, embryonic assessment of $Ehmt1^{D6cre/+}$ mice is necessary. Whilst this thesis, and most other work on *Ehmt1* knockdown models in literature, focussed only on the postnatal endophenotypes associated with disorders, embryonic focus on the development of the cortex and hippocampus would help to understand the

key developmental role of *Ehmt1* as well as parsing embryonic and postnatal phenotypes and effects of haploinsufficiency. In combination with this, single cell resolution analyses for gene expression changes during development will help identify *Ehmt1* regulated global expression patterns during development and maturation of neurons. Overlaid with chromatin data from NGS techniques such as ATAC-seq, ChIP-seq, or DNase-seq, these gene expression profiles will allow for the identification of cis regulatory elements transiently and dynamically regulated by *Ehmt1*. Together this data will lead to the temporal and spatial identification of genes as well as enhancers targeted by *Ehmt1* during development.

This will allow for the determination of specific regulated genes during development. As illustrated, ***Ehmt1's*** role is complex, to advance knowledge further focus on smaller portions of its role in terms of affected genes/pathways in a cell type specific and temporally specific manner will help unravel the complexity. Focussing on specific pathways conferring specific vulnerability to *Ehmt1* haploinsufficiency will also allow for identification of potential therapeutic targets for drug discovery in translational research in the future.

References

Acheson, S.K. et al. 1998. Impairment of semantic and figural memory by acute ethanol: age-dependent effects. *Alcoholism, clinical and experimental research* 22(7), pp. 1437–42.

Adam, M.A. and Isles, A.R. 2017. EHMT1/GLP; Biochemical Function and Association with Brain Disorders. *Epigenomes* 1(3), p. 15.

Aggleton, J.P. et al. 1989. Effects of amygdaloid and amygdaloid-hippocampal lesions on object recognition and spatial working memory in rats. *Behavioral neuroscience* 103(5), pp. 962–74.

Aggleton, J.P. et al. 2005. Sparing of the familiarity component of recognition memory in a patient with hippocampal pathology. *Neuropsychologia* 43, pp. 1810–1823.

Aggleton, J.P. and Brown, M.W. 2005. Contrasting Hippocampal and Perirhinalcortex Function using Immediate Early Gene Imaging. *The Quarterly Journal of Experimental Psychology Section B* 58, pp. 218–233.

Alarcón, J.M. et al. 2004. Chromatin acetylation, memory, and LTP are impaired in CBP+/- mice: A model for the cognitive deficit in Rubinstein-Taybi syndrome and its amelioration. *Neuron* 42(6), pp. 947–959.

Allegra, M. et al. 2017. Pharmacological rescue of adult hippocampal neurogenesis in a mouse model of X-linked intellectual disability. *Neurobiology of Disease* 100, pp. 75–86.

Allegra, M. and Caleo, M. 2017. Adult neurogenesis in intellectual disabilities. *Oncotarget* 8(28), pp. 45044–45045.

Alonso, M. et al. 2002. BDNF-triggered events in the rat hippocampus are required for both short- and long-term memory formation. *Hippocampus* 12(4), pp. 551–560.

Alves, N.D. et al. 2018. Chronic stress targets adult neurogenesis preferentially in the suprapyramidal blade of the rat dorsal dentate gyrus. *Brain Structure and Function* 223(1), pp. 415–428.

Amaral, D.G. et al. 2007. The dentate gyrus: fundamental neuroanatomical organization (dentate gyrus for dummies). In: *Progress in brain research*., pp. 3–790.

American Psychiatric Association DSM-5 Task Force. 2013. *Diagnostic and statistical manual of mental disorders: DSM-5™*. 5th ed. American Psychiatric Publishing, Inc.

Anseloni, V.Z. et al. 1995. Behavioral and pharmacological validation of the elevated plus maze constructed with transparent walls. *Brazilian journal of medical and biological research = Revista brasileira de pesquisas medicas e biologicas* 28(5), pp. 597–601.

Antunes, M. and Biala, G. 2012a. The novel object recognition memory: neurobiology, test procedure, and its modifications. *Cognitive processing* 13(2), pp. 93–110.

Antunes, M. and Biala, G. 2012b. The novel object recognition memory:

neurobiology, test procedure, and its modifications. *Cognitive processing* 13(2), pp. 93–110.

Archer, H.L. et al. 2006. NTNG1 mutations are a rare cause of Rett syndrome. *American Journal of Medical Genetics, Part A* 140 A(7), pp. 691–694.

ARNSTEN, A.F.T. and SHANSKY, R.M. 2004. Adolescence: Vulnerable Period for Stress-Induced Prefrontal Cortical Function? Introduction to Part IV. *Annals of the New York Academy of Sciences* 1021(1), pp. 143–147.

Atik, T. et al. 2015. TWINS WITH KLEEFSTRA SYNDROME DUE TO CHROMOSOME 9q34.3 MICRODELETION. *Genetic counseling (Geneva, Switzerland)* 26(4), pp. 431–5.

Bachevalier, J. and Mishkin, M. 1986. Visual recognition impairment follows ventromedial but not dorsolateral prefrontal lesions in monkeys. *Behavioural brain research* 20(3), pp. 249–61.

Balan, S. et al. 2014. Exon resequencing of H3K9 methyltransferase complex genes, EHMT1, EHTM2 and WIZ, in Japanese autism subjects. *Mol Autism* 5(1), p. 49.

Balemans, M.C.M. et al. 2010. Reduced exploration, increased anxiety, and altered social behavior: Autistic-like features of euchromatin histone methyltransferase 1 heterozygous knockout mice. *Behavioural Brain Research* 208(1), pp. 47–55.

Balemans, M.C.M. et al. 2013. Hippocampal dysfunction in the Euchromatin

histone methyltransferase 1 heterozygous knockout mouse model for Kleefstra syndrome. *Human Molecular Genetics* 22(5), pp. 852–866.

Balemans, M.C.M. et al. 2014. Reduced Euchromatin histone methyltransferase 1 causes developmental delay, hypotonia, and cranial abnormalities associated with increased bone gene expression in Kleefstra syndrome mice. *Developmental Biology* 386(2), pp. 395–407.

Ballas, N. et al. 2005. REST and Its Corepressors Mediate Plasticity of Neuronal Gene Chromatin throughout Neurogenesis. *Cell* 121(4), pp. 645–657.

Bannister, A.J. and Kouzarides, T. 2011. Regulation of chromatin by histone modifications. *Cell research* 21(3), pp. 381–95.

Barker, G.R.I. et al. 2006. The Different Effects on Recognition Memory of Perirhinal Kainate and NMDA Glutamate Receptor Antagonism: Implications for Underlying Plasticity Mechanisms. *Journal of Neuroscience* 26(13), pp. 3561–3566.

Barker, G.R.I. et al. 2007a. Recognition memory for objects, place, and temporal order: a disconnection analysis of the role of the medial prefrontal cortex and perirhinal cortex. *The Journal of neuroscience : the official journal of the Society for Neuroscience* 27(11), pp. 2948–57.

Barker, G.R.I. et al. 2007b. Recognition memory for objects, place, and temporal order: a disconnection analysis of the role of the medial prefrontal cortex and perirhinal cortex. *The Journal of neuroscience : the official journal of the Society for Neuroscience* 27(11), pp. 2948–57.

Barker, G.R.I. and Warburton, E.C. 2011. When Is the Hippocampus Involved in Recognition Memory? *Journal of Neuroscience* 31(29), pp. 10721–10731.

Bast, T. et al. 2001. Hyperactivity, decreased startle reactivity, and disrupted prepulse inhibition following disinhibition of the rat ventral hippocampus by the GABAA receptor antagonist picrotoxin. *Psychopharmacology* 156(2–3), pp. 225–233.

Baumans, V. and Van Loo, P.L.P. 2013. How to improve housing conditions of laboratory animals: The possibilities of environmental refinement. *The Veterinary Journal* 195(1), pp. 24–32.

Bedogni, F. et al. 2010. Tbr1 regulates regional and laminar identity of postmitotic neurons in developing neocortex. *Proceedings of the National Academy of Sciences of the United States of America* 107(29), pp. 13129–34.

Belin, D. et al. 2008. High Impulsivity Predicts the Switch to Compulsive Cocaine-Taking. *Science* 320(5881), pp. 1352–1355.

Belmonte, M.K. et al. 2004. Autism as a disorder of neural information processing: directions for research and targets for therapy. *Mol Psychiatry* 9(7), pp. 646–663.

Benevento, M. et al. 2015. The role of chromatin repressive marks in cognition and disease: A focus on the repressive complex GLP/G9a. *Neurobiology of Learning and Memory* 124, pp. 88–96.

Benevento, M. et al. 2016. Histone Methylation by the Kleefstra Syndrome Protein EHMT1 Mediates Homeostatic Synaptic Scaling. *Neuron* 91(2), pp. 341–355.

Benevento, M. et al. 2017. Haploinsufficiency of EHMT1 improves pattern separation and increases hippocampal cell proliferation. *Scientific Reports* 7, p. 40284.

Berg, D.A. et al. 2018. Radial glial cells in the adult dentate gyrus: what are they and where do they come from? *F1000Research* 7, p. 277.

Bergmann, O. et al. 2015. Adult neurogenesis in humans. *Cold Spring Harbor Perspectives in Medicine* 5(8), pp. 1–13.

Bird, C.M. 2017. The role of the hippocampus in recognition memory. *Cortex* 93, pp. 155–165.

Blackman, M.P. et al. 2012. A Critical and Cell-Autonomous Role for MeCP2 in Synaptic Scaling Up. *Journal of Neuroscience* 32(39), pp. 13529–13536.

Blaser, R. and Heyser, C. 2015. Spontaneous object recognition: a promising approach to the comparative study of memory. *Frontiers in behavioral neuroscience* 9, p. 183.

Bodnoff, S.R. et al. 1988. The effects of chronic antidepressant treatment in an animal model of anxiety. *Psychopharmacology* 95(3), pp. 298–302.

Bodnoff, S.R. et al. 1989. A comparison of the effects of diazepam versus several typical and atypical anti-depressant drugs in an animal model of anxiety. *Psychopharmacology* 97(2), pp. 277–9.

van Bokhoven, H. 2011. Genetic and Epigenetic Networks in Intellectual Disabilities. *Annual Review of Genetics* 45(1), pp. 81–104.

Bourin, M. et al. 2007. Animal models of anxiety in mice. *Fundamental & Clinical Pharmacology* 21(6), pp. 567–574.

van den Bout, C.J. et al. 2002. The mouse enhancer element D6 directs Cre recombinase activity in the neocortex and the hippocampus. *Mechanisms of development* 110(1–2), pp. 179–82.

Brandon, M.P. et al. 2014. Parallel and convergent processing in grid cell, head-direction cell, boundary cell, and place cell networks. *Wiley interdisciplinary reviews. Cognitive science* 5(2), pp. 207–219.

Brandt, M.D. et al. 2003. Transient calretinin expression defines early postmitotic step of neuronal differentiation in adult hippocampal neurogenesis of mice. *Molecular and Cellular Neuroscience* 24(3), pp. 603–613.

Bredy, T.W. and Barad, M. 2008. The histone deacetylase inhibitor valproic acid enhances acquisition, extinction, and reconsolidation of conditioned fear. *Learning and Memory* 15(1), pp. 39–45.

Broadbent, N.J. et al. 2004. Spatial memory, recognition memory, and the hippocampus. *Proceedings of the National Academy of Sciences* 101(40), pp. 14515–14520.

Broadbent, N.J. et al. 2010. Object recognition memory and the rodent hippocampus. *Learning & Memory* 17(1), pp. 5–11.

Brown, J.P. et al. 2003. Transient Expression of Doublecortin during Adult Neurogenesis. *Journal of Comparative Neurology* 467(1), pp. 1–10.

Brown, M.W. and Aggleton, J.P. 2001. Recognition memory: What are the roles of the perirhinal cortex and hippocampus? *Nature Reviews Neuroscience* 2(1), pp. 51–61.

Bućan, M. and Abel, T. 2002. The mouse: genetics meets behaviour. *Nature Reviews Genetics* 3(2), pp. 114–123.

Burgin, K.E. et al. 1990. In situ hybridization histochemistry of Ca2+/calmodulin-dependent protein kinase in developing rat brain. *The Journal of neuroscience : the official journal of the Society for Neuroscience* 10(6), pp. 1788–98.

Calhoon, G.G. and Tye, K.M. 2015. Resolving the neural circuits of anxiety. *Nature Neuroscience* 18(10), pp. 1394–1404.

Canitano, R. and Pallagrosi, M. 2017. Autism Spectrum Disorders and Schizophrenia Spectrum Disorders: Excitation/Inhibition Imbalance and Developmental Trajectories. *Front Psychiatry* 8, p. 69.

Caro-Maldonado, A. and Muñoz-Pinedo, C. 2011. *Dying for Something to Eat: How Cells Respond to Starvation*.

Chang, Y. et al. 2011. MPP8 mediates the interactions between DNA methyltransferase Dnmt3a and H3K9 methyltransferase GLP/G9a. *Nat Commun* 2, p. 533.

Chase, K.A. et al. 2013. Histone methylation at H3K9: evidence for a

restrictive epigenome in schizophrenia. *Schizophr Res* 149(1–3), pp. 15–20.

Chen, C.H. et al. 2017. Neuroligin 2 R215H mutant mice manifest anxiety, increased prepulse inhibition, and impaired spatial learning and memory. *Frontiers in Psychiatry* 8(NOV), p. 257.

Chen, E.S. et al. 2014. Molecular Convergence of Neurodevelopmental Disorders. *The American Journal of Human Genetics* 95(5), pp. 490–508.

Chen, X. et al. 2012. G9a/GLP-dependent histone H3K9me2 patterning during human hematopoietic stem cell lineage commitment. *Genes & development* 26(22), pp. 2499–511.

Chowdhury, D. and Hell, J.W. 2018. Homeostatic synaptic scaling: molecular regulators of synaptic AMPA-type glutamate receptors. *F1000Research* 7, p. 234.

Clapcote, S.J. et al. 2007. Behavioral Phenotypes of Disc1 Missense Mutations in Mice. *Neuron* 54(3), pp. 387–402.

Clark, R.E. et al. 2000. Impaired recognition memory in rats after damage to the hippocampus. *The Journal of neuroscience : the official journal of the Society for Neuroscience* 20(23), pp. 8853–60.

Clark, R.E. et al. 2000. Impaired Recognition Memory in Rats after Damage to the Hippocampus. *Journal of Neuroscience* 20(23), pp. 8853–8860.

Clifton, N.E. et al. 2017. Schizophrenia copy number variants and associative learning. *Molecular Psychiatry* 22(2), pp. 178–182.

Collins, R.E. et al. 2008. The ankyrin repeats of G9a and GLP histone methyltransferases are mono- and dimethyllysine binding modules. *Nat Struct Mol Biol* 15(3), pp. 245–250.

Cooper, G.M. et al. 2011. A copy number variation morbidity map of developmental delay. *Nature genetics* 43(9), pp. 838–46.

Crawley, J.N. 2012. Translational animal models of autism and neurodevelopmental disorders. *Dialogues in clinical neuroscience* 14(3), pp. 293–305.

D'Arcangelo, G. 2014. Reelin in the Years: Controlling Neuronal Migration and Maturation in the Mammalian Brain. *Advances in Neuroscience* 2014, pp. 1–19.

Daenen, E.W.P.M. et al. 2003. Neonatal lesions in the amygdala or ventral hippocampus disrupt prepulse inhibition of the acoustic startle response; implications for an animal model of neurodevelopmental disorders like schizophrenia. *European neuropsychopharmacology : the journal of the European College of Neuropsychopharmacology* 13(3), pp. 187–97.

Darvas, M. and Palmiter, R.D. 2009. Restriction of dopamine signaling to the dorsolateral striatum is sufficient for many cognitive behaviors. *Proceedings of the National Academy of Sciences* 106(34), pp. 14664–14669.

Dash, P.K. et al. 2010. Valproate administered after traumatic brain injury provides neuroprotection and improves cognitive function in rats. *PLoS ONE*

David, A. and Pierre, L. 2006. Hippocampal Neuroanatomy. In: *The*

Hippocampus Book. Oxford University Press, pp. 37–114.

Davis, B.A. and Isles, A.R. 2014. Modelling the genetic contribution to mental illness: a timely end for the psychiatric rodent? *European Journal of Neuroscience* 39(11), pp. 1933–1942.

Deaton, A.M. and Bird, A. 2011. CpG islands and the regulation of transcription. *Genes & development* 25(10), pp. 1010–22.

Deciphering Developmental Disorders, S. and Study, D.D.D. 2017. Prevalence and architecture of de novo mutations in developmental disorders. *Nature* 542(7642), pp. 433–438.

Deimling, S.J. et al. 2017. The expanding role of the Ehmt2/G9a complex in neurodevelopment. *Neurogenesis (Austin, Tex.)* 4(1), p. e1316888.

Dix, S.L. and Aggleton, J.P. 1999. Extending the spontaneous preference test of recognition: evidence of object-location and object-context recognition. *Behavioural Brain Research* 99(2), pp. 191–200.

Doeller, C.F. et al. 2008. Parallel striatal and hippocampal systems for landmarks and boundaries in spatial memory. *Proceedings of the National Academy of Sciences of the United States of America* 105(15)

Dong, K.B. et al. 2008. DNA methylation in ES cells requires the lysine methyltransferase G9a but not its catalytic activity. *EMBO J* 27(20), pp. 2691–2701.

Eastwood, S.L. and Harrison, P.J. 2008. Decreased mRNA Expression of Netrin-G1 and Netrin-G2 in the Temporal Lobe in Schizophrenia and Bipolar

Disorder. *Neuropsychopharmacology* 33(4), pp. 933–945.

Ehninger, D. and Kempermann, G. 2008a. Neurogenesis in the adult hippocampus. *Cell and Tissue Research* 331(1), pp. 243–250.

Ehninger, D. and Kempermann, G. 2008b. Neurogenesis in the adult hippocampus. *Cell and Tissue Research* 331(1), pp. 243–250.

Engelmann, M. et al. 2011. Testing declarative memory in laboratory rats and mice using the nonconditioned social discrimination procedure. *Nature Protocols* 6(8), pp. 1152–1162.

Englund, C. et al. 2005. Pax6, Tbr2, and Tbr1 Are Expressed Sequentially by Radial Glia, Intermediate Progenitor Cells, and Postmitotic Neurons in Developing Neocortex. *Journal of Neuroscience* 25(1), pp. 247–251.

Ennaceur, A. and Delacour, J. 1988. A new one-trial test for neurobiological studies of memory in rats. 1: Behavioral data. *Behavioural Brain Research* 31(1), pp. 47–59.

Epsztejn-Litman, S. et al. 2008. De novo DNA methylation promoted by G9a prevents reprogramming of embryonically silenced genes HHS Public Access Author manuscript. *Nat Struct Mol Biol* 15(11), pp. 1176–1183.

Ergorul, C. and Eichenbaum, H. 2004. The hippocampus and memory for ‘what,’ ‘where,’ and ‘when’. *Learning and Memory* 11(4), pp. 397–405.

Eriksson, P.S. et al. 1998. Neurogenesis in the adult human hippocampus. *Nature Medicine* 4(11), pp. 1313–1317.

Estève, P.O. et al. 2006. Direct interaction between DNMT1 and G9a coordinates DNA and histone methylation during replication. *Genes Dev* 20(22), pp. 3089–3103.

Feldman, N. et al. 2006. G9a-mediated irreversible epigenetic inactivation of Oct-3/4 during early embryogenesis. *NATURE CELL BIOLOGY* 8(2)

Filippov, V. et al. 2003. Subpopulation of nestin-expressing progenitor cells in the adult murine hippocampus shows electrophysiological and morphological characteristics of astrocytes. *Molecular and Cellular Neuroscience* 23(3), pp. 373–382.

Fiszbein, A. et al. 2016. Alternative Splicing of G9a Regulates Neuronal Differentiation. *Cell Reports* 14(12), pp. 2797–2808.

França, T.F.A. et al. 2017. Hippocampal neurogenesis and pattern separation: A meta-analysis of behavioral data. *Hippocampus* 27(9), pp. 937–950.

Fritsch, L. et al. 2010. A subset of the histone H3 lysine 9 methyltransferases Suv39h1, G9a, GLP, and SETDB1 participate in a multimeric complex. *Mol Cell* 37(1), pp. 46–56.

Fromer, M. et al. 2014. De novo mutations in schizophrenia implicate synaptic networks. *Nature* 506(7487), pp. 179–84.

Frost, B. et al. 2014. Tau promotes neurodegeneration through global chromatin relaxation. *Nat Neurosci* 17(3), pp. 357–366.

Fry, A.E. et al. 2016. Pathogenic copy number variants and SCN1A

mutations in patients with intellectual disability and childhood-onset epilepsy. *BMC Med Genet* 17(1), p. 34.

Fukasawa, M. et al. 2004. Case-control association study of human netrin G1 gene in Japanese schizophrenia. *Journal of medical and dental sciences* 51(2), pp. 121–8.

Fukuda, S. et al. 2003. Two distinct subpopulations of nestin-positive cells in adult mouse dentate gyrus. *The Journal of neuroscience : the official journal of the Society for Neuroscience* 23(28), pp. 9357–9366.

Gainetdinov, R.R. et al. 1999. Role of serotonin in the paradoxical calming effect of psychostimulants on hyperactivity. *Science (New York, N.Y.)* 283(5400), pp. 397–401.

Gallitano, A.L. et al. 2016. Distinct dendritic morphology across the blades of the rodent dentate gyrus. *Synapse* 70(7), pp. 277–282.

Gao, M. et al. 2010. A Specific Requirement of Arc/Arg3.1 for Visual Experience-Induced Homeostatic Synaptic Plasticity in Mouse Primary Visual Cortex. *Journal of Neuroscience* 30(21), pp. 7168–7178.

Gaskin, S. et al. 2003. Retrograde and anterograde object recognition in rats with hippocampal lesions. *Hippocampus* 13(8), pp. 962–9.

Gaskin, S. et al. 2010a. Object familiarization and novel-object preference in rats. *Behavioural Processes* 83(1), pp. 61–71.

Gaskin, S. et al. 2010b. Object familiarization and novel-object preference in rats. *Behavioural Processes* 83(1), pp. 61–71.

Gerke, P. et al. 2006. Neuronal expression and interaction with the synaptic protein CASK suggest a role for Neph1 and Neph2 in synaptogenesis. *The Journal of Comparative Neurology* 498(4), pp. 466–475.

Ghosh, S. et al. 2010. Tissue specific DNA methylation of CpG islands in normal human adult somatic tissues distinguishes neural from non-neural tissues. *Epigenetics* 5(6), pp. 527–38.

Gigek, C.O. et al. 2015. A molecular model for neurodevelopmental disorders. *Translational psychiatry* 5(5), p. e565.

Gilbert, J. and Man, H.-Y. 2017. Fundamental Elements in Autism: From Neurogenesis and Neurite Growth to Synaptic Plasticity. *Frontiers in Cellular Neuroscience* 11, p. 359.

Gilissen, C. et al. 2014. Genome sequencing identifies major causes of severe intellectual disability. *Nature* 511(7509), pp. 344–347.

Gray, J.A. et al. 2011. Distinct modes of AMPA receptor suppression at developing synapses by GluN2A and GluN2B: single-cell NMDA receptor subunit deletion in vivo. *Neuron* 71(6), pp. 1085–101.

Grozeva, D. et al. 2015. Targeted Next-Generation Sequencing Analysis of 1,000 Individuals with Intellectual Disability. *Hum Mutat* 36(12), pp. 1197–1204.

Gupta-Agarwal, S. et al. 2012a. G9a/GLP Histone Lysine Dimethyltransferase Complex Activity in the Hippocampus and the Entorhinal Cortex Is Required for Gene Activation and Silencing during Memory

Consolidation. *Journal of Neuroscience*

Gupta-Agarwal, S. et al. 2012b. G9a/GLP Histone Lysine Dimethyltransferase Complex Activity in the Hippocampus and the Entorhinal Cortex Is Required for Gene Activation and Silencing during Memory Consolidation. *Journal of Neuroscience* 32(16), pp. 5440–5453.

Gupta-Agarwal, S. et al. 2014. NMDA receptor- and ERK-dependent histone methylation changes in the lateral amygdala bidirectionally regulate fear memory formation. *Learning & Memory* 21(7), pp. 351–362.

Gupta, S. et al. 2010. Histone methylation regulates memory formation. *The Journal of neuroscience : the official journal of the Society for Neuroscience* 30(10), pp. 3589–99.

Gupta, S. et al. 2010. Histone Methylation Regulates Memory Formation. *Journal of Neuroscience*

Hadjivassiliou, G. et al. 2010. The application of cortical layer markers in the evaluation of cortical dysplasias in epilepsy. *Acta neuropathologica* 120(4), pp. 517–28.

Hadzsiev, K. et al. 2016. Kleefstra syndrome in Hungarian patients: additional symptoms besides the classic phenotype. *Mol Cytogenet* 9, p. 22.

Hamdan, F.F. et al. 2014. De novo mutations in moderate or severe intellectual disability. *PLoS Genet* 10(10), p. e1004772.

Hammond, R.S. et al. 2004. On the delay-dependent involvement of the hippocampus in object recognition memory. *Neurobiology of Learning and*

Memory 82(1), pp. 26–34.

Han, J.Y. et al. 2017. Diagnostic exome sequencing identifies a heterozygous MBD5 frameshift mutation in a family with intellectual disability and epilepsy. *Eur J Med Genet* 60(10), pp. 559–564.

Harrison, J.S. et al. 2016. Hemi-methylated DNA regulates DNA methylation inheritance through allosteric activation of H3 ubiquitylation by UHRF1. *Elife* 5

Hartley, T. et al. 2007. The hippocampus is required for short-term topographical memory in humans. *Hippocampus* 17(1), pp. 34–48.

Herz, H.M. et al. 2013. SET for life: biochemical activities and biological functions of SET domain-containing proteins. *Trends Biochem Sci* 38(12), pp. 621–639.

Hevner, R.F. 2007. Layer-Specific Markers as Probes for Neuron Type Identity in Human Neocortex and Malformations of Cortical Development. *Journal of Neuropathology and Experimental Neurology* 66(2), pp. 101–109.

Hodge, R.D. and Hevner, R.F. 2011. Expression and actions of transcription factors in adult hippocampal neurogenesis. *Developmental neurobiology* 71(8), pp. 680–9.

Hsieh, J. and Zhao, X. 2016. Genetics and epigenetics in adult neurogenesis. *Cold Spring Harbor Perspectives in Biology* 8(6), p. a018911.

Huang, J. et al. 2010. G9a and Glp methylate lysine 373 in the tumor suppressor p53. *J Biol Chem* 285(13), pp. 9636–9641.

Iacono, W.G. et al. 2014. Knowns and unknowns for psychophysiological endophenotypes: Integration and response to commentaries. *Psychophysiology* 51(12), pp. 1339–1347.

Iwakoshi, M. et al. 2004. 9q34.3 deletion syndrome in three unrelated children. *Am J Med Genet A* 126A(3), pp. 278–283.

Jakawich, S.K. et al. 2010. Local Presynaptic Activity Gates Homeostatic Changes in Presynaptic Function Driven by Dendritic BDNF Synthesis. *Neuron* 68(6), pp. 1143–1158.

Jeneson, A. et al. 2011. The role of the hippocampus in retaining relational information across short delays: the importance of memory load. *Learning & memory (Cold Spring Harbor, N.Y.)* 18(5), pp. 301–5.

Jessberger, S. et al. 2005. Seizures induce proliferation and dispersion of doublecortin-positive hippocampal progenitor cells. *Experimental Neurology* 196(2), pp. 342–351.

Ji, J. and Maren, S. 2007. Hippocampal involvement in contextual modulation of fear extinction. *Hippocampus* 17(9), pp. 749–758.

Ji, J. and Maren, S. 2008. Differential roles for hippocampal areas CA1 and CA3 in the contextual encoding and retrieval of extinguished fear. *Learning & memory (Cold Spring Harbor, N.Y.)* 15(4), pp. 244–51.

Jinno, S. 2011. Topographic differences in adult neurogenesis in the mouse hippocampus: A stereology-based study using endogenous markers. *Hippocampus* 21(5), pp. 467–480.

Jobe, E.M. and Zhao, X. 2017. DNA Methylation and Adult Neurogenesis. *Brain Plasticity* 3(1), pp. 5–26.

Jucker, M. 2010. The benefits and limitations of animal models for translational research in neurodegenerative diseases. *Nature Medicine* 16(11), pp. 1210–1214.

Kang, E. et al. 2016. Adult Neurogenesis and Psychiatric Disorders. *Cold Spring Harbor perspectives in biology* 8(9), p. a019026.

Kappel, S. et al. 2017. To Group or Not to Group? Good Practice for Housing Male Laboratory Mice. *Animals : an open access journal from MDPI* 7(12)

Kazdoba, T.M. et al. 2016. Translational Mouse Models of Autism: Advancing Toward Pharmacological Therapeutics. *Current topics in behavioral neurosciences* 28, pp. 1–52.

Kempermann, G. et al. 2003. Early determination and long-term persistence of adult-generated new neurons in the hippocampus of mice. *Development* 130(2), pp. 391–399.

Kempermann, G. 2016. Adult neurogenesis: An evolutionary perspective. *Cold Spring Harbor Perspectives in Biology* 8(2)

Kempermann, G. et al. 2018. Human Adult Neurogenesis: Evidence and Remaining Questions. *Cell Stem Cell* 23(1), pp. 25–30.

Kesner, R.P. 2007. A behavioral analysis of dentate gyrus function. *Progress in Brain Research* 163, pp. 567–576.

Khelfaoui, M. et al. 2007. Loss of X-Linked Mental Retardation Gene Oligophrenin1 in Mice Impairs Spatial Memory and Leads to Ventricular Enlargement and Dendritic Spine Immaturity. *Journal of Neuroscience* 27(35), pp. 9439–9450.

Kirov, G. et al. 2009. Neurexin 1 (NRXN1) deletions in schizophrenia. *Schizophrenia bulletin* 35(5), pp. 851–4.

Kirov, G. et al. 2012. De novo CNV analysis implicates specific abnormalities of postsynaptic signalling complexes in the pathogenesis of schizophrenia. *Mol Psychiatry* 17(2), pp. 142–153.

Kishi, N. and Macklis, J.D. 2004. MECP2 is progressively expressed in post-migratory neurons and is involved in neuronal maturation rather than cell fate decisions. *Molecular and Cellular Neuroscience* 27(3), pp. 306–321.

Klamer, D. et al. 2004. Habituation of acoustic startle is disrupted by psychotomimetic drugs: differential dependence on dopaminergic and nitric oxide modulatory mechanisms. *Psychopharmacology* 176(3–4), pp. 440–450.

Kleefstra, T. et al. 2005. Disruption of the gene Euchromatin Histone Methyl Transferase1 (Eu-HMTase1) is associated with the 9q34 subtelomeric deletion syndrome. *J Med Genet* 42(4), pp. 299–306.

Kleefstra, T. et al. 2006. Loss-of-function mutations in euchromatin histone methyl transferase 1 (EHMT1) cause the 9q34 subtelomeric deletion syndrome. *Am J Hum Genet* 79(2), pp. 370–377.

Kleefstra, T. et al. 2012. Disruption of an EHMT1-associated chromatin-modification module causes intellectual disability. *Am J Hum Genet* 91(1), pp. 73–82.

Kleefstra, T. et al. 2014. The genetics of cognitive epigenetics. *Neuropharmacology* 80, pp. 83–94.

Kleefstra, T. and de Leeuw, N. 1993. *Kleefstra Syndrome*.

Korzus, E. et al. 2004. CBP histone acetyltransferase activity is a critical component of memory consolidation. *Neuron* 42(6), pp. 961–972.

Kramer, J.M. et al. 2011. Epigenetic regulation of learning and memory by Drosophila EHMT/G9a. *PLoS Biol* 9(1), p. e1000569.

Kriegstein, A. and Alvarez-Buylla, A. 2009. The glial nature of embryonic and adult neural stem cells. *Annual review of neuroscience* 32, pp. 149–84.

Kwan, K.-M. 2002. Conditional alleles in mice: Practical considerations for tissue-specific knockouts. *Genesis* 32(2), pp. 49–62.

Kwan, K.Y. et al. 2012. Transcriptional co-regulation of neuronal migration and laminar identity in the neocortex. *Development* 139(9), pp. 1535–1546.

Lago, T. et al. 2017. Striatum on the anxiety map: Small detours into adolescence. *Brain research* 1654(Pt B), pp. 177–184.

Lang, P.J. et al. 1998. Emotion, motivation, and anxiety: brain mechanisms and psychophysiology. *Biological Psychiatry* 44(12), pp. 1248–1263.

Lawrence, M. et al. 2016. Lateral Thinking: How Histone Modifications

Regulate Gene Expression. *Trends in Genetics* 32(1), pp. 42–56.

Levitt, P. and Veenstra-VanderWeele, J. 2015. Neurodevelopment and the Origins of Brain Disorders. *Neuropsychopharmacology* 40(1) 8 January, pp. 1–3.

Lezak, K.R. et al. 2017. Behavioral methods to study anxiety in rodents. *Dialogues in clinical neuroscience* 19(2), pp. 181–191.

Li, F. et al. 1999. Integrin-linked kinase is localized to cell-matrix focal adhesions but not cell-cell adhesion sites and the focal adhesion localization of integrin-linked kinase is regulated by the PINCH-binding ANK repeats. *J Cell Sci* 112 (Pt 2, pp. 4589–4599.

Lieberwirth, C. et al. 2016. Hippocampal adult neurogenesis: Its regulation and potential role in spatial learning and memory. *Brain research* 1644, pp. 127–40.

Lienert, F. et al. 2011. Genomic prevalence of heterochromatic H3K9me2 and transcription do not discriminate pluripotent from terminally differentiated cells. *PLoS Genetics* 7(6), p. e1002090.

Lim, S. et al. 2001. Sharpin, a novel postsynaptic density protein that directly interacts with the shank family of proteins. *Mol Cell Neurosci* 17(2), pp. 385–397.

Liu, N. et al. 2015. Recognition of H3K9 methylation by GLP is required for efficient establishment of H3K9 methylation, rapid target gene repression, and mouse viability. *Genes and Development* 29(4), pp. 379–393.

Liu, X. et al. 2013. UHRF1 targets DNMT1 for DNA methylation through cooperative binding of hemi-methylated DNA and methylated H3K9. *Nat Commun* 4, p. 1563.

Liu, Y.F. et al. 2015. Autism and Intellectual Disability-Associated KIRREL3 Interacts with Neuronal Proteins MAP1B and MYO16 with Potential Roles in Neurodevelopment. Feng, Y. ed. *PLOS ONE* 10(4), p. e0123106.

Lledo, P.-M. et al. 2008. Origin and function of olfactory bulb interneuron diversity. *Trends in neurosciences* 31(8), pp. 392–400.

Lunyak, V. V. and Rosenfeld, M.G. 2005. No Rest for REST: REST/NRSF Regulation of Neurogenesis. *Cell* 121(4), pp. 499–501.

La Malfa, G. et al. 2004. Autism and intellectual disability: a study of prevalence on a sample of the Italian population. *J Intellect Disabil Res* 48(Pt 3), pp. 262–267.

Manning, E.E. and van den Buuse, M. 2013. BDNF deficiency and young-adult methamphetamine induce sex-specific effects on prepulse inhibition regulation. *Frontiers in Cellular Neuroscience* 7, p. 92.

Manto, M. et al. 2012. Consensus paper: roles of the cerebellum in motor control--the diversity of ideas on cerebellar involvement in movement. *Cerebellum (London, England)* 11(2), pp. 457–87.

Martin, E.A. et al. 2015. The intellectual disability gene Kirrel3 regulates target-specific mossy fiber synapse development in the hippocampus. *eLife* 4, p. e09395.

Matson, J.L. and Shoemaker, M. 2009. Intellectual disability and its relationship to autism spectrum disorders. *Res Dev Disabil* 30(6), pp. 1107–1114.

Maze, I. et al. 2010. Essential role of the histone methyltransferase G9a in cocaine-induced plasticity. *Science (New York, N.Y.)* 327(5962), pp. 213–6.

McCarthy, S.E. et al. 2014. De novo mutations in schizophrenia implicate chromatin remodeling and support a genetic overlap with autism and intellectual disability. *Mol Psychiatry* 19(6), pp. 652–658.

Mehler, M.F. 2008. Epigenetics and the nervous system. *Annals of Neurology* 64(6), pp. 602–617.

Mendez, P. et al. 2018. Homeostatic Plasticity in the Hippocampus Facilitates Memory Extinction. *Cell Reports* 22(6), pp. 1451–1461.

Meunier, M. et al. 1997. Effects of orbital frontal and anterior cingulate lesions on object and spatial memory in rhesus monkeys. *Neuropsychologia* 35(7), pp. 999–1015.

von Meyenn, F. et al. 2016. Impairment of DNA Methylation Maintenance Is the Main Cause of Global Demethylation in Naive Embryonic Stem Cells. *Mol Cell* 62(6), pp. 848–861.

Millan, M.J. 2013. An epigenetic framework for neurodevelopmental disorders: from pathogenesis to potential therapy. *Neuropharmacology* 68, pp. 2–82.

Ming, G. li and Song, H. 2011. Adult Neurogenesis in the Mammalian Brain:

Significant Answers and Significant Questions. *Neuron* 70(4), pp. 687–702.

Mogenson, G.J. et al. 1980. From motivation to action: functional interface between the limbic system and the motor system. *Progress in neurobiology* 14(2–3), pp. 69–97.

Mohn, A.R. et al. 1999. Mice with reduced NMDA receptor expression display behaviors related to schizophrenia. *Cell* 98(4), pp. 427–36.

Morellini, F. 2013. Spatial memory tasks in rodents: What do they model? *Cell and Tissue Research* 354(1), pp. 273–286.

Morgan, V.A. et al. 2008. Intellectual disability co-occurring with schizophrenia and other psychiatric illness: population-based study. *Br J Psychiatry* 193(5), pp. 364–372.

Morici, J.F. et al. 2015. Medial prefrontal cortex role in recognition memory in rodents. *Behavioural Brain Research* 292, pp. 241–251.

Mosavi, L.K. et al. 2004. The ankyrin repeat as molecular architecture for protein recognition. *Protein Sci* 13(6), pp. 1435–1448.

Mozzetta, C. et al. 2014. The Histone H3 Lysine 9 Methyltransferases G9a and GLP Regulate Polycomb Repressive Complex 2-Mediated Gene Silencing. *Molecular Cell* 53(2), pp. 277–289.

Mumby, D.G. et al. 2002. Hippocampal damage and exploratory preferences in rats: memory for objects, places, and contexts. *Learning & memory (Cold Spring Harbor, N.Y.)* 9(2), pp. 49–57.

Murty, V.P. et al. 2013. Hippocampal networks habituate as novelty accumulates. *Learning & memory (Cold Spring Harbor, N.Y.)* 20(4), pp. 229–35.

Nakashiba, T. et al. 2012. Young dentate granule cells mediate pattern separation, whereas old granule cells facilitate pattern completion. *Cell* 149(1), pp. 188–201.

Namburi, P. et al. 2015. A circuit mechanism for differentiating positive and negative associations. *Nature* 520(7549), pp. 675–678.

Nectoux, J. et al. 2007. Netrin G1 Mutations Are an Uncommon Cause of Atypical Rett Syndrome With or Without Epilepsy. *Pediatric Neurology* 37(4), pp. 270–274.

Niederberger, E. et al. 2017. Drugging the pain epigenome. *Nature Reviews Neurology* 13(7), pp. 434–447.

Norman, G. and Eacott, M.. 2004. Impaired object recognition with increasing levels of feature ambiguity in rats with perirhinal cortex lesions. *Behavioural Brain Research* 148(1–2), pp. 79–91.

O'Roak, B.J. et al. 2011. Exome sequencing in sporadic autism spectrum disorders identifies severe de novo mutations. *Nat Genet* 43(6), pp. 585–589.

O'Roak, B.J. et al. 2012. Sporadic autism exomes reveal a highly interconnected protein network of de novo mutations. *Nature* 485(7397), pp. 246–50.

Olsen, J.B. et al. 2016. G9a and ZNF644 Physically Associate to Suppress Progenitor Gene Expression during Neurogenesis. *Stem cell reports* 7(3), pp. 454–470.

Onay, H. et al. 2016. Mutation analysis of the NRXN1 gene in autism spectrum disorders. *Balkan journal of medical genetics : BJMG* 19(2), pp. 17–22.

Osumi, N. et al. 2015. Neurogenesis and Sensorimotor Gating: Bridging a Microphenotype and an Endophenotype. *Current Molecular Medicine* 15(2), pp. 129–137.

Peleg, S. et al. 2010. Altered histone acetylation is associated with age-dependent memory impairment in mice. *Science* 328(5979), pp. 753–756.

Pellow, S. et al. 1985. Validation of open:closed arm entries in an elevated plus-maze as a measure of anxiety in the rat. *Journal of neuroscience methods* 14(3), pp. 149–67.

Peschansky, V.J. et al. 2016. The long non-coding RNA FMR4 promotes proliferation of human neural precursor cells and epigenetic regulation of gene expression in trans. *Molecular and cellular neurosciences* 74, pp. 49–57.

Peters, A.H. et al. 2002. Histone H3 lysine 9 methylation is an epigenetic imprint of facultative heterochromatin. *Nat Genet* 30(1), pp. 77–80.

Pons-Espinal, M. et al. 2013. Functional implications of hippocampal adult neurogenesis in intellectual disabilities. *Amino Acids* 45(1), pp. 113–131.

Powell, C.M. and Miyakawa, T. 2006. Schizophrenia-relevant behavioral testing in rodent models: a uniquely human disorder? *Biological psychiatry* 59(12), pp. 1198–207.

Powell, S.B. et al. 2011. Genetic Models of Sensorimotor Gating: Relevance to Neuropsychiatric Disorders. In: *Current topics in behavioral neurosciences*., pp. 251–318.

van Praag, H. et al. 2002. Functional neurogenesis in the adult hippocampus. *Nature* 415(6875), pp. 1030–1034.

Qin, W. et al. 2015. DNA methylation requires a DNMT1 ubiquitin interacting motif (UIM) and histone ubiquitination. *Cell Res* 25(8), pp. 911–929.

Quednow, B.B. et al. 2008. Impaired Sensorimotor Gating of the Acoustic Startle Response in the Prodrome of Schizophrenia. *Biological Psychiatry* 64(9), pp. 766–773.

Quintela, I. et al. 2017. Copy number variation analysis of patients with intellectual disability from North-West Spain. *Gene* 626, pp. 189–199.

Rajagopal, L. et al. 2014. The novel object recognition test in rodents in relation to cognitive impairment in schizophrenia. *Current pharmaceutical design* 20(31), pp. 5104–14.

Rathert, P. et al. 2008. Protein lysine methyltransferase G9a acts on non-histone targets. *Nat Chem Biol* 4(6), pp. 344–346.

Rees, E. et al. 2012. De novo mutation in schizophrenia. *Schizophrenia bulletin* 38(3), pp. 377–81.

Riedel, W.J. and Blokland, A. 2015. Declarative Memory. In: Kantak, K. M. and Wettstein, J. G. eds. *Cognitive Enhancement*. Cham: Springer International Publishing, pp. 215–236.

Roopra, A. et al. 2004. Localized domains of G9a-mediated histone methylation are required for silencing of neuronal genes. *Mol Cell* 14(6), pp. 727–738.

Rudenko, A. and Tsai, L.-H. 2014. Epigenetic modifications in the nervous system and their impact upon cognitive impairments. *Neuropharmacology* 80, pp. 70–82.

Rynkiewicz, A. and Łucka, I. 2018. Autism spectrum disorder (ASD) in girls. Co-occurring psychopathology. Sex differences in clinical manifestation. *Psychiatria Polska* 52(4), pp. 629–639.

Ryu, H. et al. 2006. ESET/SETDB1 gene expression and histone H3 (K9) trimethylation in Huntington's disease. *Proc Natl Acad Sci U S A* 103(50), pp. 19176–19181.

Sahay, A. and Hen, R. 2007. Adult hippocampal neurogenesis in depression. *Nature Neuroscience* 10(9), pp. 1110–1115.

Della Sala, G. and Pizzorusso, T. 2014. Synaptic plasticity and signaling in rett syndrome. *Developmental Neurobiology* 74(2), pp. 178–196.

Salgado, J.V. and Sandner, G. 2013. A critical overview of animal models of psychiatric disorders: challenges and perspectives. *Revista Brasileira de Psiquiatria* 35(suppl 2), pp. S77–S81.

Samocha, K.E. et al. 2014. A framework for the interpretation of de novo mutation in human disease. *Nature Genetics* 46(9), pp. 944–950.

Sarti, F. et al. 2013. Rapid Suppression of Inhibitory Synaptic Transmission by Retinoic Acid. *Journal of Neuroscience* 33(28), pp. 11440–11450.

Saunderson, E.A. et al. 2016. Stress-induced gene expression and behavior are controlled by DNA methylation and methyl donor availability in the dentate gyrus. *Proceedings of the National Academy of Sciences of the United States of America* 113(17), pp. 4830–5.

Schaefer, A. et al. 2009. Control of Cognition and Adaptive Behavior by the GLP/G9a Epigenetic Suppressor Complex. *Neuron* 64(5), pp. 678–691.

Schmid, S. et al. 2014. Habituation mechanisms and their importance for cognitive function. *Frontiers in integrative neuroscience* 8, p. 97.

Schmidt, B. et al. 2012. Disambiguating the similar: The dentate gyrus and pattern separation. *Behavioural Brain Research* 226(1), pp. 56–65.

Schoenbaum, G. et al. 2007. A role for BDNF in cocaine reward and relapse. *Nature neuroscience* 10(8), pp. 935–6.

Selemon, L.D. 2013. A role for synaptic plasticity in the adolescent development of executive function. *Translational psychiatry* 3(3), p. e238.

Sharma, M. et al. 2016. Inhibition of G9a/GLP Complex Promotes Long-Term Potentiation and Synaptic Tagging/Capture in Hippocampal CA1 Pyramidal Neurons. *Cerebral Cortex* 27(6), p. bhw170.

Sharma, M. et al. 2017. Epigenetic regulation by G9a/GLP complex ameliorates amyloid-beta 1-42 induced deficits in long-term plasticity and synaptic tagging/capture in hippocampal pyramidal neurons. *Aging Cell* 16(5), pp. 1062–1072.

Shinkai, Y. and Tachibana, M. 2011. H3K9 methyltransferase G9a and the related molecule GLP. *Genes Dev* 25(8), pp. 781–788.

Silverman, J.L. et al. 2010. Behavioural phenotyping assays for mouse models of autism. *Nature reviews. Neuroscience* 11(7), p. 490.

Smrt, R.D. et al. 2007. Mecp2 deficiency leads to delayed maturation and altered gene expression in hippocampal neurons. *Neurobiology of disease* 27(1), pp. 77–89.

Snyder, J.S. et al. 2005. A role for adult neurogenesis in spatial long-term memory. *Neuroscience* 130(4), pp. 843–852.

Snyder, J.S. et al. 2009. Anatomical gradients of adult neurogenesis and activity: young neurons in the ventral dentate gyrus are activated by water maze training. *Hippocampus* 19(4), pp. 360–70.

Snyder, J.S. et al. 2012. Late maturation of adult-born neurons in the temporal dentate gyrus. *PloS one* 7(11), p. e48757.

Soden, M.E. and Chen, L. 2010. Fragile X Protein FMRP Is Required for Homeostatic Plasticity and Regulation of Synaptic Strength by Retinoic Acid. *Journal of Neuroscience* 30(50), pp. 16910–16921.

Soldati, C. et al. 2012. Repressor Element 1 Silencing Transcription Factor

Couples Loss of Pluripotency with Neural Induction and Neural Differentiation. *STEM CELLS* 30(3), pp. 425–434.

van der Staay, F.J. et al. 2009. Evaluation of animal models of neurobehavioral disorders. *Behavioral and Brain Functions* 5(1), p. 11.

Steimer, T. 2011. Animal models of anxiety disorders in rats and mice: some conceptual issues. *Dialogues in clinical neuroscience* 13(4), pp. 495–506.

Steiner, B. et al. 2006. Type-2 cells as link between glial and neuronal lineage in adult hippocampal neurogenesis. *GLIA* 54(8), pp. 805–814.

Südhof, T.C. 2008. Neuroligins and neurexins link synaptic function to cognitive disease. *Nature* 455(7215), pp. 903–911.

Sugeno, N. et al. 2016. α-Synuclein enhances histone H3 lysine-9 dimethylation and H3K9me2-dependent transcriptional responses. *Sci Rep* 6, p. 36328.

Sun, J. et al. 2011. Epigenetic regulation of neurogenesis in the adult mammalian brain. *The European journal of neuroscience* 33(6), pp. 1087–93.

Suzuki, W.A. et al. 1993. Lesions of the perirhinal and parahippocampal cortices in the monkey produce long-lasting memory impairment in the visual and tactual modalities. *The Journal of neuroscience : the official journal of the Society for Neuroscience* 13(6), pp. 2430–51.

Swank, M.W. and Sweatt, J.D. 2001. Increased histone acetyltransferase and lysine acetyltransferase activity and biphasic activation of the ERK/RSK

cascade in insular cortex during novel taste learning. *The Journal of neuroscience : the official journal of the Society for Neuroscience* 21(10), pp. 3383–91.

Swerdlow, N.R. et al. 2001. Neural circuit regulation of prepulse inhibition of startle in the rat: current knowledge and future challenges. *Psychopharmacology* 156(2–3), pp. 194–215.

Swerdlow, N.R. et al. 2004. The ventral hippocampal regulation of prepulse inhibition and its disruption by apomorphine in rats are not mediated via the fornix. *Neuroscience* 123(3), pp. 675–85.

Tachibana, M. et al. 2001. Set domain-containing protein, G9a, is a novel lysine-preferring mammalian histone methyltransferase with hyperactivity and specific selectivity to lysines 9 and 27 of histone H3. *J Biol Chem* 276(27), pp. 25309–25317.

Tachibana, M. et al. 2002. G9a histone methyltransferase plays a dominant role in euchromatic histone H3 lysine 9 methylation and is essential for early embryogenesis. *Genes and Development* 16(14), pp. 1779–1791.

Tachibana, M. et al. 2005. Histone methyltransferases G9a and GLP form heteromeric complexes and are both crucial for methylation of euchromatin at H3-K9. *Genes Dev* 19(7), pp. 815–826.

Takata, A. et al. 2016. De Novo Synonymous Mutations in Regulatory Elements Contribute to the Genetic Etiology of Autism and Schizophrenia. *Neuron* 89(5), pp. 940–947.

Talkowski, M.E. et al. 2012. Sequencing chromosomal abnormalities reveals neurodevelopmental loci that confer risk across diagnostic boundaries. *Cell* 149(3), pp. 525–537.

Tamminga, C.A. et al. 2003. Evaluating glutamatergic transmission in schizophrenia. *Annals of the New York Academy of Sciences* 1003, pp. 113–8.

Trievel, R.C. et al. 2002. Structure and catalytic mechanism of a SET domain protein methyltransferase. *Cell* 111(1), pp. 91–103.

Tsujimura, K. et al. 2009. Neuronal differentiation of neural precursor cells is promoted by the methyl-CpG-binding protein MeCP2. *Experimental Neurology* 219(1), pp. 104–111.

Verhoeven, W.M. et al. 2011. Kleefstra syndrome in three adult patients: further delineation of the behavioral and neurological phenotype shows aspects of a neurodegenerative course. *Am J Med Genet A* 155A(10), pp. 2409–2415.

Vermeulen, K. et al. 2017. Sleep Disturbance as a Precursor of Severe Regression in Kleefstra Syndrome Suggests a Need for Firm and Rapid Pharmacological Treatment. *Clin Neuropharmacol* 40(4), pp. 185–188.

Vianna, M.R. et al. 2004. Role of the hippocampus and amygdala in the extinction of fear-motivated learning. *Current neurovascular research* 1(1), pp. 55–60.

Vogel-Ciernia, A. and Wood, M.A. 2014. Examining object location and

object recognition memory in mice. *Current protocols in neuroscience* 69, p. 8.31.1-17.

Vorhees, C. V and Williams, M.T. 2014. Assessing spatial learning and memory in rodents. *ILAR journal* 55(2), pp. 310–32.

Walf, A.A. and Frye, C.A. 2007. The use of the elevated plus maze as an assay of anxiety-related behavior in rodents. *Nature protocols* 2(2), pp. 322–8.

Walker, M.P. et al. 2013. Reversible epigenetic histone modifications and Bdnf expression in neurons with aging and from a mouse model of Alzheimer's disease. *Age* 35(3), pp. 519–531.

Wan, H. et al. 1999. Different contributions of the hippocampus and perirhinal cortex to recognition memory. *The Journal of neuroscience : the official journal of the Society for Neuroscience* 19(3), pp. 1142–8.

Ware, J.S. et al. 2015. Interpreting de novo Variation in Human Disease Using denovolyzeR. *Current protocols in human genetics* 87, p. 7.25.1-7.25.15.

West, P.T. et al. 2014. Genomic distribution of H3K9me2 and DNA methylation in a maize genome. *PLoS One* 9(8), p. e105267.

Williams, L.E. et al. 2013. Reduced habituation in patients with schizophrenia. *Schizophrenia research* 151(1–3), pp. 124–32.

Wondolowski, J. and Dickman, D. 2013. Emerging links between homeostatic synaptic plasticity and neurological disease. *Frontiers in cellular*

neuroscience 7, p. 223.

Wu, H. and Sun, Y.E. 2006. Epigenetic Regulation of Stem Cell Differentiation. *Pediatric Research* 59(4 Pt 2), p. 21R–25R.

Xiang, J.-Z. and Brown, M.W. 2004. Neuronal Responses Related to Long-Term Recognition Memory Processes in Prefrontal Cortex. *Neuron* 42(5), pp. 817–829.

Xin, Z. et al. 2003. Role of histone methyltransferase G9a in CpG methylation of the Prader-Willi syndrome imprinting center. *J Biol Chem* 278(17), pp. 14996–15000.

Yamaguchi, M. et al. 2000. Visualization of neurogenesis in the central nervous system using nestin promoter-GFP transgenic mice. *NeuroReport* 11(9), pp. 1991–1996.

Yamaguchi, S. et al. 2004. Rapid Prefrontal-Hippocampal Habituation to Novel Events. *Journal of Neuroscience* 24(23), pp. 5356–5363.

Yao, B. et al. 2016. Epigenetic mechanisms in neurogenesis. *Nature Reviews Neuroscience* 17(9), pp. 537–549.

Yashiro, K. and Philpot, B.D. 2008. Regulation of NMDA receptor subunit expression and its implications for LTD, LTP, and metaplasticity. *Neuropharmacology* 55(7), pp. 1081–1094.

Zeng, L. et al. 2013. Functional Impacts of NRXN1 Knockdown on Neurodevelopment in Stem Cell Models. Arking, D. E. ed. *PLoS ONE* 8(3), p. e59685.

Zhang, T. et al. 2016. G9a/GLP Complex Maintains Imprinted DNA Methylation in Embryonic Stem Cells. *Cell Rep* 15(1), pp. 77–85.

Zylicz, J.J. et al. 2015. Chromatin dynamics and the role of G9a in gene regulation and enhancer silencing during early mouse development. *eLife* 4, p. e09571.

Appendix A

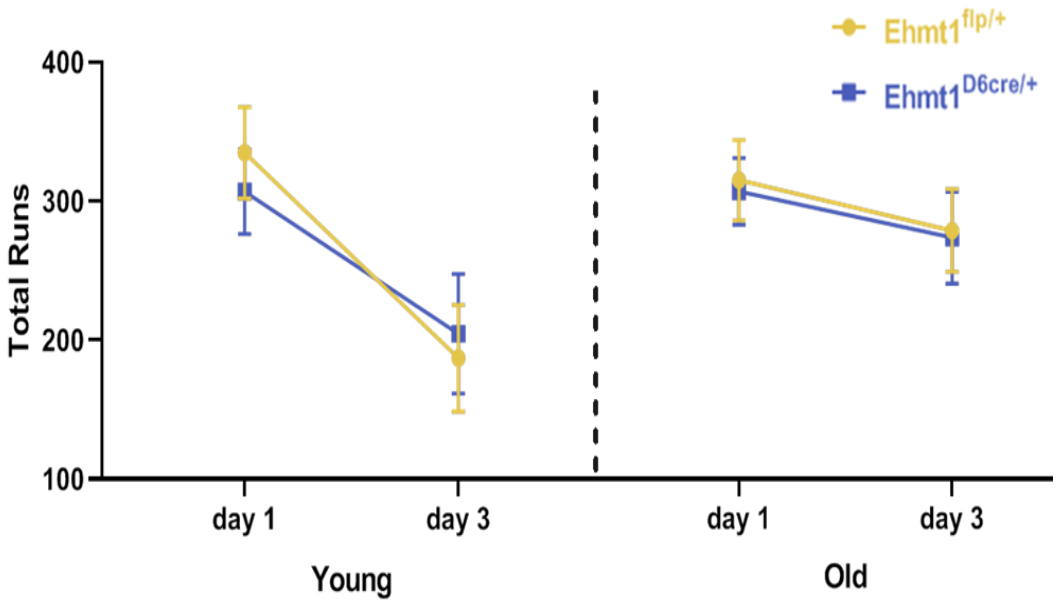

Figure A. 1 Total number of RUNS, defined by consequetive breaks of both beams, performed in the first and last session at young and old timepoints, all data presented as mean and SEM, *Ehmt1*$^{flp/+}$: 20, *Ehmt1*$^{D6cre/+}$: 17.

Appendix B

Table B. 1 Table of Primary and Secondary Antibodies used in Chapters 4 and 5 IHC/ICC

Antibody	ICC	IHC	Supplier & Cat No.
Mouse α-nestin	1:500	not used	Milipore **MAB353**
Rat α-GFAP Rabbit	1:1000	not used	ThermoFisher **13-0300**
Goat α-DCX	1:500	not used	Santa Cruz **sc-8066**
Mouse α-BrdU	1:250	1:200	BD Biosciences **347580**
Rabbit α-NeuN	not used	1:500	Abcam **ab177487**
Rabbit α-Ki67	1:1000	1:1000	Abcam **ab15580**
Rabbit α-Cleaved Caspase 3	1:500	not used	Cell Signal **#9661**
Alexa Fluor® 488 Donkey α-mouse	not used	1:1000	Life Technologies **A-21202**
AlexaFluor® 488 Donkey α-rat	1:1000	not used	Life Technologies **A-11006**
AlexaFluor® 555 Donkey α-mouse	1:1000	not used	Life Technologies **A-31570**
AlexaFluor® 647 Donkey α-rabbit	1:1000	1:1000	Life Technologies **A-31571**
Alexa Fluor® 647 Donkey α-goaT	1:1000	not used	Life Technologies **A-21447**

Appendix C

Table C. 1 Gene Ontology Enrichment of differentially DOWNREGULATED genes of baseline WT versus shRNA treated cultures.

GO Terms	PValue	Fold Enrichment	FDR
rno03010:Ribosome	1.87E-16	9.522643819	2.66E-13
Ribosomal protein	8.75E-12	6.531891936	1.12E-08
GO:0005925 focal adhesion	3.09E-10	4.71302169	4.10E-07
Ribonucleoprotein	6.54E-10	5.225513549	8.35E-07
GO:0003735 structural constituent of ribosome	4.73E-08	4.097387173	6.56E-05
GO:0022627 cytosolic small ribosomal subunit	2.84E-07	8.050423821	3.78E-04
GO:0006412 translation	1.44E-06	3.802367942	0.002356764
GO:0070062 extracellular exosome	4.12E-06	1.763375462	0.00547977
GO:0044822 poly(A) RNA binding	6.49E-06	2.314814815	0.008992583
GO:0022625 cytosolic large ribosomal subunit	2.92E-05	5.008112493	0.038867233

Table C. 2 Gene Ontology Enrichment of differentially UPREGULATED genes of baseline WT versus shRNA treated cultures.

GO Terms	PValue	Fold Enrichment	FDR
GO:0043025 neuronal cell body	1.32E-11	3.894848	1.76E-08
GO:0030425 dendrite	5.40E-11	4.008211	7.20E-08
Synapse	5.03E-10	5.049653	6.54E-07
Lipoprotein	4.99E-09	3.742185	6.48E-06
Phosphoprotein	2.68E-08	1.656391	3.48E-05
GO:0005515 protein binding	2.70E-08	2.17979	3.83E-05
Cell junction	4.60E-08	3.580884	5.97E-05
GO:0030424 axon	2.85E-07	3.722223	3.80E-04
GO:0030054 cell junction	6.50E-07	3.419866	8.67E-04
GO:0045202 synapse	7.79E-07	3.974334	0.001039
GO:0043005 neuron projection	1.18E-06	3.419141	0.001581
GO:0030426 growth cone	9.10E-06	5.131725	0.012138
Cytoplasm	9.27E-06	1.72556	0.01203
Glycoprotein	1.01E-05	1.783414	0.013059

Table C. 3 Gene Ontology Enrichment of differentially DOWNREGULATED genes of TTX-Conditioned WT versus shRNA treated cultures.

GO Terms	PValue	Fold Enrichment	FDR
GO:0044822 poly(A) RNA binding	3.15E-13	2.426612207	4.76E-10
GO:0005737 cytoplasm	2.16E-10	1.449466929	3.05E-07
Phosphoprotein	2.32E-09	1.533150666	3.05E-06
rno03010:Ribosome	1.06E-07	4.184509784	1.35E-04
GO:0042552 myelination	2.65E-07	7.840375587	4.64E-04
RNA-binding	3.52E-07	3.227112038	4.63E-04
GO:0016020 membrane	3.56E-07	1.641437088	5.03E-04
GO:0005925 focal adhesion	4.02E-07	2.834404653	5.68E-04
Methylation	1.30E-06	2.589082786	0.001707815
GO:0005634 nucleus	1.56E-06	1.354919782	0.002201369
GO:0003723 RNA binding	1.70E-06	2.546902416	0.002557229
Ribonucleoprotein	2.29E-06	3.000765986	0.003018618
Ubl conjugation	5.13E-06	2.103750253	0.006743182
GO:0030529 intracellular ribonucleoprotein complex	8.11E-06	4.384469697	0.011459339
GO:0070062 extracellular exosome	1.18E-05	1.484688151	0.016705918
IPR009030:Insulin-like growth factor binding protein, N-terminal	1.25E-05	4.230097765	0.01991842
GO:0048709 oligodendrocyte differentiation	1.96E-05	7.560362173	0.034369674
GO:0005654 nucleoplasm	2.13E-05	1.608979705	0.030045139

Table C. 4 Gene Ontology Enrichment of differentially UPNREGULATED genes of TTX-Conditioned WT versus shRNA treated cultures

GO Terms	PValue	Fold Enrichment	FDR
Phosphoprotein	2.19E-23	1.957760817	2.91E-20
Synapse	2.48E-19	5.726033505	3.28E-16
Cytoplasm	4.96E-18	2.16946636	6.56E-15
Cell junction	1.22E-17	4.296855627	1.61E-14
GO:0005515 protein binding	4.31E-17	2.444933921	6.42E-14
GO:0030424 axon	1.27E-14	4.327941361	1.76E-11
GO:0030054 cell junction	4.15E-14	3.996587373	5.79E-11
GO:0043025 neuronal cell body	5.12E-13	3.387288523	7.13E-10
GO:0043005 neuron projection	4.21E-12	3.781610279	5.86E-09
GO:0045202 synapse	9.95E-12	4.277315865	1.39E-08
GO:0030426 growth cone	4.46E-11	5.922033144	6.22E-08
Lipoprotein	9.89E-11	3.344579515	1.31E-07
Acetylation	1.03E-10	2.039251369	1.37E-07
GO:0030425 dendrite	1.22E-10	3.24820547	1.69E-07
Methylation	4.64E-10	3.23407047	6.14E-07
Alternative splicing	1.15E-09	2.443985516	1.53E-06
GO:0043195 terminal bouton	2.27E-09	6.033607682	3.16E-06
GO:0043209 myelin sheath	6.32E-09	4.588800552	8.82E-06
GO:0005737 cytoplasm	5.29E-08	1.399759558	7.38E-05
Cytoskeleton	1.01E-07	2.740491788	1.34E-04
Postsynaptic cell membrane	1.85E-07	4.858619033	2.44E-04
GO:0030672 synaptic vesicle membrane	3.19E-07	7.750575434	4.45E-04
GO:0043204 perikaryon	3.85E-07	4.603529704	5.37E-04
Transport	4.53E-07	1.937885073	6.00E-04
Glycoprotein	9.72E-07	1.686035144	0.001286114
GO:0045211 postsynaptic membrane	1.11E-06	3.868730547	0.001543874
Cell projection	1.28E-06	2.940260895	0.001698261
GO:0014069 postsynaptic density	1.31E-06	3.522495418	0.001826417
Ion channel	1.54E-06	3.260965027	0.002036933
Cytoplasmic vesicle	1.72E-06	3.239079356	0.002282885
Palmitate	2.51E-06	3.672928645	0.003323469
GO:0001975 response to amphetamine	2.77E-06	8.18016421	0.004782531
GO:0007268 chemical synaptic transmission	3.40E-06	3.937893003	0.005883066
GO:0043679 axon terminus	3.90E-06	5.50434385	0.005441987
GO:0048488 synaptic vesicle endocytosis	4.77E-06	14.63340486	0.008245106
GO:0005829 cytosol	5.88E-06	1.725599814	0.008191853
rno05032:Morphine addiction	7.55E-06	5.089573269	0.009684435
Membrane	7.93E-06	1.265464719	0.010496173
GO:0048306 calcium-dependent protein binding	1.22E-05	6.056547619	0.018142156
Calcium	1.37E-05	2.317680228	0.018086371
GO:0048471 perinuclear region of cytoplasm	1.60E-05	2.196197582	0.022272623
Ion transport	1.61E-05	2.416231838	0.021251926
Ubl conjugation	1.72E-05	2.087292804	0.022723838
GO:0042220 response to cocaine	1.74E-05	6.601536029	0.03015947
GO:0016020 membrane	1.76E-05	1.55821428	0.024601054
GO:0044325 ion channel binding	1.91E-05	4.37007874	0.028382263
Nitration	2.05E-05	9.192815695	0.027099653
GO:0008021 synaptic vesicle	3.45E-05	4.135642964	0.048054001

Table C. 5 MGI Mammalian phenotype enrichment of differentially UPREGULATED genes of baseline WT versus shRNA treated cultures.

MP Terms	P	FDR
MP:0003633 abnormal nervous system physiology	1.85E-09	3.97E-06
MP:0014114 abnormal cognition	2.65E-09	3.97E-06
MP:0002063 abnormal learning/memory/conditioning	2.65E-09	3.97E-06
MP:0002572 abnormal emotion/affect behaviour	9.01E-09	1.02E-05
MP:0003635 abnormal synaptic transmission	1.16E-07	0.000104
MP:0001362 abnormal anxiety-related response	9.85E-07	0.00074
MP:0002065 abnormal fear/anxiety-related behaviour	3.63E-06	0.002335
MP:0002206 abnormal CNS synaptic transmission	6.19E-06	0.00349
MP:0002062 abnormal associative learning	3.26E-05	0.016302
MP:0001454 abnormal cued conditioning behaviour	7.60E-05	0.034234

Table C. 6 MGI Mammalian phenotype enrichment of differentially UPREGULATED genes of TTX-Conditioned WT versus shRNA treated cultures.

MP Terms	P	FDR
MP:0003635 abnormal synaptic transmission	1.32E-16	5.94E-13
MP:0002206 abnormal CNS synaptic transmission	1.76E-15	3.96E-12
MP:0003633 abnormal nervous system physiology	5.79E-13	8.70E-10
MP:0014114 abnormal cognition	3.73E-12	3.36E-09
MP:0002063 abnormal learning/memory/conditioning	3.73E-12	3.36E-09
MP:0002572 abnormal emotion/affect behaviour	5.50E-10	4.13E-07
MP:0002062 abnormal associative learning	1.81E-08	1.17E-05
MP:0002066 abnormal motor capabilities/coordination/movement	4.36E-08	2.46E-05
MP:0001399 hyperactivity	7.63E-08	3.60E-05
MP:0001968 abnormal touch/ nociception	7.98E-08	3.60E-05
MP:0002067 abnormal sensory capabilities/reflexes/nociception	1.92E-07	7.87E-05
MP:0004753 abnormal miniature excitatory postsynaptic currents	3.90E-07	0.000146
MP:0002065 abnormal fear/anxiety-related behaviour	5.48E-07	0.00019
MP:0001362 abnormal anxiety-related response	2.89E-06	0.000932
MP:0009745 abnormal behavioural response to xenobiotic	3.30E-06	0.000971
MP:0001463 abnormal spatial learning	3.45E-06	0.000971
MP:0002910 abnormal excitatory postsynaptic currents	5.00E-06	0.001327
MP:0002945 abnormal inhibitory postsynaptic currents	6.13E-06	0.001534
MP:0002272 abnormal nervous system electrophysiology	7.28E-06	0.001676
MP:0012349 increased susceptibility to induction of seizure by inducing agent	7.44E-06	0.001676
MP:0001970 abnormal pain threshold	9.77E-06	0.002096
MP:0001392 abnormal locomotor behaviour	1.36E-05	0.002783
MP:0002064 seizures	1.51E-05	0.002863
MP:0001468 abnormal temporal memory	1.52E-05	0.002863
MP:0002915 abnormal synaptic depression	1.76E-05	0.003077
MP:0009538 abnormal synapse morphology	1.77E-05	0.003077
MP:0001364 decreased anxiety-related response	2.18E-05	0.00364
MP:0003491 abnormal voluntary movement	2.54E-05	0.003973
MP:0002906 increased susceptibility to pharmacologically induced seizures	2.56E-05	0.003973
MP:0003313 abnormal locomotor activation	3.42E-05	0.005138
MP:0002207 abnormal long term potentiation	4.23E-05	0.006146
MP:0002557 abnormal social/conspecific interaction	5.02E-05	0.007073
MP:0002882 abnormal neuron morphology	5.71E-05	0.007793
MP:0000950 abnormal seizure response to pharmacological agent	7.81E-05	0.010358
MP:0001462 abnormal avoidance learning behaviour	8.73E-05	0.011244
MP:0004769 abnormal synaptic vesicle morphology	9.41E-05	0.011776
MP:0001454 abnormal cued conditioning behaviour	9.83E-05	0.011974
MP:0001473 reduced long term potentiation	0.00014	0.016528
MP:0001486 abnormal startle reflex	0.000143	0.016528
MP:0009357 abnormal seizure response to inducing agent	0.000149	0.016755
MP:0001488 increased startle reflex	0.00016	0.017579
MP:0004008 abnormal GABA-mediated receptor currents	0.000286	0.030721
MP:0000947 convulsive seizures	0.000302	0.031687
MP:0012315 impaired learning	0.000329	0.033723
MP:0005136 decreased growth hormone level	0.000399	0.039991
MP:0004811 abnormal neuron physiology	0.00044	0.041274
MP:0008840 abnormal spike wave discharge	0.000444	0.041274
MP:0004770 abnormal synaptic vesicle recycling	0.000444	0.041274
MP:0001469 abnormal contextual conditioning behaviour	0.000449	0.041274
MP:0003990 decreased neurotransmitter release	0.000544	0.049046

Table C. 7 MGI Mammalian phenotype enrichment of differentially DOWNREGULATED genes of TTX-Conditioned WT versus shRNA treated cultures.

MP Terms	P	FDR
MP:0003077 abnormal cell cycle	6.12E-07	0.002757
MP:0010867 abnormal bone trabecula morphology	4.65E-06	0.010484
MP:0003723 abnormal long bone morphology	3.59E-05	0.046787
MP:0004023 abnormal chromosome number	4.15E-05	0.046787